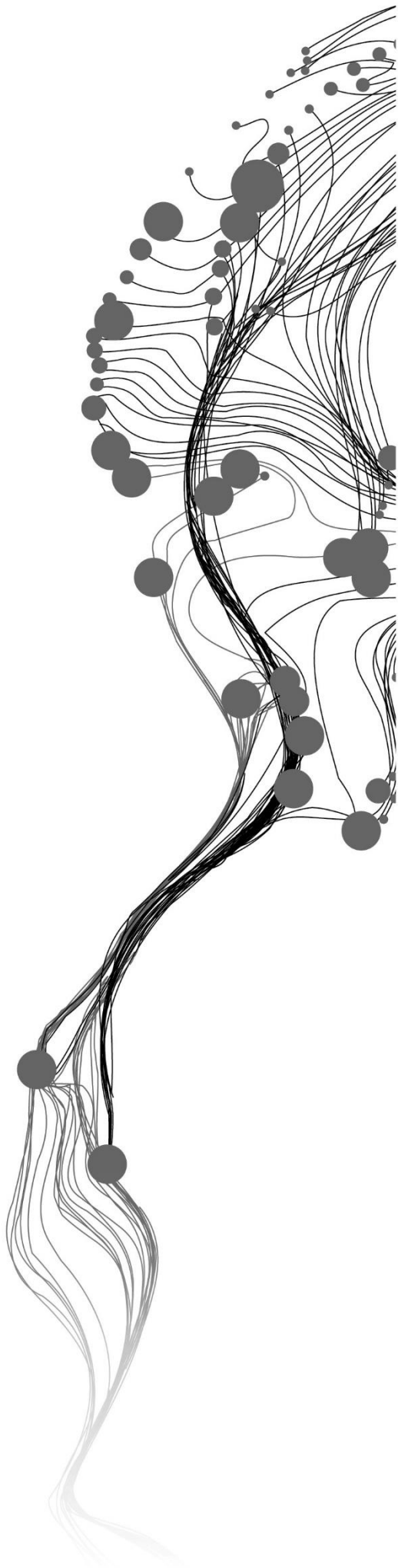# Assessment of methods for mangrove cover mapping on shrimp farms using high spatial resolution remote sensing

FINN BENJAMIN MÜNCH
JULY 2023

SUPERVISORS:
Dr. Iris van Duren
Dr. Panagiotis Nyktas

Assessment of methods for mangrove cover mapping on shrimp farms using high spatial resolution remote sensing

FINN BENJAMIN MÜNCH
Enschede, The Netherlands, July, 2023

Thesis submitted to the Faculty of Geo-Information Science and Earth Observation of the University of Twente in partial fulfillment of the requirements for the degree of Master of Science in Geo-information Science and Earth Observation.

Specialization: Natural Resource Management

SUPERVISORS:
Dr. Iris van Duren
Dr. Panagiotis Nyktas

External supervisor:
Dr. Vo Quoc Tuan

THESIS ASSESSMENT BOARD:
Dr. Kees de Bie (Chair)
Prof. Dr. Daphne van der Wal (External Examiner, ITC University of Twente & Koninklijk Nederlands Instituut voor Onderzoek der Zee (NIOZ))

ABSTRACT

Mangroves are tropical and subtropical coastal wetlands that provide valuable ecosystem services. Although mangroves have important environmental functions like climate regulation and water purification, they decline mainly due to anthropogenic influence. This development can be observed particularly well in the Mekong Delta in Vietnam, where the decline of the mangrove area is mainly triggered by the land use change from mangrove to shrimp farms. Addressing deforestation as well as the demand for more sustainable shrimp production, hybrid systems, called mixed mangrove-shrimp farms, aim to conserve 60% of mangrove cover and cultivate ecological shrimp in low-intensity aquacultures. Observation and mapping of mangrove ecosystems are necessary to provide evidence-based information for preserving and managing this natural resource. Satellite remote sensing offers more transparent and efficient mangrove monitoring than the currently applied laborious field surveys. Data on the present land cover in the study area was collected during a sampling campaign in March 2023. This study compared an object-based and a pixel-based approach to classify high-resolution imagery to assess mangroves on shrimp farms. A SPOT-7 image was classified using a Random Forest machine learning algorithm in eCognition to investigate the mangrove classification accuracy on mixed mangrove-shrimp farms in a Vietnamese protection and production forest. The resulting mangrove maps achieved an overall accuracy of 96% with a spatial resolution of 1.5 m. The McNemar test indicated that there is no statistically significant difference between the classification accuracy of the object-based and pixel-based approach. The discrepancy between the farmer's perspective and the classification-based shrimp farm mangrove ratios suggested ground-based estimates to be challenging. Resulting from the spatial analysis, a higher mangrove ratio was revealed in the protection forest compared to the production forest. This indicates more successful mangrove conservation or reforestation on the shrimp farms in the protection forest zone, which correlates with the funding for mangrove sapling replantation in the respective forest zone. However, the continued replantation of *Rhyzophora* is likely to maintain the dominance of monocultures that may benefit timber production but do not preserve or reintroduce biodiverse mangrove ecosystems and their valuable services. Consequently, the application of a hybrid mangrove observation approach that uses satellite and UAV remote sensing data is proposed for the assessment of mangrove ratios on shrimp farms in the study area.

ACKNOWLEDGMENTS

TABLE OF CONTENTS

LIST OF FIGURES

LIST OF MAPS

LIST OF TABLES

LIST OF ACRONYMS

GPS	Global Positioning System
GTPs	Ground Truth Points
Kappa	Kappa coefficient or Kappa index
Kappa$_m$	mangrove specific Kappa coefficient
k-NN	k-Nearest Neighbor
LAI	Leaf Area Index
NDVI	Normalized Difference Vegetation Index
NDWI	Normalized Difference Water Index
NIR	Near Infra-Red
OA	Overall accuracy
OBIA	Object-based image analysis
PA	Producer accuracy
PA$_m$	Producer accuracy of the mangrove class
RF	Random Forest
SVM	Support Vector Machine
UA	User accuracy
UA$_m$	User accuracy of the mangrove class
UAV	Unmanned Aerial Vehicle
VND	Vietnamese Dong

1. INTRODUCTION

Coastal areas inhabit highly productive and carbon-dense ecosystems that play a vital role in climate change mitigation. Therefore, ecosystems like mangroves and saltmarshes are termed blue carbon ecosystems (Klemas, 2013; Pham et al., 2019b). Blue carbon ecosystems efficiently sequester carbon dioxide, which leads to a storage of about 10 times more carbon dioxide than in terrestrial green carbon ecosystems like forests (Huang et al., 2022). Mangroves are defined as tidally influenced trees, shrubs, palms, or ferns that grow in coastal or estuarine environments (Massó i Alemán et al., 2010). About 70 species of 25 genera and 19 families are considered as mangroves (Ellison et al., 2020). Mangroves inherit a buffer function by dissipating wave energy and adapting to sea level rise (Duarte et al., 2013; Horstman et al., 2014). The water quality and sedimentation are enhanced by mangroves via the filtration of nutrients as well as organic and inorganic matter (Alongi, 2018; Hock & Su, 2020). As a result, mangroves prevent eutrophication by acting as a nutrient sink (Hock & Su, 2020). The mentioned functions like climate regulation, flood regulation, and water purification are considered regulating ecosystem services (Vo et al., 2012). Mangroves provide a variety of further ecosystem services that can be divided into provisioning, supporting, and cultural services. The provision of food, fresh water, and wood is associated with provisioning services (Vo et al., 2012). Also, the provision of habitat for a diversity of fauna ranging from birds over reptiles to shellfish is considerable. Particularly the mangrove's root system serves as a shelter and nursery for juvenile fish (Hock & Su, 2020). Supporting services refer to the nutrient cycling, soil formation, and primary production of mangrove ecosystems. At last, the cultural services include the aesthetic, spiritual, educational, and recreational value that mangrove ecosystems contribute (Vo et al., 2012).

Despite the important services they provide, the loss of mangroves is an issue that occurs on tropical and subtropical coasts worldwide (Polidoro et al., 2010). Goldberg et al. (2020) modeled that 2.1% of the global mangrove area, which relates to 3,363 km², was lost from 2000 to 2016. 62% of this loss was anthropogenically caused with the transition from mangrove to commodities being the primary driver accounting for 47% (about 1,586 km²) of the observed global mangrove depletion (Goldberg et al., 2020). Mangroves rapidly decline due to anthropocentric impact (Klemas, 2013; Pham et al., 2019b). This is triggered, because the density of the population in coastal areas strongly increases, which exemplifies the pressure on adjacent ecosystems by anthropogenic activities (Bouma et al., 2014). 82% of the human-induced mangrove loss originates in the six Southeast Asian nations Indonesia, Myanmar, Malaysia, the Philippines, Thailand, and Vietnam, with the Mekong Delta representing one of the hotspots (Goldberg et al., 2020). Anthropogenic stress on mangrove ecosystems via the conversion of mangroves to aquaculture or human settlement as stated by Pham et al., (2019b) was observed in Vietnam's Mekong Delta. Son et al. (2015) mapped a 74% decline in mangrove forests between 1979 and 2013 in the Mekong Delta's Cà Mau province. The boom in the aquaculture industry was cited as the main reason for the decline (Son et al., 2015). The Vietnamese Mekong Delta accounts for more than 85% of the national shrimp production (Lai et al., 2022). In 2018 Vietnam was the fourth-largest shrimp exporter and third-largest producer in the world, which makes shrimp farming an important business in the country (Lai et al., 2022; Xuan et al., 2021). The Vietnamese government plans to increase revenues from shrimp aquaculture to 10 billion US$ by 2025 (Lai et al., 2022). But the conversion of land use from mangroves to shrimp aquaculture leads to a loss of biodiversity and negative environmental impacts (Lai et al., 2022; Nguyen et al., 2018; Van et al., 2015). Additionally, the charcoal production in the Cà Mau province leads

to the plantation of *Rhizophora* and *Melaleuca* monocultures, which does not support the improvement of biodiversity (Ha et al., 2014; Nguyen et al., 2023). The depletion of mangrove ecosystems leads to the loss of important ecosystem services like carbon sequestration via primary production, flood regulation, and water purification (Estoque et al., 2018; Friess et al., 2016; Vo et al., 2012). The alarming loss of mangrove forests in the Mekong Delta must be tackled to preserve the valuable ecosystem services they provide. Therefore, the monitoring and management of mangrove forested areas is of special importance for the Mekong Delta.

From 1975 to 1994 mangrove forests in Vietnam were managed by the State Forest Enterprises and state-owned organizations. The mangrove forest area drastically decreased during that period due to the conversion of mangroves into aquaculture ponds and the exploitation of timber and non-timber forest resources. This was backed by the State Forest Enterprises since Vietnam's mangrove forests were defined as state-owned national assets. In 1994 the forest management was decentralized, and a forestland devolution policy was adopted (Truong et al., 2021). This led to the introduction of two main forest use rights, the land use certificate also called the red book, and the contract-based allocation called green book. Production forests like barren land or plantations were listed in the red book. The land use certificate ensuring 50-year forestland use right for those areas was transferred by the state to households. Special-use forests for nature conservation, and protection forests used for watershed protection, soil erosion prevention, and natural hazard mitigation are allocated in the green book. Households can lease limited use rights with a maximum contract term of 20 years for green book areas from Forest Management Boards or forest companies (Truong et al., 2021). The level of mangrove coverage is the most important regulation. Depending on the contract, tenants are allowed to convert 20 to 40% of the allotted forest into land uses like agriculture, aquaculture, or housing (Truong & Do, 2018). Hogestijn (2023, p. 17) lists a detailed overview with respect to the development of legal instruments concerning the mangrove management on shrimp farms from 1961 until 2022. Moreover, the Vietnamese jurisdictional system that decides on the legal instruments for the mangrove forest management is presented (Hogestijn, 2023, p. 6).

The conservation zones in Vietnam are divided into full protection zones where all land must be forested and conserved, and buffer zones, where 60% mangrove forest cover must prevail. Farmers can lease a land use right for the remaining 40% of the area. This land use right can only be renewed if the farmers respect the legislation and maintain 60% mangrove forest cover in the area (Vo et al., 2013).

Despite the risk of losing the land use right, increasing the profit by extending the aquaculture area to more than 40% is tempting for farmers (Vo et al., 2013). Consequently, mangrove forests in the buffer zones are at risk to be harvested and converted into shrimp ponds, as this seems more profitable for the farmers that lease the use right. However, Truong & Do (2018) found that about 60% is the optimal mangrove coverage for shrimp farming in terms of productivity and profitability. The integration of mangroves into shrimp aquacultures reduces the risk of water pollution or shrimp diseases to affect productivity (Nguyen et al., 2020a). Bosma et al. (2016) found that ponds with 30-50% mangrove cover had the highest shrimp yields. Integrated mangrove-shrimp aquacultures need less or no feed input and fertilization, which reduces production costs (Nguyen et al., 2020a). Moreover, certified organic shrimps from mangrove-shrimp aquacultures with a minimum of 50% mangrove cover in the ponds can be sold for a premium shrimp price (Lai et al., 2022). The certification of regular and organic shrimp becomes a prerequisite for accessing most world markets (Bosma et al., 2016), which is crucial given Vietnam's intention to increase shrimp exports (Lai et al., 2022). Certification organizations like the Global Aquaculture Alliance Best Aquaculture Practices (GAA-BAP), the Aquaculture Stewardship Council (ASC), and Naturland vouch for sustainable and ecological shrimp production with their labels (Baumgartner & Nguyen, 2017; Havice & Iles, 2015). Among other criteria, a mangrove to pond ratio greater than 50% is required to qualify as an organic shrimp farm (Joffre et al., 2015). Audits assessing the

compliance of a shrimp farm with the organic standards consider the mangrove measurements and maps that are recorded and reported by the local Forest Management office, a visual assessment on-site as well as the confirmation of the Protection Mangrove Forest Management Committee to verify that the mangrove plantation area within the farm's land is greater than 50% (Gruber et al., 2020, p. 27).

A variety of ministries, departments, administrations, and institutes with independent and overlapping responsibilities at national, provincial, and district levels are involved in the monitoring and management of mangroves in Vietnam (Hogestijn, 2023, p. 52). The lack of interaction between the involved parties leads to ineffective and insufficient monitoring, particularly on a small scale. The People's Committees that are responsible on the district and commune level face challenges to afford forest surveyors and managers that monitor the local mangrove area (Hogestijn, 2023). The monitoring of the mangrove forest to aquaculture ratio is important to control if the farmers that manage the land comply with the regulations and incentivize sustainable land use management according to the requirements. The lack of human resources causes the enforcement of forestry regulations by the Forest Management Boards to be weak. Only about three cases of community-level violations are detected annually. But a survey found that 50% of the investigated households cleared the mangrove forest beyond the regulated level (Truong et al., 2021). The prevention of mangrove coverage violations by the limited number of patrolling foresters is unlikely to be successful, due to the size of the monitored area and the vast distribution of the numerous shrimp farms. The assessment of the forest assignment policy enforcement indicated that the focus must be on the quality of the enforcement, not the quantity (Truong et al., 2021). Currently, aquacultures are usually mapped with field surveys using handheld GPS devices, by visual analysis and delineation using remote sensing images, or via a hybrid approach that combines both methods (Virdis, 2014). This subjective and untransparent assessment of the mangrove coverage on shrimp farms does not enable a quantification of inaccuracies. This potentially leads to uncertainty in terms of achieving a mangrove cover threshold value, since there is no consideration of an error range. Research demonstrated the potential of satellite remote sensing applications for the inventorying, monitoring, and management of aquacultures (Virdis, 2014; Vo et al., 2013). An accuracy assessed remote sensing-based classification of mangroves could assist the forest administrations to efficiently detect violations as well as facilitate the awarding and verification of eco-labels by certification organizations.

1.1.   Literature review on the remote sensing of mangroves

The following section reviews literature on the object-based and pixel-based approach for the classification of satellite remote sensing imagery for mangrove mapping purposes as well as the application of Unmanned Aerial Vehicles (UAV).

The lack of monitoring data on coastal ecosystems hinders the successful implementation of management and preservation frameworks since continuous environmental observation is required (El Mahrad et al., 2020; Muller-Karger et al., 2018). Accordingly, research on accurate observation methods is necessary. satellite-based remote sensing technologies introduced a cost-effective solution to complement data gaps with regular temporal and wide spatial coverage (El Mahrad et al., 2020). Still coastal habitats, including wetlands like mangroves, "remain among the most undersampled habitats on the Earth's surface" (Muller-Karger et al., 2018, p. 750). But an integration of multisensor and multitemporal data can benefit blue carbon ecosystem mapping, monitoring, and risk assessment as well as the analysis of key drivers causing changes (Guo et al., 2017; Pham et al., 2019b; Reif & Theel, 2017; White et al., 2015). Additionally, the flexible application of Unmanned Aerial Vehicles (UAVs) as sensor platforms can

improve the database to observe the dynamic processes of coastal environments on fine temporal and spatial scales (Doughty & Cavanaugh, 2019; Zhu et al., 2019). The comparison of very high spatial resolution UAV datasets (0.03 m/pixel) to moderate spatial resolution satellite remote sensing datasets of 10 and 25 m/pixel showed that satellite-based monitoring tends to overestimate the mangrove area (Hsu et al., 2020). For small areas, UAVs present a valuable alternative to satellite remote sensing, because they can classify mangroves with even higher accuracies than very high spatial resolution satellite imagery like Pleiades-1B (Ruwaimana et al., 2018). But the long processing time of UAV data compared to satellite images was stated by Ruwaimana et al. (2018) to be the main disadvantage.

Tropical regions like Vietnam are particularly challenging for optical remote sensing in terms of atmospheric moisture content, haze, and cloud cover. Cloud and cloud shadow masking prevents the consideration of pixels which could lead to inaccurate classifications (Nguyen et al., 2020b).

The review of Pham et al. (2019c) presents the successful mapping of mangroves with object-based and pixel-based classification methods using satellite remote sensing data. Taking this as a starting point the following paragraph first introduces the pixel-based and then the object-based classification approach in more detail.

Pixel-based classifications consider the spectral signature of each individual pixel of a satellite image (Maurya et al., 2021). Also, the computation of indices that combine the spectral information of different bands, for instance, the Normalized Difference Vegetation Index (NDVI) and the Soil Adjusted Vegetation Index (SAVI), are applicable input data (Rhyma et al., 2020). The distinction between moderately and high vegetation biomass using the NDVI is challenging due to its saturation issue. The Enhanced Vegetation Index (EVI) was found to have a higher correlation with field measurements than the NDVI (Tran et al., 2022). The Enhanced Vegetation Index corrects canopy background noise from soil and atmospheric conditions, which makes it valuable for classifications in mangrove ecosystems where soil, water, and vegetation contribute to the pixel composition (Tran et al., 2022).

Supervised classifications like the Maximum Likelihood (ML) classification use Ground Truth Points (GTPs) on the present land cover as training data to build a probability density function for the investigated land cover classes (Rhyma et al., 2020). The pixels of the image are classified according to their respective probability to belong to the classes represented by the training data. The ML classifier is the most applied pixel-based classifier (Maurya et al., 2021). It assumes that the training data is normally distributed, which can lead to erroneous classification in case the values do not follow a normal distribution (Myint et al., 2008). Pixel-based classifications were frequently applied for mangrove species distribution mapping that resulted in up to 82% overall accuracy when using Pleiades-1 imagery that was pan-sharpened to a spatial resolution of 0.5 m (Wang et al., 2018b). Wang et al. (2018b) found the salt-and-pepper appearance of the pixel-based classifiers to represent the investigated mangrove species smaller and patchier than the object-based approach.

Object-based classification methods account for spectral, and spatial aspects to distinguish mangrove areas (Ridha & Kamal, 2021). Spatial aspects are segmentation parameters like shape, scale, compactness, and smoothness (Dawod & Sharafuddin, 2021). Dawod & Sharafuddin (2021) found that the scale is the most important of the stated parameters since it determines the size of the objects. High spatial resolution imagery is advantageous for the segmentation process of an object-based image analysis (OBIA) considering the finer resolution of spatial aspects (GISGeography, 2022a).

The application of multiple segmentation levels is commonly used in OBIA mangrove classification approaches. The first level of segmentation can classify water pixels according to Normalized Difference Water Index (NDWI) and NDVI threshold values or the Near-Infrared (NIR) band (Pham et al., 2019a; Pham & Brabyn, 2017; Valderrama-Landeros et al., 2018; Vo et al., 2013). Then a second-level

segmentation can distinguish vegetation from other land cover types. NDVI threshold values of NDVI > 0.3 or NDVI > 0.4 are commonly applied to classify vegetation (Pham et al., 2019a; Pham & Brabyn, 2017; Valderrama-Landeros et al., 2018; Vo et al., 2013).

This research's literature review revealed that the study of Vo et al. (2013) is unique in mapping mangroves on shrimp farms. The application of an object-based classification on a SPOT-5 image using the NDVI as an additional band was the subject of the study. SPOT 5 records the multispectral bands with a 10 m spatial resolution. It was stated that the accurate classification of mangroves in mixed shrimp farm mangrove systems remains challenging (Vo et al., 2013). An integrated mangrove shrimp farm is a diked aquaculture characterized by narrow, elongated ditches between rows of mangroves that are planted on soil platforms (Lai et al., 2022). A pixel size of 10 meters spans over both narrow mangrove rows as well as the water in between illustrated in *Figure 1*. Accordingly, a finer spatial resolution than 10 m is necessary to depict mangrove rows on integrated mangrove shrimp farms with satellite remote sensing imagery.

Figure 1. Rows of mangroves on an integrated mangrove shrimp farm in the Cà Mau province, Vietnam. (Source: own photograph, 2023).

The accuracy of classifications can be assessed with the validation data, which is the remaining part of the Ground Truth Points (GTPs) that is not used for the training of the machine learning algorithm. A confusion matrix can be used to calculate descriptive and analytic statistics (Manandhar et al., 2009). The user, producer, and overall accuracies as well as the Kappa coefficient, are used to report the accuracy of classifications (Pham & Brabyn, 2017). The producer accuracy assesses the map from the point of view of the map producer. It refers to the probability that a respective land cover class's reference GTP on the

ground is correctly classified by the map. Whereas the user accuracy focuses on the reliability of the map from a user perspective. It states the probability that a pixel on the classified map really represents that land cover class on the ground (Liu et al., 2007). The overall accuracy is computed by dividing the correctly classified GTPs by the total amount of GTPs in the confusion matrix (Liu et al., 2007). A minimum land cover interpretation accuracy of 85% should be achieved (Manandhar et al., 2009). The Kappa accounts for GTP and mapped land cover agreements that may be caused by chance (Liu et al., 2007). In terms of accuracy, object-based approaches tend to outperform pixel-based classifications (Kamal & Phinn, 2011; Pham & Brabyn, 2017; Pham et al., 2019c; Trang et al., 2016; Wang et al., 2018a). However, OBIAs involve more workload than pixel-based classifications. The segmentation process increases the labor input and processing time of object-based approaches. Therefore, pixel-based classifications are attractive in terms of time and effort, but the extra effort for object-based classifications can pay off in terms of higher accuracies.

Artificial intelligence is applied for remote sensing-based earth observation. Wang et al. (2020) reviewed rule-based, data-driven, and reinforcement approaches as well as ensemble methods used for remote sensing data mining and analysis. A variety of machine learning algorithms are applied for mangrove classification and mapping. Previous studies conclude that Random Forest (RF) outperformed the Support Vector Machine (SVM), decision tree, and Maximum Likelihood (ML) approaches in mangrove classification problems (Jhonnerie et al., 2015; Jiang et al., 2021; Luo et al., 2016). The Random Forest, being a non-parametric ensemble machine learning algorithm, constructs a defined number of individual decision trees, which is determined during the setup by n-trees. Each decision tree has one vote for the classification. The random forest classification result bases on the majority vote of all its individual decision trees (Talukdar et al., 2020). It is a non-linear and adaptive classification model that avoids overfitting and performs well with noisy datasets (Luo et al., 2016). Ensemble methods like Random Forest obtain better results than data-driven approaches such as SVM, k-Nearest Neighbor (k-NN), and Bayes or rule-based approaches such as decision tree. Accordingly, the Random Forest ensemble learning method is most commonly applied for classification tasks (Wang et al., 2020).

1.2. Problem statement

In summary, mangroves are important for various reasons, but severe mangrove forest degradation caused by the establishment of, and cultivation practices on shrimp farms is observed in Vietnam. The land use contracts for the protection and production forest zone require the shrimp farmers to maintain 60% mangrove cover on their property. Additionally, mangrove cover greater than 50% is necessary for the certification of ecological shrimps. Due to these requirements, monitoring the ratio of mangroves to other land use is needed. However, the Vietnamese forest management authorities as well as certification organizations lack accurate methods for the observation and quantification of mangroves on a shrimp farm scale. The currently applied field surveys are subjective, inaccurate, and time-consuming. Remote sensing-based mangrove monitoring has great potential to provide more accurate, transparent, and regular observations. Most mangrove classification studies are based on medium spatial resolution satellite data for large-scale mangrove distribution mapping. The spatial resolution of Landsat 9, SPOT 5, or the Sentinel-2 multispectral instrument is too coarse to depict individual rows or patches of mangroves on a shrimp farm scale. Therefore, this proposed study is going to assess the accuracy of object-based and pixel-based mangrove classifications on shrimp farm scale, based on a high spatial resolution image. Pixel-based and object-based classifications have opposing trade-offs in terms of workload and accuracy. However, it is not yet clear to what extent these methods perform in terms of accuracy and acceptance of

a certain inaccuracy on the shrimp farm level. The stated trade-offs must be considered to investigate the applicability of the methods for Vietnamese forest managers as well as eco-labeling organizations.

1.3.   Research objectives and research questions

This study's general research objective is to investigate the applicability of remote sensing imagery for the observation and mapping of mangroves on mixed mangrove shrimp farm systems. The necessity of accurate and cost-effective mangrove classification methods for forest managers as well as eco-labeling organizations leads to the following research objective and question.

RO1. To compare two commonly used classification methods for mapping mangroves on shrimp farms using high spatial-resolution imagery.

> **RQ1.** What is the difference in accuracy between an object-based and pixel-based classification for mangrove mapping on shrimp farms with high spatial-resolution imagery?

Mangrove monitoring by the Forest Management Board and certification organizations intends to investigate the mangrove ratio present on the shrimp farms. Consequently, this leads to the second research objective and question.

RO2. To compare the effect of forest management zones regarding mangrove prevalence on shrimp farms.

> **RQ2.** What is the difference in the ratio of mangrove cover on shrimp farms in the protection, production and no forest zones?

Although the farmers work and live on the shrimp farms, the estimation of the mangrove ratio is likely to be challenging from a ground-based perspective. Accordingly, the third research objective and question arise.

RO3. To assess the agreement or discrepancy between ground-based and satellite-based mangrove ratio estimates.

> **RQ3.** How do ground-based estimates differ from satellite-based mangrove ratios?

This research aims to study the stated objectives and questions by performing pixel-based, and object-based mangrove classification methods at a study area in the Năm Căn district of the Cà Mau province, Vietnam. The intended results are relative mangrove area maps of the investigated shrimp farms in the study area. Maps of the land cover on aquacultures estimated by a SPOT-7 satellite image are going to be generated. Moreover, the accuracy assessment with the Producer Accuracy, User Accuracy, Overall Accuracy and Kappa coefficient is going to be performed with ground truthing data from the study area. In particular, the producer and user accuracy of the mangrove class is important to estimate the performance of the classification. The Overall Accuracy for the binary classification of mangrove and non-mangrove land cover will be computed and used to indicate the classification's accuracy and error range. It is particularly important to report the error margin of the mangrove classification to reduce the

risk of shrimp farms being incorrectly indicated to comply with the mangrove ratio specified in the regulation. Additionally, an interview with a Vietnamese forest manager provided qualitative information on surveying practices as well as the consideration of error margins in meeting the mangrove cover threshold. Furthermore, the application of remote sensing-based monitoring will be debated in the discussion section.

2.   MATERIALS AND METHODS

This section gives an overview of the materials and methods used in this study. First, the study area will be introduced before the utilized datasets and applied methods are presented.

2.1.   Study area

The coast of southern Vietnam provides good conditions for mangrove growth. It is the largest and richest mangrove ecosystem in the country (Veettil et al., 2019). The most common mangrove genera that occur in Vietnam are *Rhizophora* and *Aviciennia* (Veettil et al., 2019). Changes in the hydrology of the Mekong River, due to dams, canals, and levees, lead to a reduced sediment load, which impacts coastal mangrove ecosystems. However, mangrove losses were mainly anthropogenically driven by chemical warfare with herbicides during the Vietnam War as well as the conversion of mangrove areas into aquacultures (Van et al., 2015). Pham et al. (2022) found that of the Mekong Delta's provinces, Cà Mau hosts the largest area of mangrove forests and even experienced a slight increase in mangrove area during the time from 2016 to 2020. Cà Mau province, the Southernmost province of Vietnam, hosts an abundance of mangrove forests and shrimp farms (Truong & Do, 2018). The Mekong Delta represents Vietnam's largest farming and aquaculture region. Therefore, the Cà Mau province, which accommodates 58,285 ha of the about 100,000 ha of the Mekong Delta's total mangrove area (Truong & Do, 2018), is especially interesting for a remote sensing mangrove observation case study.

The confrontation of both the largest aquaculture and mangrove forest located in the Cà Mau province holds the potential to escalate in the conversion of mangrove land cover to aquacultural land use as observed by Son et al. (2015). The government encouraged farmers with financial incentives to replant and protect mangroves to counteract the mangrove loss (Lai et al., 2022). Moreover, a reforestation project introduced by the Vietnamese government recovered about 6,800 ha of mangroves on mangrove-shrimp farms in the Cà Mau province (Son et al., 2015). This raises a special interest in the monitoring of the aquaculture to mangrove forest dynamics in the Cà Mau province, particularly the ratio of mangrove cover present on shrimp farms. Bosma et al. (2016) point out three main types of mixed mangrove shrimp farm systems. Rows of mangroves are present in the ponds of integrated mangrove-shrimp farm systems. Associated mangrove-shrimp farm systems host continuous patches of mangrove in the pond. In separated systems, the mangroves do not grow in the pond but on the land surrounding it (Bosma et al., 2016). Integrated mangrove-shrimp farming systems are typical for the Năm Căn and Ngoc Hien districts of the Cà Mau province (Ha et al., 2012). Accordingly, mixed mangrove shrimp farm systems in the Cà Mau province' Năm Căn district are defined as areas of interest to investigate the objective of mangrove coverage. The Cửa Lớn River represents the Southern border of the Năm Căn district and is the major river in the study area (*Map 1*). The study area in Năm Căn district contains a special-use, protection, and production forest indicated in *Map 1*. Additionally, a non-forested zone is located in the Northeast of the study area. The predominant mixed mangrove aquaculture model in the study area are integrated mangrove shrimp farms.
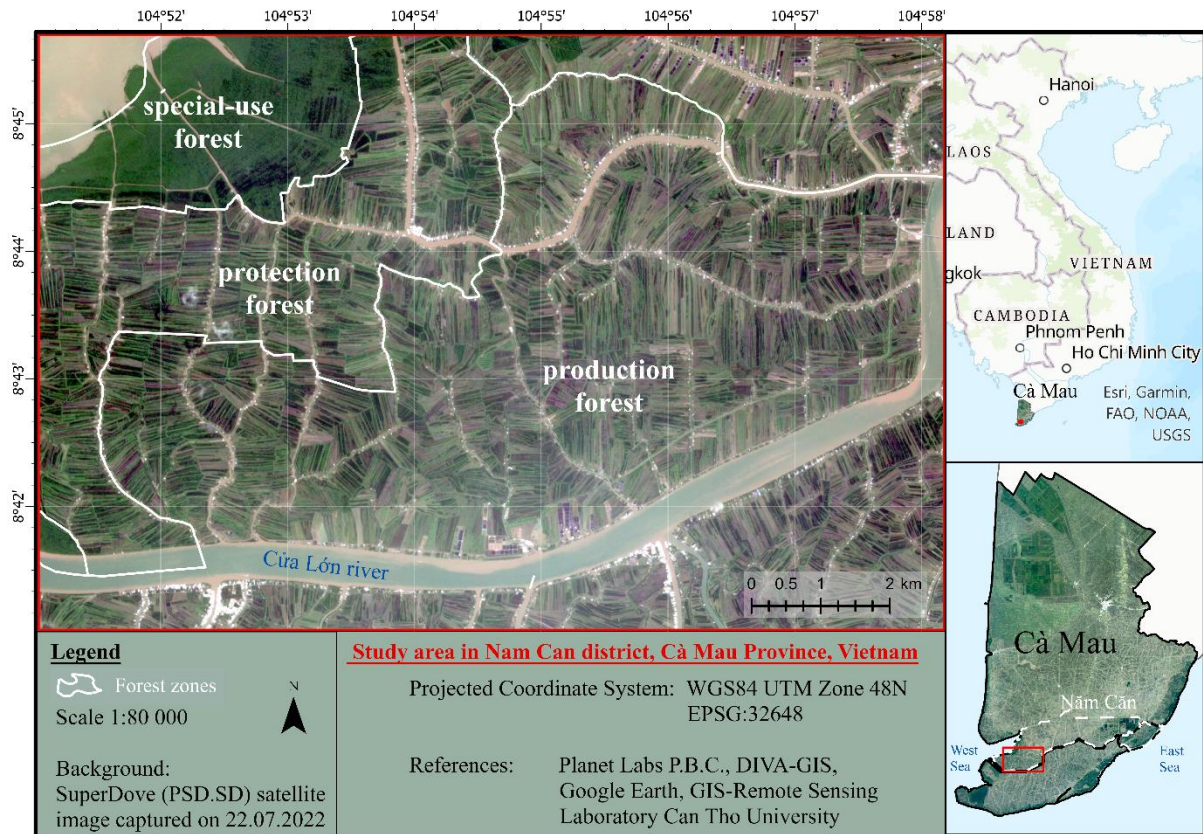
Map 1. Study area covering forest zones and integrated mangrove-shrimp farm systems in Năm Căn district, Cà Mau province, Vietnam (Google Earth, 2023; Hijmans et al., n.d.; Planet Labs PBC., 2022b).

An equatorial tropical climate prevails in Cà Mau. Two seasons, the dry season caused by the Northeast monsoon from December until April, and the wet season caused by the southwest monsoon from May to November, influence the atmospheric conditions (Groenewold et al., 2015). The Southwest monsoon's winds transport moist, water-saturated air parcels from the Gulf of Thailand to Cà Mau, which leads to heavy precipitation events during the wet season (Groenewold et al., 2015). An average annual precipitation of about 2000 mm and temperatures ranging from 20 to 35°C are recorded (Muoi et al., 2022). The wet season's Southwest winds and the dry season's Northeast winds also influence Cà Mau's wave environment. The highest waves occur at the coastlines facing the wind direction. Accordingly, the study area, which is located on the West coast, experiences the highest waves during the southwest monsoon caused by wind speeds up to 4.5 mm (Groenewold et al., 2015). Diurnal tides with a maximum tidal range of +1 m prevail in the West Sea which borders the study area (Luom et al., 2021). Cà Mau province is prone to flooding as it is a flat, low-lying area with an altitude ranging from -1 to 3 m above sea level (Tran et al., 2015).

2.2. Overview of materials and methods

This subsection gives an overview of the methods and materials. The research process is going to be presented with a flow chart.

Figure 2 illustrates the workflow of the process from the raw satellite image to maps indicating the mangrove ratio per forest zone and the mangrove ratio on the shrimp farms covered in the study area. The main steps involve the image pre-processing in the first block of *Figure 2*, followed by the classification with both approaches and the accuracy assessment in the second block. At last, the

mangrove ratio is calculated and analyzed in the third processing block. The subsequent sections of this chapter will explain the processing steps as well as the field data collection of Ground Truth Points (GTPs) in detail.
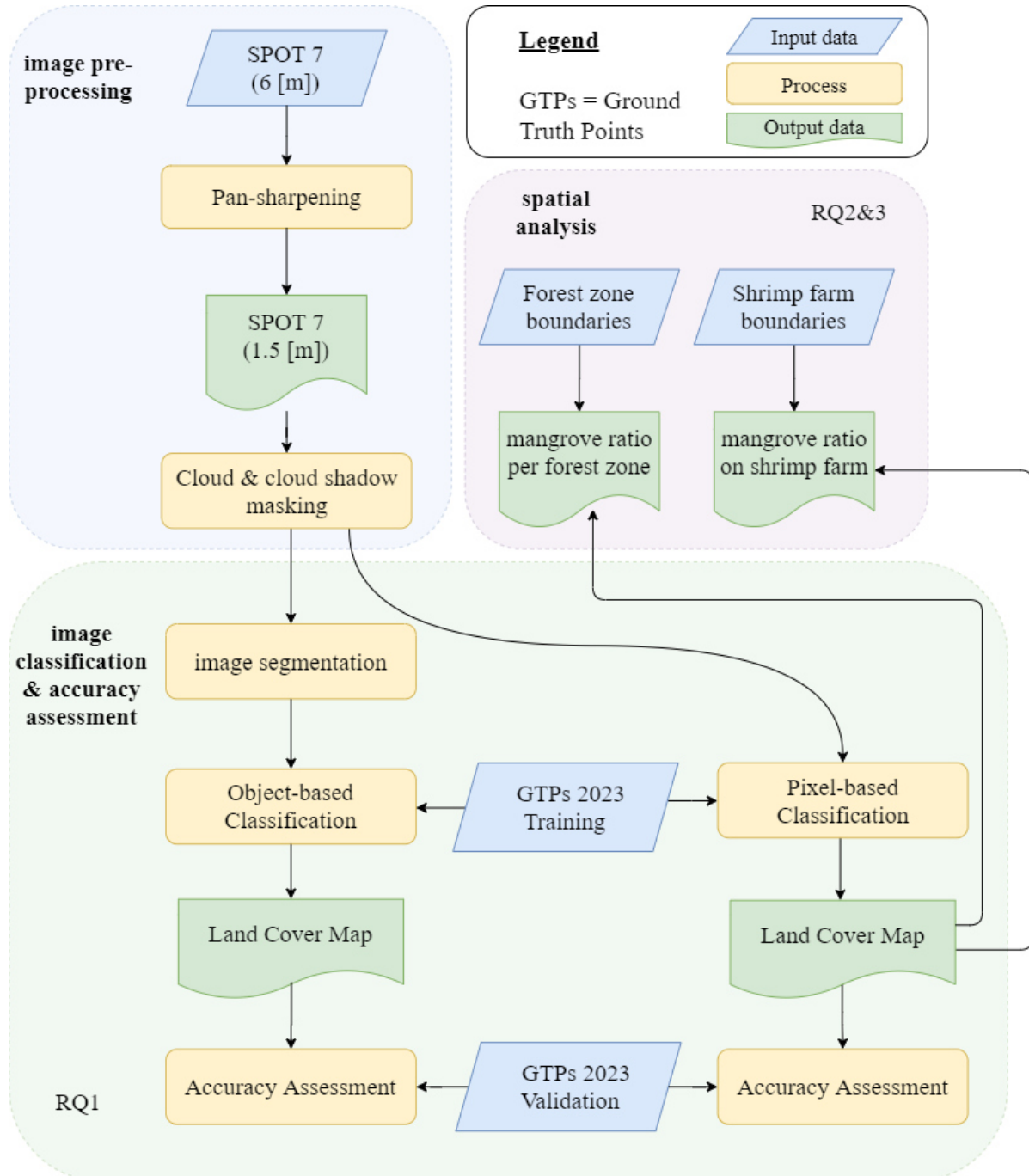
Figure 2. Flow chart on the processing steps of the study. The process is grouped into image processing, image classification & accuracy assessment, and spatial analysis. The accuracy assessment addresses research question one (RQ1) and the spatial analysis addresses research question two and three (RQ2 & 3).

2.3. Data

The datasets that were used in this study are listed in *Table 1*. The blue parallelograms in *Figure 2* represent the input data, which is listed in *Table 1*. The qualitative interview is not represented in the processing workflow since it is used as background information on the Forest Management Board's mangrove monitoring practices applied in the study area. The questionnaire survey of Prof. Dr. Vo and the Geo Eye mangrove map of Julia Hogestijn were used to compare the mangrove ratio created in this study with the estimates of alternative approaches.

Table 1. List of applied datasets. Where .shp represents shapefile, .tif represents tagged image file, .m4a represents MPEG-4 audio file, and .docx represents Microsoft Word file.

Name	Type, resolution & format	Date	Source of data
shrimp farm boundaries	Vector (polygon) [.shp]		Vo Quoc Tuan
forest zone boundaries	Vector (polygon) [.shp]		Vo Quoc Tuan
questionnaire survey	Vector (point) [.shp]	2022	Vo Quoc Tuan
Ground Truth Points (GTPs) 2023	Vector (point) [.shp]	2023	Vo Quoc Tuan & Finn Münch
SPOT-7 satellite image	Raster (pan 1.5 m, multispectral 6 m) [.tif]	2022	Airbus and European Space Agency (ESA)
qualitative interview	Record & notes (.m4a & .docx)	2023	Vo Quoc Tuan & Finn Münch
Geo Eye mangrove map	Vector (polygon) [.shp]	2019	Julia Hogestijn

2.4. Pre-processing of satellite imagery

Several parameters can be taken into account for the comparison of candidate remote sensing images to perform a land cover observation task (Phinn et al., 2003). The spatial and spectral resolution was considered to be most important for the mangrove mapping on shrimp farms. Therefore, a high spatial resolution satellite remote sensing image captured during the field survey of Prof. Dr. Tuan Quoc Vo from the 21st to the 25th of July 2022 was obtained. The Satellite pour l'Observation de la Terre 7 (SPOT-7) image was recorded at 09:16 AM on the 25th of July 2022. This image also represents the least cloud cover over the study area found in the SPOT and Pleiades archive from 2020 up to the present. A proposal to obtain this SPOT-7 orthophoto bundle package from ESA was submitted and accepted in January 2023. With the consent of Airbus and the European Space Agency (ESA), the corresponding data was downloaded (Airbus, 2022). SPOT-7 captures the Near Infrared (NIR), red, green, and blue band with a spatial resolution of 6 meters (*Table 2*). The SPOT-7 satellite also provides measurements with a panchromatic band that has a 1.5 m spatial resolution. The obtained product is geometrically and radiometrically processed. The image was delivered orthorectified. The pixel values represent radiometrically and atmospherically corrected reflectance scaled to 10,000 (Airbus, n.d.).

Table 2. Spectral bands and spatial resolution of the SPOT-7 satellite (European Space Agency (ESA), n.d). Where PAN represents the panchromatic band. NIR represents the Near-Infrared band.

Spectral Band	Wavelengths [nm]	Spatial resolution [m]
PAN	450-750	1.5
Blue	450-520	6
Green	530-600	6
Red	620-690	6
NIR	760-890	6

Considering the panchromatic and multispectral bands the applicable pan-sharpening weights were calculated with the 'Calculate pan sharpen weights' tool in Arc GIS Pro. The SPOT-7 image was pansharpened with the Gram-Schmidt algorithm according to the calculated pan-sharpening weight for the respective band (*Figure 2*). Gram Schmidt was selected since it performs better than the Principal Component Analysis (PCA) and the Intensity-Hue-Saturation (HIS) pan-sharpening methods in terms of the spectral deviation for high spatial resolution WorldView-2 and medium-scale Landsat-8 satellite imagery (Mahmoudi & Karami, 2020). Gram Schmidt achieved the best spectral match with the least spectral deviation between the multispectral and the pan-sharpened image (Mahmoudi & Karami, 2020). Therefore, Gram Schmidt was applied to minimize spectral distortion during the pan-sharpening process. A cloud mask was created using a supervised Support Vector Machine (SVM) classifier in Arc GIS Pro to improve the cloud mask that was delivered with the SPOT-7 image. Training polygons representing the classes cloud, cloud shadow, mangrove, vegetation, water, infrastructure, and soil were created. The spectral signature of the SPOT-7 image's pixels within the respective class's polygons was used to train the SVM classifier. The land cover map resulting from the supervised classification was used to indicate areas covered by cloud or cloud shadow. A natural color composite using the red, green, and blue bands of the SPOT-7 image was used to visually inspect the performance of the cloud and cloud shadow areas. Moreover, the blue band as well as the red band was individually visualized with a grey scale to detect haze and thin clouds. The grey scale visualizations were stretched to represent the value range greater than the 85th percentile. As a result, land covers that cause low reflections in the blue and red band are shown as black whereas haze and clouds are visualized according to the grey scale due to the spectral signature's sensitivity to red and blue wavelengths (GISGeography, 2022b). The overlay of the classified cloud map, the natural color composite as well as the blue and red band that underwent spectral stretching indicated where the SVM classifier did not detect haze or clouds. All stated layers were used to manually create a cloud mask that covers the haze and cloud pixels of the SPOT-7 image. According to the date, time, and location of the SPOT-7 image caption, the position of the sun can be estimated. Considering the sun's position, the angle between the cloud and cloud shadow was estimated. Cloud shadows were detected using a digitized cloud mask, the estimation of the angle between the clouds and their shadow as well as the previously mentioned red band, green band, and natural color composite. The generated cloud shadow and cloud mask were merged and then rasterized according to the panchromatic band of the SPOT-7 image. Cloud and cloud shadow pixels are represented as NoData and all other pixels with a value of 1. The cloud and cloud shadow mask was applied to the pansharpened SPOT-7 image with the 'raster calculator' tool (*Figure 2*). The mask layer was multiplied with the pansharpened SPOT-7 to create a cloud and shadow-masked, pansharpened SPOT-7 image.

2.5. Field survey

A QGIS project was created for the Ground Truth Point (GTP) sampling campaign. The workflow for the QGIS project generation is described in the QGIS and QField tutorial in *Appendix A*. The created project and the applied data were packaged and then transferred to the mobile QField devices. The QGIS project's layers include a vector polygon shapefile of the reference shrimp farms of interest. Twenty-five shrimp farms in each, the protection and production, forest zone were randomly selected using the random point generator with a minimum distance of 700 m. This minimum distance was chosen since it enabled the distribution of 25 random points in the respective forest zone of interest. The area of the observed forest zones was not large enough to generate 25 randomly distributed points with minimum distances greater than 700 m. The terrain in the protection and production forest is characterized by rivers, channels, sluices, and shrimp ponds, which limit accessibility via land routes. Considering the expenses of hiring vehicles, efficient transport between the sampling sites was aspired. To reduce the travel time in the difficult terrain, increase the number of GTPs, and improve the sampling efficiency one shrimp farm adjacent to each randomly selected shrimp farm was added as a reference shrimp farm of interest. Accordingly, clusters of two reference shrimp farms of interest were generated. The limited network of paths and bridges was displayed in the QField application using an open street map shapefile. The SPOT-7 satellite image with a spatial resolution of 1.5 m and Google Earth imagery with a spatial resolution of 0.5 m were used as background in QField to facilitate orientation and navigation during the field survey. A training for the QField application was developed from the 13th to the 16th of March 2023. A total of four training sessions were held. Prof. Dr Tuan Quoc Vo (Can Tho University), Dr. Iris van Duren (ITC University of Twente) as well as four students, namely Sagittarus Tinh, Thanh Loc, Thuat Ngon, and Huynh Nhat Hao, participated in the QField tutorial and practical. The training introduced the field survey and the sampling procedure. The conveyed QField skills and tools covered during the practical are summarized in the QField application tutorial in *Appendix A*. Students were instructed to locate the sampling points in the center of the areas representing the respective land cover. Edges or transition zones of one to another land cover should be avoided and not sampled. The pan-sharpened SPOT-7 image with a spatial resolution of 1.5 m was used to ensure that the point is located on a pixel that is surrounded by a buffer of as many pixels representing the same land cover as possible. At least a buffer of one pixel of the same land cover must surround a pixel of interest to create a sample point. This ensures that no mixed pixels are used as Ground Truth Points (GTPs).

The creation of a GTP with the QField application involved three main steps.

1. Defining the 'Code' of the GTP.
   Individual code letters, ranging from A to D, were assigned to each student. The respective student's code letter was used as the first item of the GTP's code. Then a unique number starting with 001 for the first GTP and then counting upwards to 002, 003, etc. was designated. Considering the first student's samples this procedure resulted in the following codes A001, A002, A003, etc.
2. Defining the 'Class' of the GTP.
   The land cover class of the surveyed sample point was selected from a drop-down menu. This drop-down menu was previously set up in the QField project to make the sampling quicker and more convenient. It presented the land cover classes of interest 'Mangrove', 'Water', 'Vegetation', 'Infrastructure', and 'Soil'.
3. Taking an image of the GTP.
   The surveyed sample point was photographed with the inbuilt camera of the used device and directly linked to the GTP. The image provides proof of the surveyed land cover. Moreover, it can indicate the location of the surveyor as well as the direction and distance to the GTP.

These three steps were mandatory. A GTP could not be saved if one of the three features was missing. This condition was set up in the created QField project to avoid incomplete GTPs. Another condition defined that the individual 'Code' for the GTPs must be unique. In case a code was duplicated, a warning was displayed and the GTP could not be saved. The date of the GTP record was automatically generated according to the device's date. The final optional step was to write a comment. The 'Comment' section was used to record land cover change during the SPOT-7 image caption and the field survey, the specification of the water subclasses pond water or river water, etc. The described step-wise sampling procedure with the QField interface is visualized in *Figure 3*.

Figure 3. Interface of the 'GTPs_NamCan_A' QField project that was applied during the field survey.

The field survey took place on the 22nd and 23rd of March 2023. The students paired up. Each duo rode with a motorbike to the reference shrimp farms of interest in the two strata protection forest and production forest. An equal number of shrimp farms was aimed in both forest zones to sample each forest zone with a similar number of GTPs. A forest manager guided the students to the pairs of reference shrimp farms of interest that were previously selected according to a random cluster sampling. Always two adjacent shrimp farms were sampled by one pair of students. The first student sampled one and the second student the other shrimp farm. The land cover classes mangrove, water, vegetation, soil, and infrastructure characterize the study area's landscape. The mentioned land cover classes were sampled on each reference shrimp farm of interest. The mangrove land cover class was defined as trees and shrubs of the genera listed in the mangrove floristics of the world table presented by Ragavan et al. (2021, p. 40 - 43). A minimum height of three meters was considered to neglect mangrove propagules and saplings, which contribute less to the functions and ecosystem services of a mangrove forest than grown mangroves. A minimum height of five meters specified by the Forest Protection Department to ensure

the protective function, which is reached about 5 years after planting the seedling[1], was not considered because only a few mangroves in the study area reached this height. Whereas the vegetation land cover class was defined as non-mangrove vegetation for instance, grass, vegetables, fruit trees, etcetera. Since water and mangroves dominated in the study area, two GTPs for each, the water and mangrove, land cover class were created on the respectively investigated shrimp farm. One water GTP within the shrimp pond and one in the channel or river bordering the respectively investigated shrimp farm were sampled to account for the spectral properties of the water bodies caused by the different depth and total suspended matter (TSM) like sediment or organic components (Das et al., 2017). The mangroves in the shallow aquaculture ponds lead to more dissolved organic matter (DOM) in the water column. Particularly the chromophoric dissolved organic matter (CDOM) influences the light absorption and consequently the color of the water (Das et al., 2017; Juhls et al., 2019). The sediment transport in the deeper water of rivers and channels leads to a higher load of suspended sediment in the water column, which increases the backscatter of light (Juhls et al., 2019). If the intended land cover was not located on the shrimp farm it was compensated by the closest respective land cover in the vicinity of the shrimp farm. On the second fieldwork day, the students traveled by boat to the reference shrimp farms of interest that were not accessible via the land route. In total, the four students collected 778 GTPs, which are listed according to the represented land cover in *Table 10* of *Appendix B*.

2.5.1.   Ground Truth Point (GTP) quality assessment

A quality assessment of the GTPs was performed in QGIS. The location and class as well as the captured image of the respective land cover of each GTP, were checked. The presence of surrounding buffer pixels of the same land cover class as the GTP located amidst was investigated. Moreover, the minimum distance between GTPs of the same land cover class was examined.

GTPs presenting nonconformity with the requirements defined in the field sampling manual (*Appendix A*) were noted. It appeared that a subsequent number of 199 GTPs would not be usable considering the predefined requirements. The neglection of these GTPs would have led to the loss of about 25% of the GTPs. Therefore, the following assumptions were made.

1. A distance of 50 m between land cover GTPs of the same class ensures to gain of the added value of independent spectral reflectance observations for the respective land cover class. This assumption bases on the heterogeneity observed for the respective land cover classes in the study area.

2. The spectral signature of the sub-land cover classes pond water and river water differ significantly. Therefore, a pond water and river water GTP with a distance of less than 50 m are relevant since they are not part of one homogeneous water body.

3. Separate buildings of the infrastructure GTPs with a distance of less than 50 m between each other are also relevant since they do not represent one homogeneous surface build of the same material. Spatial autocorrelation may not apply for infrastructure GTPs since the used materials can vary regardless of the distance between the individual complex of infrastructure. Field observations of corrugated iron, roof tiles, palm leaves, and concrete being used as construction material showed that the spectral signature of adjacent infrastructure varied according to the utilized material.

After the GTP quality assessment on a pixel level, it was also performed on an object level according to the results of the segmentation. Some GTPs of the water class were located within one object. In this case either one of the GTPs was neglected or moved to an adjacent object. Some objects included more pixels

---

[1] Zoom meeting with the technical manager of the West Sea Protection Forest Management Board and Prof. Dr. Vo Quoc Tuan (Head of the GIS and remote sensing laboratory, Can Tho University). 14.04.2023.

of another land cover class than the GTP's class. In this case either the class of the GTP was adjusted or the GTP was moved to an adjacent object representing pixels of the correct land cover class.

Considering the stated assumptions and the relocation of ill-positioned GTPs to locations complying with the requirements, the quality assessment resulted in the neglect of 63 GTPs. Reasons for neglecting GTPs ranged from the risk of introducing mixed pixels as reference for a particular land cover class to misclassifications to an insufficient distance between GTPs of the same land cover. Particularly the collection of explicit soil land cover sample points was problematic. Often a mixture of vegetation and soil prevailed in the study area, which would result in mixed pixels or objects used to identify soil areas. This could introduce unclear decisions in the classification algorithm. In total, 29 soil GTPs were neglected due to their unclear representation of the respective land cover.

2.5.2. Training and Validation dataset

A script to divide the quality assessed GTPs into a training and a validation dataset was written in RStudio. The division of GTPs into random 70% and 30% datasets was commonly applied in published research articles performing random forest land cover classifications (Behera et al., 2021; Guo et al., 2022; Pham et al., 2020; Wasniewski et al., 2020). Accordingly, the R script divides the available GTPs into a training dataset containing a random selection of 70% for each land cover class's GTPs (mangrove, water, vegetation, soil, infrastructure) and a validation dataset containing the remaining 30% of each land cover class's GTPs. The GTPs were split proportional to the respective strata to ensure that the resulting training dataset contained 70% of each land cover class's GTPs. A *for loop*[2] facilitated to create ten different pairs of training and validation datasets with randomly selected GTPs. After each iteration of the *for loop*, the seed incremented by one to generate seeds from one to ten. During each loop, one individual seed was used to ensure that individual training and validation datasets are created. After the performance of each loop, a matrix illustrating the ratio as well as an absolute number for each class of the training and validation dataset was printed to the console and controlled. The classification and accuracy assessment was performed with all dataset pairs to investigate the consistency of the calculated accuracy.

2.6. Classification

A classification of satellite remote sensing imagery involves the raster file of the captured image as well as Ground Truth Points defining land cover classes within the satellite image. In this study, the pansharpened, cloud, and cloud shadow masked SPOT-7 image, after this referred to as SPOT-7 image as well as the quality assessed GTPs, in the following parts referred to as GTPs, serve as input for the classification. In this study, object-based and pixel-based classifications were performed and compared. The subsequent subchapters describe the respective classification in more detail.

2.6.1. Object-based Classification

The object-based classification was performed with eCognition Developer 10.3. It involves three main steps, the image segmentation into objects, the classification assigning a land cover class to each object, and the accuracy assessment investigating the classification's performance (*Figure 2*). First, objects are created with the segmentation process. The 'Estimation of Scale Parameter' (ESP2) tool was used to estimate the most appropriate scale parameter for the segmentation of the SPOT-7 image (Drăguţ et al., 2010, 2014; Trimble Inc., 2020). The ESP2 tool was applied to five representative subsets that respectively cover several integrated mangrove-shrimp farms, channels as well as parts of the river and its

---

[2] A *for loop* is a function that enables repeatedly executing a section of code until a defined condition is met.

riverbank. The maximum local variance of the five subsets ranged from 92.78 to 101.63. The local variance peaked at a scale of 50 for each investigated subset. This indicates that a scale parameter of 50 is the most appropriate for the segmentation of the SPOT-7 image. The shape parameter and the compactness were set to 0.1 to attribute most of the weight to the spectral information. Due to the spatial resolution of the SPOT-7 image, less importance was attributed to the shape of the objects compared to the spectral signature. The segmentation based on the four pan-sharpened spectral bands of the SPOT-7 image with a spatial resolution of 1.5 m as well as on two spectral indices that were computed using the relevant pan-sharpened SPOT-7 bands. The image layer weight was set to 1 to give equal weight to each input layer in the segmentation process.

The 'Index Layer Calculation' of eCognition was used to create a respective layer for the Normalized Difference Vegetation Index (NDVI) and the Normalized Difference Water Index (NDWI). The NDVI was calculated as follows:

$$NDVI = \frac{(NIR - Red)}{(NIR + Red)}$$

where *NIR* represents the Near-Infrared band, and *Red* represents the red band of the SPOT-7 satellite remote sensing image (Gupta et al., 2018).

The NDWI was computed with the following equation:

$$NDWI = \frac{(NIR - Green)}{(NIR + Green)}$$

where *NIR* represents the Near-Infrared band, and *Green* represents the green band of the SPOT-7 satellite remote sensing image (Gupta et al., 2018).

Jhonnerie et al. (2015) found that the more input data was used, for instance, including spectral indices like the NDVI and NDWI in addition to the information of the spectral bands, the better the RF classifier performed. The NDWI was found to be the third most important input variable for the pixel-based mangrove classification (Jhonnerie et al., 2017). Whereas the study by Chen (2020) indicated NDVI to be the second most important variable for the Random Forest (RF) image classification approach. Also, the study by Shi et al. (2016) indicates that the use of the spectral metrics, for instance the Normalized Difference Mangrove Index (NDMI), outperformed the use of the raw band reflectance in terms of the User (UA), Producer (PA), and Overall Accuracy (OA). This result was verified by the McNemar test results of Shi et al., (2016), which indicated that the classification that used the spectral metrics performed significantly better than the classification that is based on the raw band reflectance (Shi et al., 2016). Therefore, the NDVI and NDWI were used as additional input layers for the segmentation as well as the classification. The application of the vegetation and water index supported the discrimination between the predominant land cover classes in the study area, namely water and mangrove as well as the residual land cover classes.

A variety of classification test runs were executed to assess the performance of different classifiers and input layers. The Bayes, k-NN, SVM, decision tree, and Random Forest supervised classifiers that are available in eCognition were investigated. Furthermore, different input data was used in the test runs to examine the effect of the NDVI and NDWI as additional input layers besides the red, green, blue, and NIR bands on the respective classifier's performance. The performance was investigated via accuracy assessments based on the independent validation GTPs and the visual inspection of classification results in eCognition. The classifier and input data that revealed high accuracies were chosen for this study. The

selection of a classifier that performs better for one of the approaches would not be valid for a fair comparison. Therefore, Random Forest was selected to avoid introducing a bias, since it indicated equal accuracies for the object-based and pixel-based classification. Moreover, the result of the Random Forest classifier indicated one of the highest mangrove class-specific accuracies for both the object-based and pixel-based approach. The applicability of the Random Forest algorithm for the classification of mangroves is confirmed by scientific literature stating that Random Forest outperforms other classifiers like SVM, decision tree, Maximum Likelihood, Bayes and k-NN (Jhonnerie et al., 2015; Jiang et al., 2021; Luo et al., 2016; Talukdar et al., 2020; L. Wang et al., 2020) Therefore, the selection of the Random Forest classifier was based on the literature review as well as the comparison of the classifiers' test runs. The 'Accuracy Assessment' tool was used to create a confusion matrix and calculate the Overall Accuracy (OA), Kappa as well as the User Accuracy (UA), Producer Accuracy (PA), and Kappa per class (Trimble Inc., n.d.). The Overall Accuracy (OA) and Kappa were considered as statistics indicating the classifications' accuracy. Since this study focuses on the classification of mangroves, particularly the mangrove class's User Accuracy (UA) and Producer Accuracy (PA) as well as the Kappa for the mangrove class were considered to select suitable classifiers and input data.

The Random Forest classifier with a maximum number of 50 decision trees and the input data were used to perform ten supervised classification replicates in eCognition. The standard setting of 50 decision trees suggested by eCognition was applied since using more decision trees than required would unnecessarily increase the processing time (Talukdar et al., 2020). Investigating the robustness of the result's classification accuracy using different replicates of GTPs as training and validation data is of interest to test its applicability. Therefore, each classification used an individual pair of the ten training and validation GTP datasets that were previously generated in RStudio. Subsequently, an accuracy assessment was performed, and the confusion matrix was exported for the result of each classification. A table including the mangrove class's User Accuracy (UA), Producer Accuracy (PA), and Kappa as well as the Overall Accuracy (OA) and Kappa of the ten classifications, was compiled. This table was used to calculate the descriptive statistics Minimum, Average, Median, Maximum, and Range, which facilitated the illustration as box plots. The ten classification replications indicate the robustness or variability of the assessed accuracies according to the used training and validation GTPs. Moreover, each of the ten exported confusion matrices containing the classes mangrove, water, vegetation, infrastructure, and soil was reclassified to a two-by-two confusion matrix representing the mangrove class and another class called non-mangrove, which represents all remaining land cover classes. Subsequently, the Overall Accuracy for the classification of the classes mangrove and non-mangrove was computed for each of the ten confusion matrices. The object-based Random Forest classification that achieved the median mangrove class-specific accuracies was exported from eCognition to further investigate the land cover map in Arc GIS Pro.

2.6.2. Pixel-based Classification

The pixel-based classification was also performed with eCognition Developer 10.3 to ensure the comparability of the resulting object-based and pixel-based classification. The 'chess board' segmentation was used to create one object per pixel. The test runs investigating the performance of machine learning algorithms and input data for the classification task were also performed for the pixel-based approach. Subsequently, a classifier that achieved high and similar accuracies for both the object-based and pixel-based approach was selected. The applicability of the Random Forest classifier was also confirmed by the literature, which stated it to be a well performing, commonly used classifier. Accordingly, a pixel-based land cover classification using the same settings for the Random Forest classifier with 50 decision trees

and the available SPOT-7, NDVI, and NDWI input data as for the object-based approach was performed for each of the ten individual GTP replicates (*Figure 2*). Subsequently, the accuracy assessment was replicated for each of the ten GTP replicates to assess the robustness of the pixel-based classification. Also, the pixel-based Random Forest classification that achieved the median mangrove class-specific accuracies was exported from eCognition for further processing and analysis.

A land cover map of the entire study area with a spatial scale of 1:50 000 was created in Arc GIS Pro using the result of the object-based and pixel-based Random Forest classification. The fine differences between the studied approaches cannot be perceived on that scale. Therefore, a subset of the land cover map and the mangrove cover map covering the protection and production forest zone as well as the no forest zone was generated for the investigation of differences on a finer spatial scale of 1:15 000. Furthermore, a mangrove cover difference map was produced with the 'Symmetrical Difference' tool of Arc GIS Pro's overlay toolset to illustrate discrepancies between the object-based and pixel-based approach.

2.6.3. McNemar test

The McNemar test was used to compare the overall performance of the object-based and pixel-based classifier. The reference validation GTPs were used to indicate misclassified objects or pixels. The count n of misclassified GTPs of one approach, which were correctly classified by the other approach and vice versa was used to perform the McNemar test with one degree of freedom. The following formula was considered:

$$x^2 = \frac{\left(|n_{op} - n_{po}| - 1\right)^2}{n_{op} + n_{po}}$$

where n_{op} represents the number of objects misclassified by the object-based classification o but correctly classified by the pixel-based classification p, and n_{po} indicates the number of pixels misclassified by the pixel-based classification p but correctly classified by the object-based classification o. A x^2 value greater than 3.84 indicates a statistically significant difference in the performance between the compared classifications at a confidence interval of 95% (Kavzoglu, 2017).

The McNemar test was performed with the ten individual validation GTP replicates for both the object-based and pixel-based classifications resulting from the respective GTP training dataset. Moreover, the McNemar test was specifically applied on mangrove misclassifications to directly assess the classifications' performance for the mangrove land cover class. Therefore, the mangrove validation GTPs were used for the mangrove specific McNemar test to indicate misclassified mangrove objects or pixels.

The following hypotheses were investigated with the McNemar test on all land cover misclassifications as well as the McNemar test specifically focusing on the mangrove land cover misclassifications:
H_0 There is no difference in the number of misclassified GTPs for the object-based and pixel-based approach.
H_1 There is a difference in the number of misclassified GTPs for the object-based and pixel-based approach.

2.7. Mangrove to shrimp farm ratio map

The ten supervised object-based and pixel-based classification replicates were investigated. The land cover map of the respective classification approach that achieved the median in the mangrove-specific accuracies, namely the User and Producer accuracy of the mangrove class (PA_m & UA_m) as well as the mangrove-specific Kappa coefficient ($Kappa_m$), was exported from eCognition. The exported classification and the shrimp farm boundaries for the study area were used to create a mangrove to shrimp farm ratio map with the 'Summarize within' analysis tool in Arc GIS Pro (*Figure 2*). The mangrove specific Overall Accuracy, calculated by merging all other classes into one class called 'non-mangrove', was computed for each individual object-based and pixel-based classification replicate. The median Overall Accuracy of the ten replicates for the respective classification approach was considered as the error margin of the mangrove class. This error margin was used to indicate shrimp farms that have a relative mangrove area within the range of 60% plus or minus the error margin on a map. Shrimp farms that present a mangrove ratio greater than 60% plus the error margin are indicated to comply with the regulations. On the other hand, shrimp farms with mangrove ratios smaller than 60% minus the error margin do not have enough relative mangrove cover to comply with the regulations in the protection and production forest zone. Shrimp farms with mangrove ratios within the transition range from complying to not complying with the 50% regulation for the certification of ecological shrimps are indicated according to the mangrove ratio error margin. Also, the extrema of greater than 99% and smaller than 1% relative mangrove area on the shrimp farm are illustrated in individual classes. Only shrimp farms with an area greater than 1 ha were displayed on the maps. Shrimp farms smaller than 1 ha, and properties that mainly presented urban land use were neglected.

The computed shrimp farm mangrove ratios for the protection and production forest zone were compared to investigate differences in compliance with the regulations in the zones. Moreover, the ratios of the forest zones were compared to the mangrove ratio on the shrimp farms that are located outside of the forest zones. The Shapiro-Wilk test was applied to test if the mangrove ratios of the three populations, protection forest, production forest, and non-forest, were normally distributed. Subsequently, the non-parametric Mann-Whitney U test was used to test if the mangrove ratios in the assessed zones are different.

The following hypotheses were investigated:

H_0 There is no difference in the mangrove ratio.

H_1 There is a difference in the mangrove ratio.

2.7.1. Validation of Mangrove to shrimp farm ratio map

To further investigate the reliability of the mangrove ratio computed considering the pixel-based classification was compared to a manual digitization of mangroves on shrimp farms performed by Julia Hogestijn (2023). A Geo Eye image captured in 2019 with a spatial resolution of 0.4 m was used by Julia Hogestijn to manually delineate the mangroves (Hogestijn, 2023). The manual mangrove mapping is also one of the methods applied by the Protection Forest Management Board, raising interest in comparison to the machine learning classification. The difference in the mangrove ratio based on the manual mangrove mapping with the Geo Eye image and the pixel-based SPOT-7 classification was calculated for 50 shrimp farms in the study area. For this comparison, it was assumed that the mangrove cover did not change significantly between 2019 and 2022. This comparison also investigated the effect of the satellite images' spatial resolution on the relative mangrove cover observed on the shrimp farms.

2.7.2. Farmers perception of mangrove cover

The mangrove ratios resulting from the object-based and pixel-based classification were compared to the estimates of the farmers that cultivate the respective shrimp farm. The statements of the shrimp farm owners' mangrove cover estimate based on the field survey performed by Prof. Dr. Vo and his colleagues from Can Tho University in 2022. One question of the performed survey focuses on the shrimp farmer's perception of the relative mangrove cover on the property in percent (Vo, 2022). This data was used to compare the farmers' estimates with the object-based and pixel-based computation. The purpose of the comparison was to examine the ability of farmers to assess and maintain the mandatory mangrove ratio on their property based on observation from the ground. The mangrove ratio based on the classification trained with the GTP training dataset that revealed the median values for the mangrove-specific accuracies, namely the mangrove class's Producer Accuracy (PA_m), mangrove class's User Accuracy (UA_m), and mangrove class's Kappa ($Kappa_m$), was used for the comparison. The accuracies investigated the reliability of the respective classification. Moreover, the accuracy assessment assured that robust mangrove ratios were used for the comparison that are representative for the ten classification replicates and not ratios resulting from a classification that achieved a maximum or minimum value in the investigated accuracies.

2.8. Expert interview

Prior to the expert interview, a questionnaire was prepared to gain insider knowledge on the currently applied mangrove monitoring practices in the study area. The questions were translated into Vietnamese with Google Translate and then shared with Thanh Loc who checked the Vietnamese questions for comprehensibility. After small adjustments, Prof. Dr. Vo Quoc Tuan forwarded the questionnaire to a technical manager that works for the Forest Protection Department of the Biển Tây (West Sea) Protection Forest Management Board. After the technical manager filled out the questionnaire, Prof. Dr. Vo and I held a Zoom meeting to elaborate on the questions and clarify the given responses. The digital meeting took place on the 14th of April 2023. Prof. Dr. Vo translated from Vietnamese to English and vice versa to enable the dialogue with the technical manager.

3. RESULTS

This section will start by giving an overview of the object-based and pixel-based classifications' performance in terms of accuracy to address the first research question (RQ1). The resulting land cover maps and maps indicating the relative mangrove cover on the shrimp farms in the protection forest, production forest and non-forest zone of the study area are going to be presented approach the second research question (RQ2). Moreover, the relative mangrove cover computed with both classification approaches will be compared to the estimates of shrimp farmers that live and work in the study area to answer the third research question (RQ3). To validate the results on farm level, the mangrove ratio estimated in this study is verified with a manual mangrove digitization.

3.1.   Ground Truth Points (GTPs)

Map 2 illustrates the GTPs that were sampled during the field survey on the 22nd and 23rd of March 2023 after checking for their quality.

Ground Truth Points (GTPs) in the study area's protection and production forest
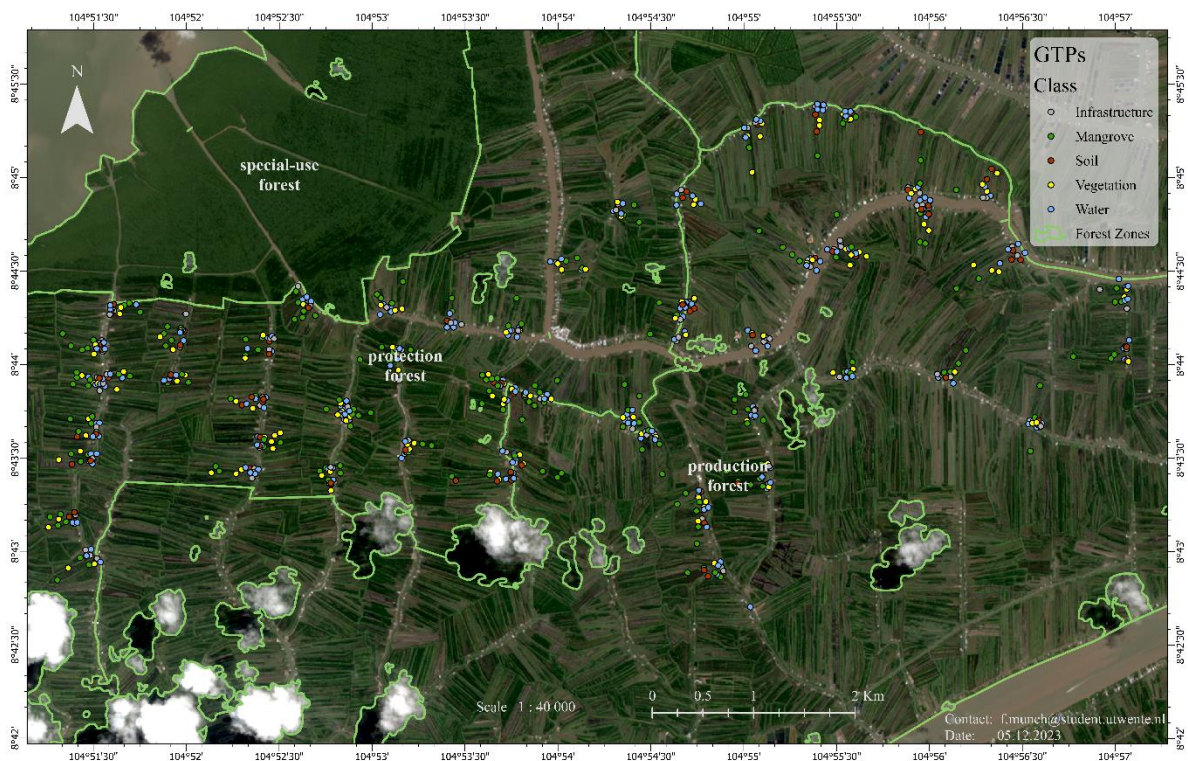
Map 2. Ground Truth Points (GTPs) in the study area's protection and production forest (Airbus, 2022).

In total 407 GTPs were sampled in the protection forest and 308 GTPs in the production forest (*Table 3*). The water class represents the largest group of GTPs (210) followed by the mangrove class with 187 GTPs. The 79 soil GTPs account for the smallest group of the sampled land cover GTPs.

Table 3. Count [n] of quality assessed Ground Truth Points (GTPs) in the production forest, protection forest, and entire study area per land cover class.

	Production forest GTPs [n]	Protection forest GTPs [n]	Total [n]
Mangrove	75	112	187
Water	88	122	210
Vegetation	57	74	131
Infrastructure	49	59	108
Soil	39	40	79
Total	308	407	715

3.2. Classifier comparison

This section compares a number of commonly used classifiers to select the most appropriate data, machine learning algorithm for the object-based and pixel-based approach.

The assessment of the classification test runs revealed that the Bayes, Random Forest, and Decision Tree classifiers resulted in highest accuracies in terms of the Kappa and Overall Accuracy (OA) as well as the Producer Accuracy (PA), User Accuracy (UA) and Kappa for the Mangrove class (*Table 4* & *Table 5*). *Figure 4* and *Figure 5* illustrate the result from the Bayes classifier using the available SPOT-7 spectral bands and the NDVI for the pixel-based and object-based approach. In terms of the mangrove-specific User Accuracy (UA_m), which indicates the reliability of the mangrove classification for the map user, this classifier and input data resulted in the highest values for both approaches (*Table 4* & *Table 5*). However, the residual mangrove-specific accuracies, mangrove Producer Accuracy (PA_m), and mangrove Kappa ($Kappa_m$) were not complemented that well by this classifier.
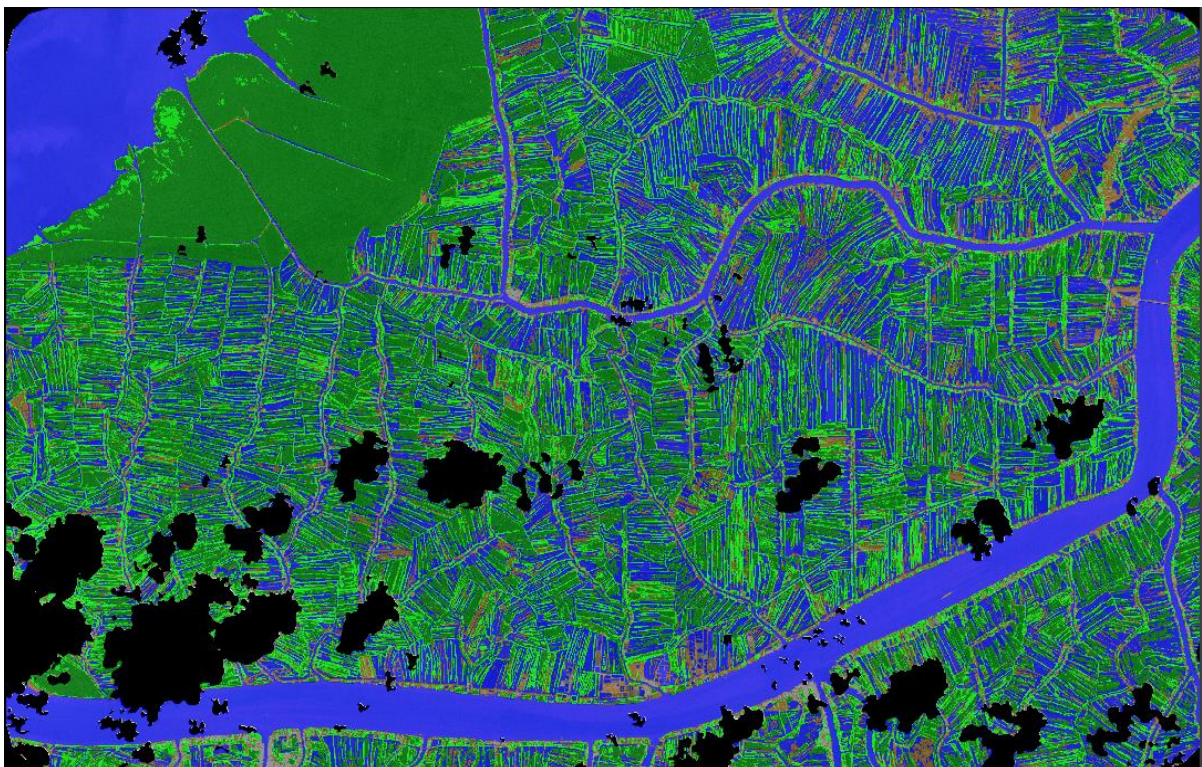
Figure 4. Classification results from the object-based Bayes classifier using the Red, Green, Blue, Near-Infrared, and NDVI layers as input data. Where the illustrated land cover classes represent water (blue), mangrove (dark green),

vegetation (light green), soil (brown), and infrastructure (grey). No data values are represented by black areas, which mainly relate to clouds and cloud shadows.
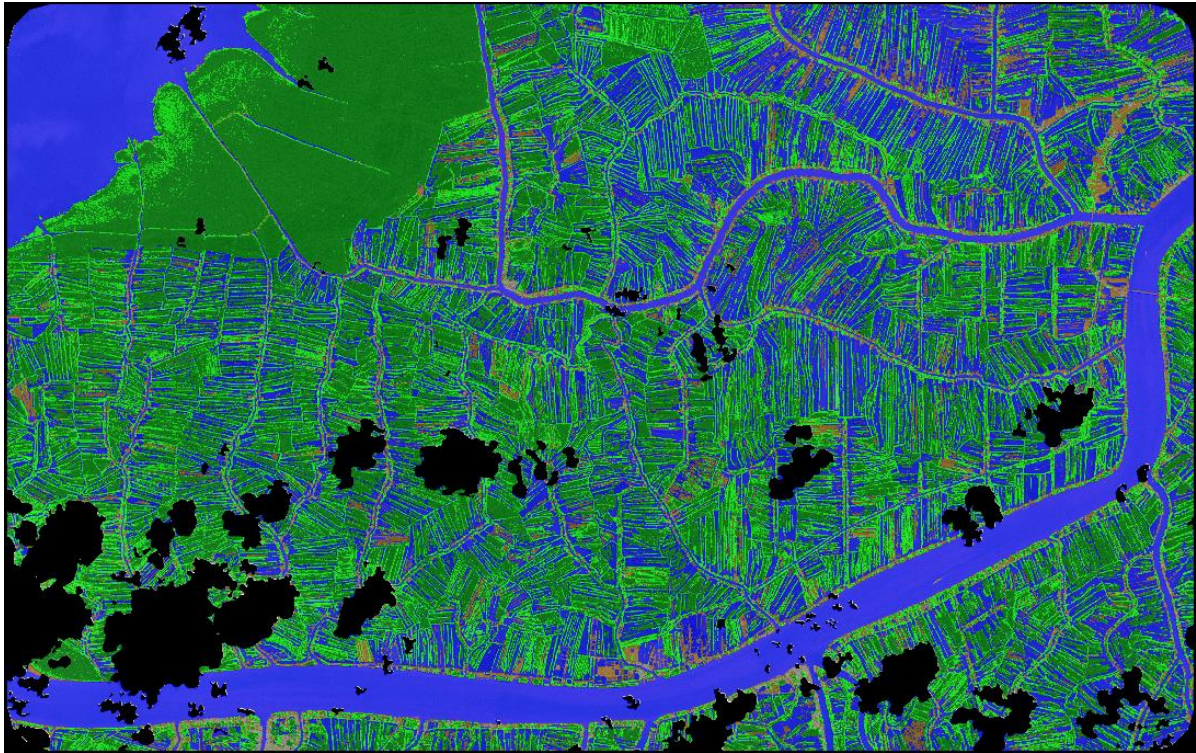
Figure 5. Classification results from the pixel-based Bayes classifier using the Red, Green, Blue, Near-Infrared, and NDVI layers as input data. Where the illustrated land cover classes represent water (blue), mangrove (dark green), vegetation (light green), soil (brown), and infrastructure (grey). No data values are represented by black areas, which mainly relate to clouds and cloud shadows.

Considering all three accuracies that specifically focus on the performance of the mangrove classification, the Random Forest algorithm performed the classification task well with balanced high values for the mangrove Producer Accuracy (PA_m), mangrove User Accuracy (UA_m), and mangrove Kappa ($Kappa_m$) (*Table 4* & *Table 5*).

The accuracy assessment of the three best-performing classifiers, Bayes, Random Forest (RF), and Decision Tree, displayed in *Table 4* and *Table 5* indicate that the mangrove classification performance given by the mangrove specific accuracies, mangrove Producer Accuracy (PA_m), mangrove User Accuracy (UA_m) and mangrove Kappa ($Kappa_m$), can improve the more input data was used. The classifiers using all available spectral bands of SPOT-7 as well as the NDVI and NDWI, resulted in high accuracies when assessing the mangrove-specific classification. This is less clearly indicated by the Overall Accuracy and the Kappa coefficient, which indicate the accuracy considering all land cover classes.

Table 4. Accuracy assessment comparison of object-based classifiers. The respective input data is defined in parentheses following the classifier name. RGB NIR represents the four SPOT-7 bands Red, Green, Blue and, Near-Infrared. NDVI: Normalized Difference Vegetation Index. NDWI: Normalized Difference Water Index. PA_m & UA_m represent mangrove-specific Producer and User Accuracy. $Kappa_m$: Kappa coefficient for the mangrove class. Accuracy considering all land cover classes is given by the Kappa and Overall Accuracy (OA).

Object-based classifier	PA_m [%]	UA_m [%]	$Kappa_m$	Kappa	OA [%]
Bayes (RGB NIR)	89.1	96.1	0.86	0.84	87.2
Random Forest (RGB NIR)	94.6	91.2	0.93	0.82	85.8
Decision Tree (RGB NIR)	89.1	92.5	0.85	0.77	82.0
Bayes (RGB NIR NDVI)	89.1	**98.0**	0.86	0.86	**89.1**
Random Forest (RGB NIR NDVI)	94.6	92.9	0.93	0.81	84.8
Decision Tree (RGB NIR NDVI)	89.1	94.2	0.86	0.76	81.0
Bayes (RGB NIR NDWI NDVI)	92.7	96.2	0.90	0.85	88.1
Random Forest (RGB NIR NDWI NDVI)	96.4	93.0	0.95	0.81	85.2
Decision Tree (RGB NIR NDWI NDVI)	96.4	94.6	0.95	0.79	83.8

Table 5. Accuracy assessment comparison of pixel-based classifiers. The respective input data is defined in parentheses following the classifier name. RGB NIR represents the four SPOT-7 bands Red, Green, Blue and, Near-Infrared. NDVI: Normalized Difference Vegetation Index. NDWI: Normalized Difference Water Index. PA_m & UA_m represent mangrove-specific Producer and User Accuracy. $Kappa_m$: Kappa coefficient for the mangrove class. Accuracy considering all land cover classes is given by the Kappa and Overall Accuracy (OA).

Pixel-based classifier	PA_m [%]	UA_m [%]	$Kappa_m$	Kappa	OA [%]
Bayes (RGB NIR)	94.6	96.3	0.93	0.88	90.6
Random Forest (RGB NIR)	94.6	92.9	0.93	0.84	87.3
Decision Tree (RGB NIR)	98.2	93.1	0.98	0.84	87.7
Bayes (RGB NIR NDVI)	94.6	**98.1**	0.93	0.89	**91.5**
Random Forest (RGB NIR NDVI)	94.6	94.6	0.93	0.85	88.2
Decision Tree (RGB NIR NDVI)	94.6	94.6	0.93	0.84	87.3
Bayes (RGB NIR NDWI NDVI)	96.4	96.4	0.95	0.87	90.1
Random Forest (RGB NIR NDWI NDVI)	96.4	93.0	0.95	0.87	89.6
Decision Tree (RGB NIR NDWI NDVI)	94.6	94.6	0.93	0.84	87.3

The smallest deviation of the mangrove class-specific accuracies is indicated for the object-based and pixel-based Random Forest classification, which used the SPOT-7 spectral bands as well as the NDVI and NDWI as input data (*Table 4* & *Table 5*). The other investigated classifiers indicated different mangrove Producer Accuracies, mangrove User Accuracies, and mangrove Kappas for the object-based and pixel-based approach. Moreover, this specific Random Forest classifier and input data represent some of the highest mangrove class-specific accuracies for both approaches.

3.3. Accuracy Assessments

This section presents the replicated accuracy assessment using the ten individual training and validation GTP replicates for the object-based and pixel-based Random Forest classifications. Consequently, this section addresses the first research objective (RO1) and question (RQ1). Furthermore, the accuracy assessment indicates which classification is used to create a land cover map of the study area.

3.3.1. Object-based classification

This section presents the results of the replicated accuracy assessment for the object-based Random Forest classification. *Figure 6* illustrates boxplots on the replicated accuracies and *Figure 7* displays boxplots on the replicated Kappa indices. For visualization purposes the accuracies are presented in the range from 75 to 100% and the Kappa indices in the range from 0.75 to 1 instead of presenting the entire value range from 0 to 100% and -1 to 1 respectively.

Regarding the mangrove-specific accuracies and Kappa, *Figure 6* and *Figure 7* illustrate that the maximum of the Producer mangrove accuracy (PA_m) peaked at 100% and the maximum of the mangrove Kappa at 1. Both represent the absolute maximum value that can be achieved and result from the classification using the seventh GTP training and validation dataset. The second highest PA_m of 98% and $Kappa_m$ of 0.97 were computed for the classification performed with the fifth GTP training and validation dataset. Whereas the mangrove-specific User Accuracy (UA_m) performed best with 93% using the sixth training and validation GTP for the classification. Both the maximum Overall Accuracy (OA) of 89% and the maximum Kappa of 85% were calculated for the classification using the third GTP dataset. In contrast, the classification based on the fourth GTP training and validation data revealed the minimum for the mangrove-specific Producer Accuracy (84%) and Kappa (0.78). Both minima were indicated as outliers. The second lowest PA_m and $Kappa_m$ are 92% and 0.9 respectively. The difference between the PA_m and $Kappa_m$ minimum, represented by the outliers, and the maximum resulted in a considerably larger range for both accuracies. PA_m presented a range of 16%. $Kappa_m$ spanned a range of 0.22. The UA_m performed worst with a minimum of 85% considering the second GTP replicate for the classification, indicating a UA_m range of 7%. The minimum for both the Overall Accuracy (83%) and Kappa (0.78) resulted from the classification that utilized the ninth GTP training and validation dataset. Concerning the mangrove-specific accuracies UA_m indicated the lowest median value of 89%. The median calculation of $Kappa_m$ and PA_m, considering the values of all ten individual GTP replicates, resulted in 0.93 and 95% respectively. Whereas the median of the generic accuracies, indicating the performance in respect of all land cover classes, was 0.81 for the Kappa and 85% for the Overall Accuracy.

Figure 6. Boxplots on the accuracies of the replicated object-based classification using Random Forest. Where PA_m represents the mangrove-specific Producer Accuracy in percent, UA_m represents the mangrove-specific User Accuracy in percent, OA represents the Overall Accuracy in percent.
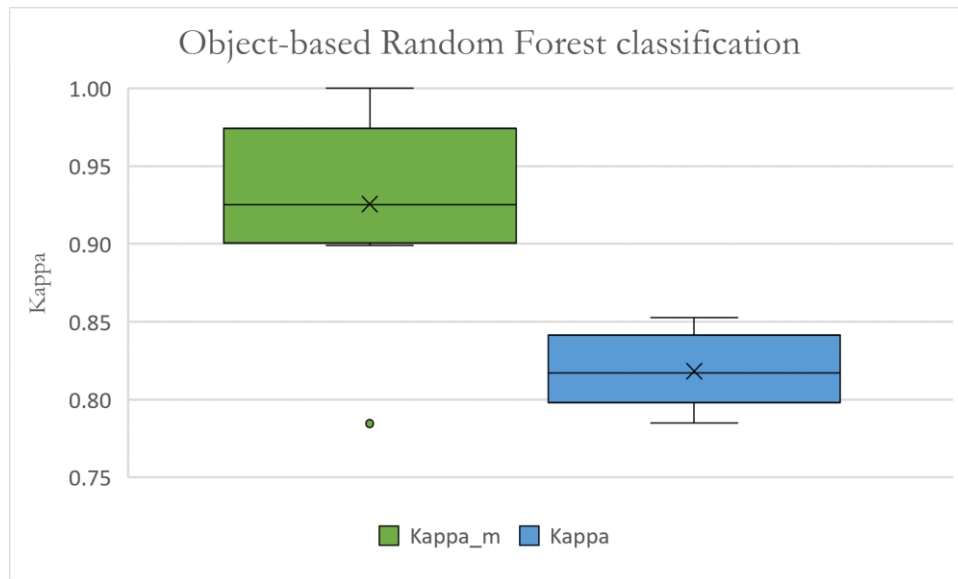
Figure 7. Boxplots on the Kappa of the replicated object-based classification using Random Forest. Where Kappa_m represents the mangrove-specific Kappa, Kappa represents the Kappa index.

3.3.2. Pixel-based classification

In this section, the results for the accuracy assessment of the replicated pixel-based Random Forest classifications are presented. *Figure 8* visualizes the boxplots of the replicated accuracies and *Figure 9* illustrates the replicated Kappa. For visualization and comparability purposes the value range is displayed as for the object-based counterparts (*Figure 6* & *Figure 7*).

Concerning the pixel-based classifications, all three mangrove specific accuracies indicated mean and median values greater than 90%. *Figure 8* illustrates that the median PA_m and UA_m were 95% and 91% respectively, whereas the $Kappa_m$ was 0.93 (*Figure 9*). The maximum values for the mangrove-specific accuracies, with 98% mangrove Producer Accuracy, 93% mangrove User Accuracy, and a value of 0.98 for the mangrove-specific Kappa, were achieved using the second GTP training and validation replicate for the pixel-based approach. The minimum value of 91% for the mangrove-specific Producer accuracy and 0.88 for the mangrove-specific Kappa resulted from the fifth GTP dataset and were marked as outliers. $Kappa_m$ indicated the largest value range of 0.1 from the maximum of 0.98 to the minimum of 0.88.

Regarding the accuracies that consider all land cover classes, the maximum for the Overall Accuracy (OA) and Kappa of 89% and 0.86 was computed using the fourth GTP replicate (*Figure 8* & *Figure 9*). Whereas the eighth GTP training and validation replicate dataset resulted in a minimum Overall Accuracy (OA) of 86% and minimum Kappa of 0.82. The OA presented the smallest value range of 3% from maximum to minimum with a median of 87.5%. The Kappa indices were distributed around the median of 0.84 within a range of 0.4.
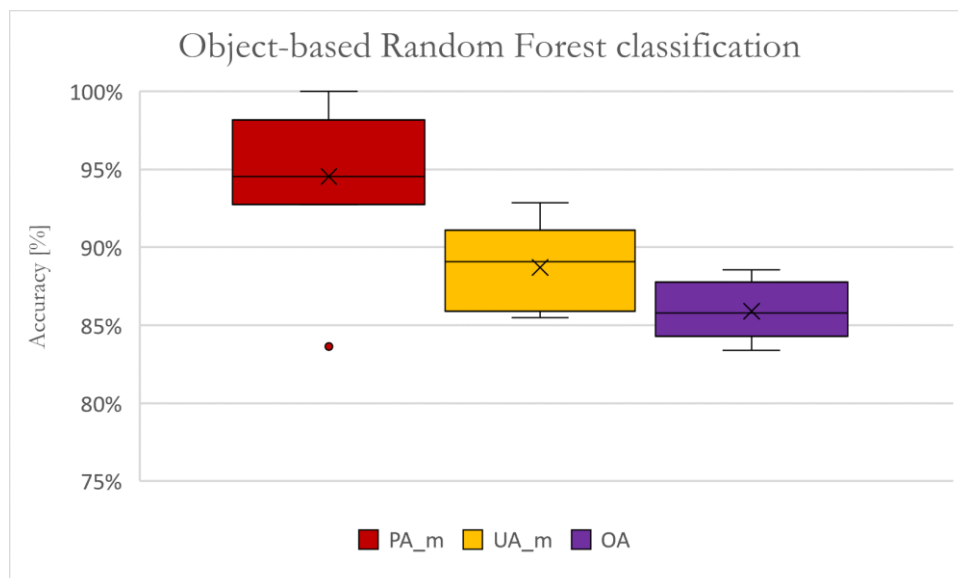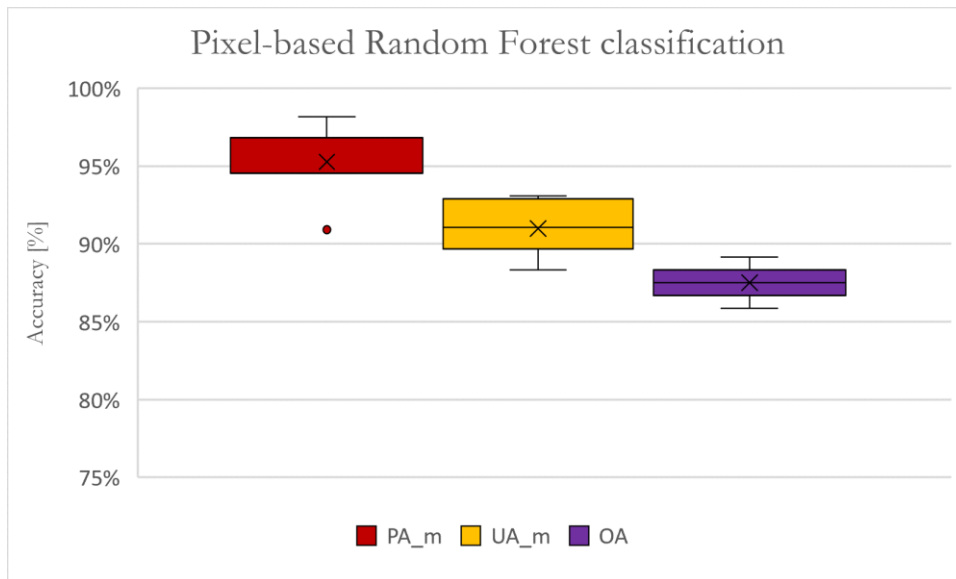
Figure 8. Boxplots on the accuracies of the replicated pixel-based classification using Random Forest. Where PA_m represents the mangrove-specific Producer Accuracy in percent, UA_m represents the mangrove-specific User Accuracy in percent, OA represents the Overall Accuracy in percent.
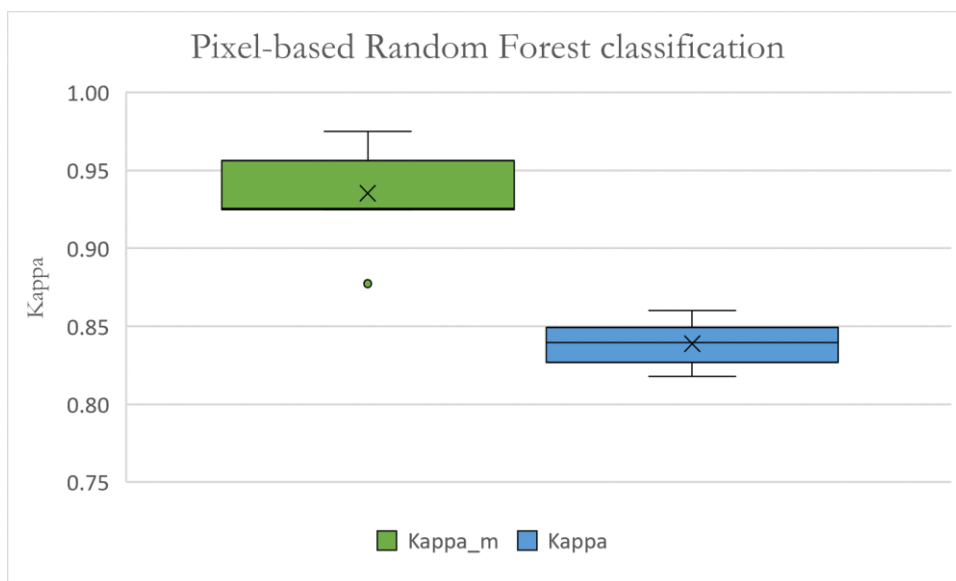
Figure 9. Boxplots on the Kappa of the replicated pixel-based classification using Random Forest. Where Kappa_m represents the mangrove-specific Kappa, Kappa represents the Kappa index.

3.3.3. Comparison of object-based and pixel-based classification

The replicates of the object- and pixel-based classifications that map two classes, one mangrove class and a non-mangrove class for all other land covers, indicated a median overall accuracy (OA) of 95.5% for the object-based and 96.2% for the pixel-based maps (*Figure 10*). The object-based OA ranged from a minimum of 93% to a maximum of about 96.6% and the pixel-based OA from a minimum of 95% to a maximum of 97.6%. The value range of both approaches varied by 0.91 percent. Also, the interquartile range of the pixel-based OA was 0.27% smaller than for the object-based approach.
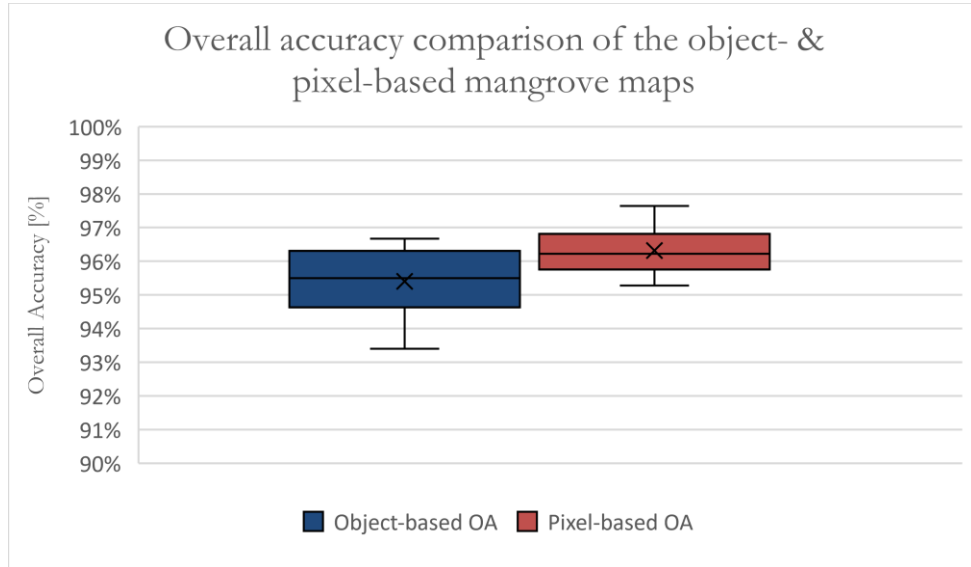
Figure 10. Overall accuracy comparison of the object- & pixel-based mangrove maps using the Random Forest classifier.

According to the McNemar test, all investigated object-based and pixel-based classification pairs resulted in x^2 values below the significance threshold of 3.84 (*Table 6*). Therefore, the null hypothesis (H_0) was accepted, which indicates that there is no difference in the classification of GTPs by the object-based and pixel-based approach. The comparison of the object- and pixel-based classification for the three training and validation datasets $GTPs_4$, $GTPs_5$, and $GTPs_6$ resulted in the minimum x^2 value of 0. The maximum x^2 value of 1.939 was computed using the $GTPs_{10}$ training dataset for the classification and the $GTPs_{10}$ validation dataset for the accuracy assessment indicating correctly and erroneously classified objects or pixels.

Table 6. Results of all land cover classes McNemar test for the ten GTP replicates. n_{op}: number of GTPs misclassified by the OBIA that were correctly classified by the pixel-based classification. n_{po}: number of GTPs misclassified by the pixel-based classification that were correctly classified by the OBIA. x^2 represents the calculated result of the McNemar test that indicates a statistically significant difference if x^2 is greater than 3.84 at a 95% confidence interval.

	$GTPs_1$	$GTPs_2$	$GTPs_3$	$GTPs_4$	$GTPs_5$	$GTPs_6$	$GTPs_7$	$GTPs_8$	$GTPs_9$	$GTPs_{10}$
n_{op}	9	7	14	15	12	9	15	8	8	21
n_{po}	15	12	10	14	13	10	17	10	6	12
x^2	1.042	0.842	0.375	0.000	0.000	0.000	0.031	0.056	0.071	1.939

The results of the McNemar test that specifically focused on the classification performance of the mangrove land cover class are presented in *Table 7*. All mangrove specific x^2 values were below the significance threshold of 3.84. This led to the acceptance of the null hypothesis (H_0). Accordingly, there was no statistically significant difference in terms of the mangrove misclassification for the investigated object-based and pixel-based classifier considering the ten utilized GTP datasets. The classifications using the $GTPs_3$, $GTPs_5$, $GTPs_8$ and $GTPs_9$ dataset indicated the minimum x^2 values of 0. In contrast, the maximum x^2 value of 2.25 was computed using the $GTPs_6$ training and validation dataset. In this case, four mangrove GTPs were misclassified by the pixel-based classification that were correctly classified by the object-based classification. Whereas the object-based classification misclassified none of the mangrove GTPs.

Table 7. Results of the mangrove-specific McNemar test for the ten GTP replicates. n_{op}: number of GTPs misclassified by the OBIA that were correctly classified by the pixel-based classification. n_{po}: number of GTPs misclassified by the pixel-based classification that were correctly classified by the OBIA. x^2 represents the calculated result of the mangrove-specific McNemar test that indicates a statistically significant difference if x^2 is greater than 3.84 at a 95% confidence interval.

	GTPs$_1$	GTPs$_2$	GTPs$_3$	GTPs$_4$	GTPs$_5$	GTPs$_6$	GTPs$_7$	GTPs$_8$	GTPs$_9$	GTPs$_{10}$
n_{op}	0	3	4	4	2	0	5	0	2	5
n_{po}	2	3	3	1	1	4	2	1	1	1
x^2	0.500	0.167	0.000	0.800	0.000	2.250	0.571	0.000	0.000	1.500

Table 9 illustrates that the water and mangrove class present the smallest differences with 0.7% for the average of the object-based and pixel-based Producer Accuracies. Whereas the infrastructure average Producer Accuracy presents the maximum difference (3.9%) from the object-based to the pixel-based classification but the minimum difference for the average User Accuracy (0.5%). Comparing both approaches the soil User Accuracy achieved the maximum difference of 2.8%. Accordingly, the differences between both classification approaches' average Producer and User Accuracy for the respective land cover classes ranged below 4%. Both classification approaches indicated the soil class to have the minimum Producer and User Accuracy (*Table 9*).

Table 8. Class specific average Producer and User Accuracy for the pixel-based and object-based approach according to the ten individual replicated classifications.

	Accuracy	Water	Infrastructure	Soil	Vegetation	Mangrove
Pixel	Producer Accuracy [%]	92.1	96.3	**58.8**	79.5	95.3
Based	User Accuracy [%]	91.9	92.5	**64.0**	85.2	91.0
Object	Producer Accuracy [%]	91.4	92.4	**56.8**	78.7	94.6
Based	User Accuracy [%]	91.0	93.0	**61.2**	83.4	88.7

3.4. Land cover and relative mangrove area per forest zone

This section presents the respective land cover map resulting from the object-based and pixel-based classification to compare both approaches via visual inspection (RO1). Additionally, the ratio of mangrove to non-mangrove land cover within the forest zones in the study area is indicated on the maps to address RO2 and RQ2.

3.4.1. Object-based forest zone mangrove ratios

The computation and illustration of the relative mangrove area in the study area's forest zones in *Map 3* indicates that the special-use forest presented the maximum overall mangrove ratio with 93% of its area being covered by mangroves. In the protection forest 48% overall mangrove cover prevailed. The mangrove class was the predominant land cover in the special-use and protection forest. Whereas a mangrove ratio of 33% was present in the production forest. In this forest zone water, covering 40% of the area, was the major land cover class. An area, that is not a forest zone is located in the north-east of *Map 3*. This no forest zone hosted a mangrove cover of 20%, which was the minimum mangrove ratio for the investigated zones. The cluster of the shrimp farms with a higher mangrove ratio in the north of the no forest zone at about 104°55' East was noteworthy since it substantially contributes to this zone's

relative mangrove cover of 20%. Most of the non-forest zone was covered by water, which accounts for 52% of the area.

Object-based relative mangrove area per forest zone
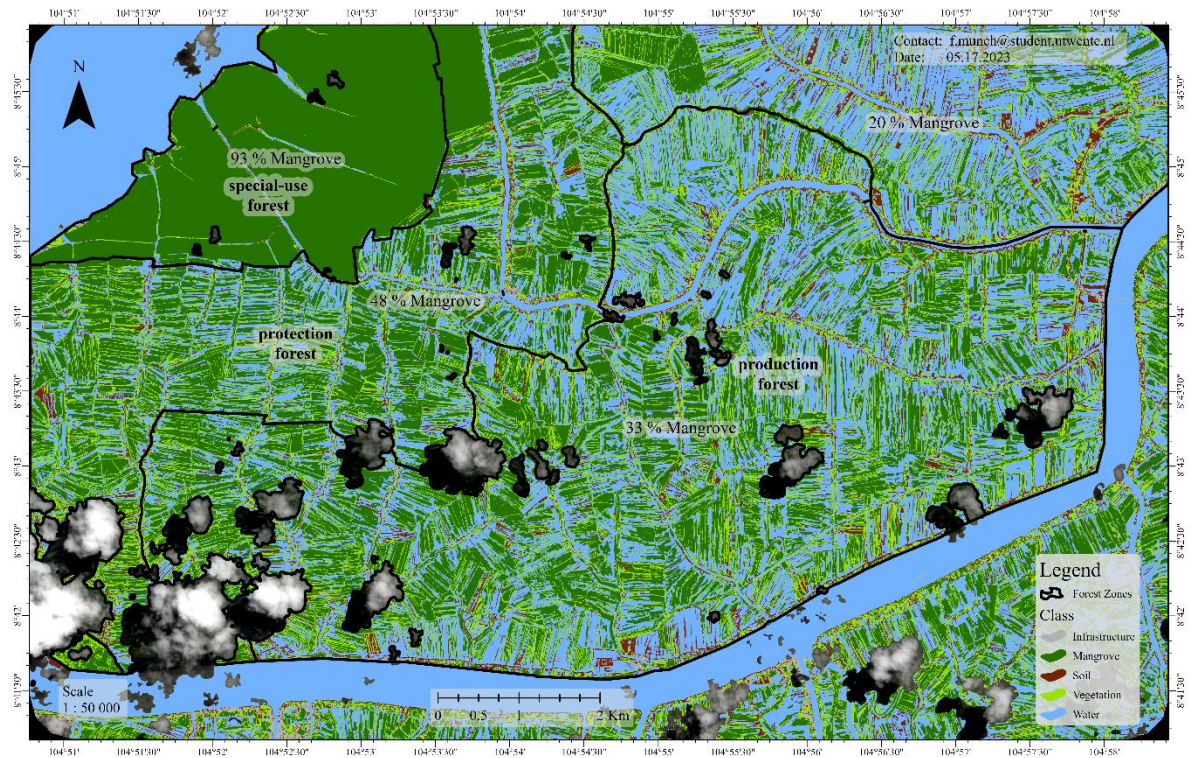
Map 3. Object-based land cover classification and the relative mangrove area per forest zone in percent. The SPOT-7 image serves as background to illustrate the neglected cloud and cloud shadow-covered areas (Airbus, 2022).

3.4.2.   Pixel-based forest zone mangrove ratios

The land cover map, resulting from the pixel-based classification, illustrated in *Map 4* indicates the maximum mangrove ratio of 93% in the special-use forest. Mangroves were also the dominant land cover in the protection forest, where 48% of the area was covered by this class. In the production forest mangroves accounted for 33% of the area. Water covered 41% of the production forest, making it the main land cover class in this zone. In comparison to the other zones, the minimum mangrove ratio of 20% was present in the non-forest zone. Water also represented the dominant land cover class in the non-forest zone, covering 52% of the area.

Pixel-based relative mangrove area per forest zone

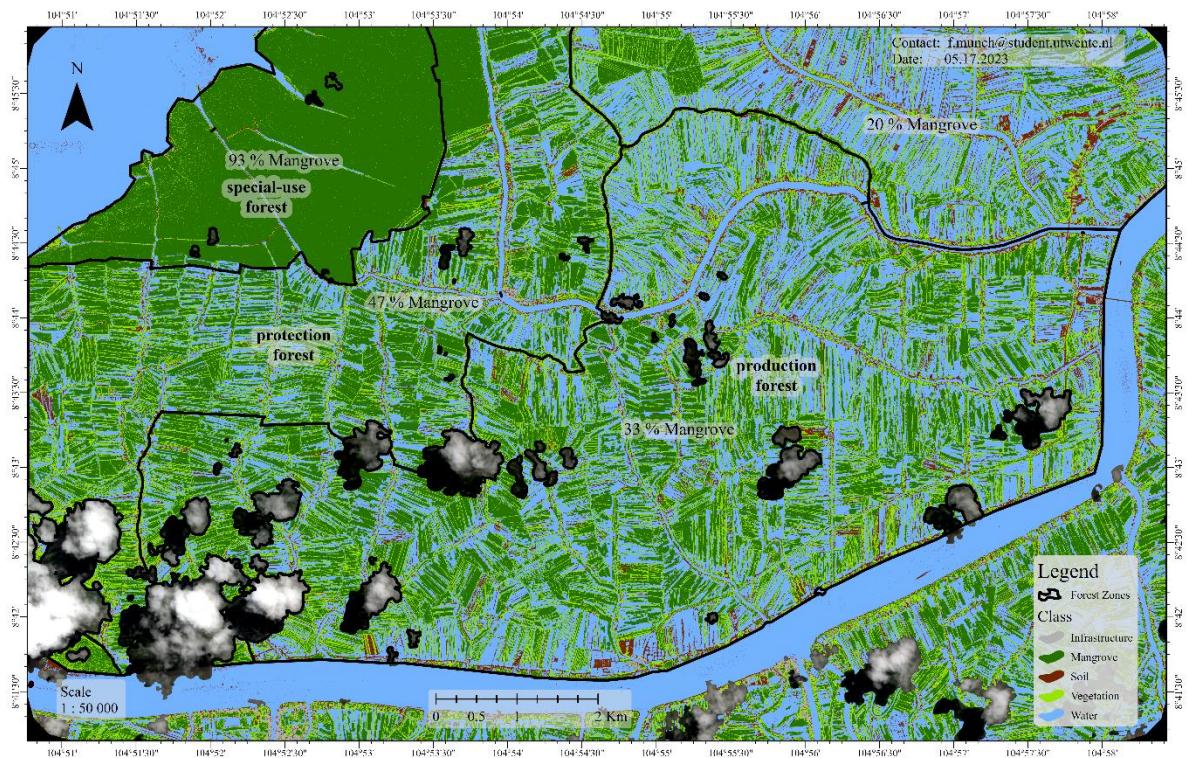Map 4. Pixel-based land cover classification and the relative mangrove area per forest zone in percent. The SPOT-7 image serves as a background to illustrate the neglected cloud and cloud shadow-covered areas (Airbus, 2022).

3.4.3. Subset comparison

In this section, subsets of the land cover map as well as the binary mangrove-non-mangrove map are presented to visually inspect and compare the results of the object-based and pixel-based classification according to the first research objective (RO1).

A subset covering the intersection of the protection and production forest as well as a non-forest area, is illustrated in *Map 5*. This map facilitates the comparison of both the object-based and pixel-based classification with the pan-sharpened SPOT-7 image. The classifications display similar results in the observed subset. However, fine differences exist.

The classification of the pixel-based approach illustrates the land cover in a more pixelated or grainier manner than the object-based classification. This salt and pepper effect can be observed for the pixel-based classification. For instance, in the north of the subset, the mangrove area appeared heterogeneous with vegetation pixels interrupting the mangrove canopy. Whereas the object-based classification indicated more homogeneous rows of mangroves. The pixel-based salt and pepper effect as well as the more homogeneous object-based representation, was also valid for the other land cover classes. This is exemplified by the soil in the southeast of the production forest in *Map 5*. The rows of bare soil in the shrimp pond were displayed with fine lines of soil pixels, whereas the object-based approach depicted one continuous water area.
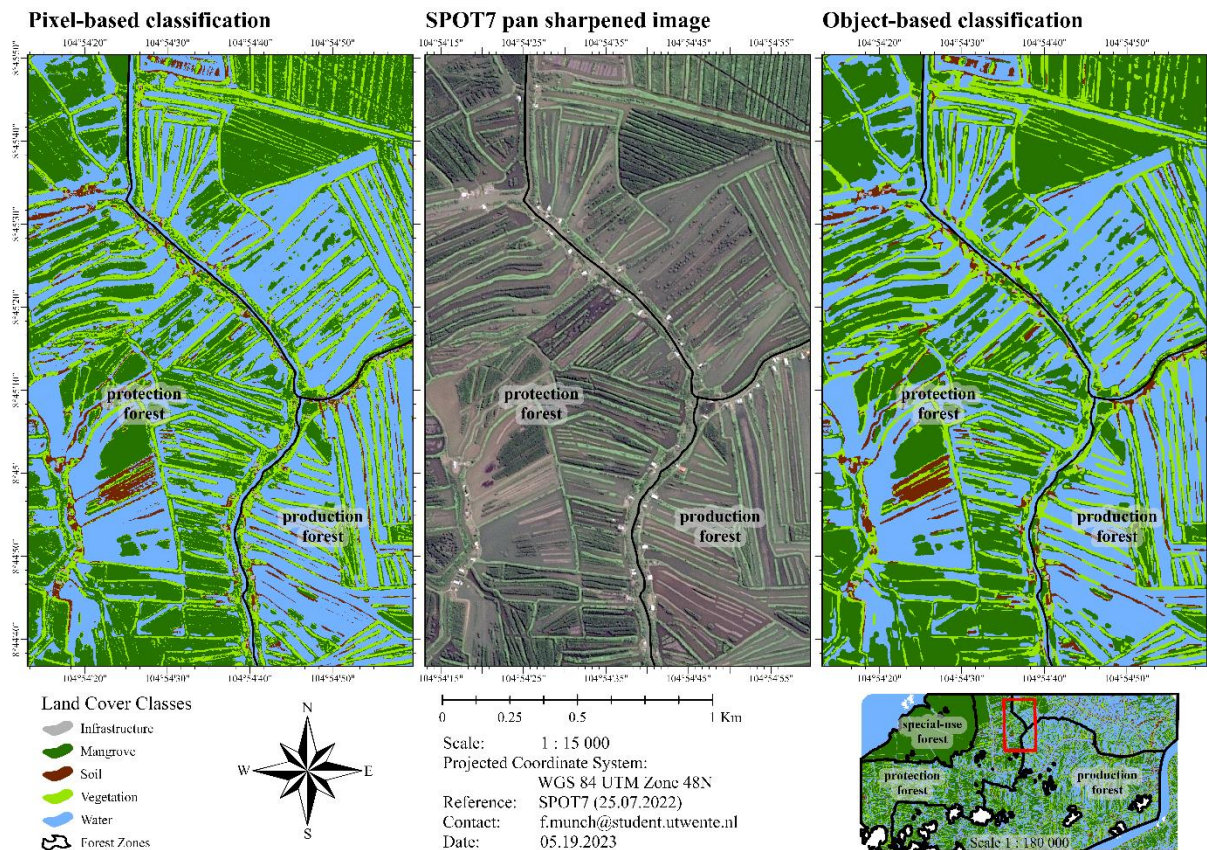
Map 5. Comparison of the pixel-based and object-based classification as well as the pan-sharpened SPOT-7 image for a subset covering the protection and production forest (Airbus, 2022).

Map 6 illustrates the difference between the object-based and pixel-based mangrove map. Blue indicates a total area of 465 ha, which represents spaces that were classified as mangrove by the object-based but not by the pixel-based mangrove map. Conversely, the red indicated patches, that sum up to an area of 412 ha, outline mangroves depicted by the pixel-based map that were not represented as mangrove by the object-based mangrove map. Accordingly, disagreement between the pixel-based and object-based approach in *Map 6* is mainly observed at the boundary of the mangrove cover. The transition from mangrove to another land cover like water, vegetation, or soil is represented differently for the investigated approaches. Moreover, differences can be observed for small patches and narrow rows of mangroves. This indicates the representation as mangrove by one and the neglection by the other approach. Mangrove stands that are presented as one continuous patch by the object-based classification tend to be interrupted by vegetation pixels and clusters in the pixel-based mangrove map. This grainier representation of mangrove stands and canopies can be seen in the mangrove cover maps as well as the difference map (*Map 6*).
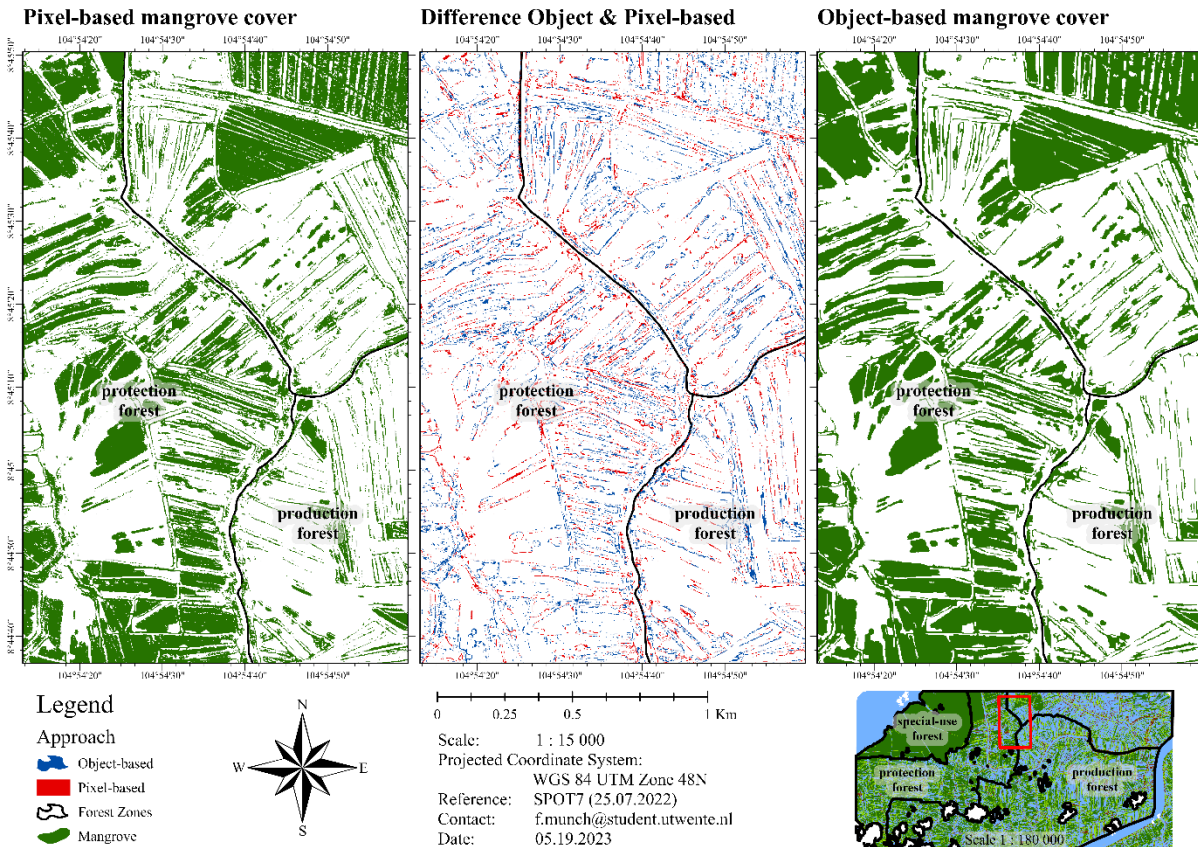
Map 6. Comparison of the pixel-based and object-based mangrove cover for a subset covering the protection and production forest. Where blue indicated areas represent spaces that were classified as mangrove by the object-based but not by the pixel-based mangrove map. Red demonstrates patches that were indicated as mangrove by the pixel-based map that were not depicted as mangrove by the object-based map.

3.5.   Mangrove to shrimp farm ratio maps

In this section, the land cover map is used to estimate the relative mangrove area on the study area's shrimp farms. Consequently, the forest management's effect on the shrimp farms' mangrove ratio in the observed forest zones is investigated to account for the second research objective and question (RO2 & RQ2). The ratio of mangrove to non-mangrove land cover on the shrimp farms was mapped to indicate farmers that achieve 60% mangrove conservation on their property. Moreover, shrimp farms that have a relative mangrove area ranging within the mangrove classification's error margin were illustrated to closer investigate if the properties' mangrove ratio is above or below the threshold. Also, shrimp farms that presented less than 60% mangrove cover were displayed to locate properties that are suitable for the replantation of mangrove saplings. Finally, the farmer's perception of the mangrove cover was compared to the classification estimates to answer the third research objective and question (RO3 & RQ3).

3.5.1.   Shrimp farm mangrove ratio mapping

In total, there were 1,677 shrimp farms with an area greater than 1 ha present in the study area. *Map 7* and *Map 9* represent the object-based and pixel-based mangrove ratio maps of the investigated shrimp farms. The visual comparison of the maps as well as *Table 12*, indicate that both maps are identical. *Map 7* illustrates 33 red-indicated shrimp farms that have less than 1% mangrove cover. These shrimp farms were distributed in different forest zones. The majority of 20 shrimp farms with less than 1% mangrove cover were located in the production forest zone, which was the largest zone covering 43,757 km² of the study area (*Table 11*). The protection forest zone covered 21,116 km² of the study area and hosted 2

shrimp farms that had a mangrove ratio of less than 1%. In the non-forest zone about 11,474 km² were covered by shrimp farms of which 11 presented a mangrove cover of less than 1%. Relative to its area the non-forest zone revealed the most frequent occurrence of 0.96 n/km² shrimp farms per square kilometer with a mangrove to shrimp farm ratio of less than 1%, followed by the production forest with 0.43 n/km² (*Table 11*). In the protection forest 125 and in the production forest 118 shrimp farms had a mangrove to shrimp farm ratio ranging from 64 to 99% relative mangrove cover. The area of the observed protection forest was about half the size of the production forest. Therefore, 5.87 n/km² shrimp farms per square kilometer of protection forest conserved the required relative mangrove cover on the property, whereas it was 2.86 n/km² in the production forest.

Pixel-based mangrove to shrimp farm ratio
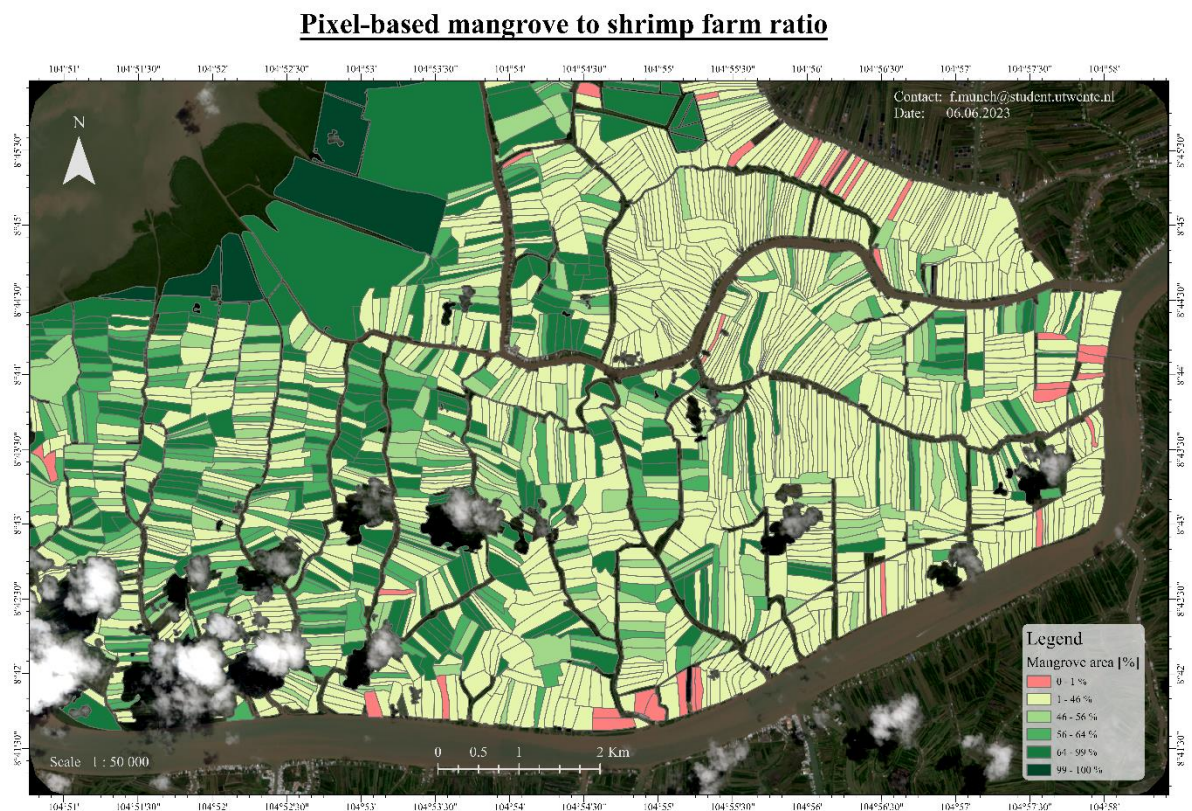
Map 7. Relative mangrove area on the shrimp farms in percent according to the pixel-based classification (Airbus, 2022).

In the special-use forest zone, seven properties with a mangrove cover exceeding 99% were indicated in the darkest shade of green (*Map 7*). It was the only zone with properties that achieved that high relative mangrove cover. Shrimp farms with a relative mangrove area between 46 and 56%, indicated in light green, potentially are eligible to apply for an eco-label certificate in terms of achieving the necessary 50% mangrove ratio. The class labeled with 56 to 64% represented the transition from not complying to complying with the regulation of 60% relative mangrove cover. The percentage range of this class is based on the consideration of the 4% error margin for the mangrove classification. It avoided including (false negatives) falsely neglected and exclude (false positives) falsely considered shrimp farms from the 64 to 99% class, which included all properties that achieved the regulation of 60% mangrove cover.

Table 9 displays that 25% of the shrimp farms in the protection forest achieved a relative mangrove coverage greater than 64%, complying with the regulation of 60% considering the 4% error margin, followed by 11% and 7% of the respective shrimp farms in the production forest and no forest zone. In

the protection forest, 14% were in the transition class of 56 to 64% relative mangrove cover, which was defined by the 4% error margin. 9% of the shrimp farms in the production forest and 1% of the shrimp farms outside of the forest zones were part of the 56 to 64% mangrove ratio class. Outside of the forest zones, 92% of the shrimp farms had a relative mangrove cover of less than 56%. Whereas 80% of the shrimp farms within the production forest and 62% within the protection forest had a mangrove ratio below 56%.

Table 9. The percentage of shrimp farms in the respective forest zone that have a relative mangrove cover of less than 56%, between 56 and 64%, and greater than 64%.

Forest Zone	Area [km²]	Shrimp farms [n]	< 56 % mangrove cover	56 to 64 % mangrove cover	> 64 % mangrove cover
Protection forest	21,116	505	62%	14%	25%
Production forest	43,757	1036	80%	9%	11%
Not forestry	11,477	136	92%	1%	7%
Total	76,350	1677	75%	10%	16%

Since the shrimp farm mangrove ratios indicated by the pixel-based *Map 7* and object-based *Map 9* are identical, the presented results on the relative mangrove cover on the shrimp farms in the different forest zones, that base on *Table 9* and *Table 11*, are applicable for both the object-based and the pixel-based approach.

The p-values derived from the Mann-Whitney U test, comparing the protection with the production forest zone, protection with the non-forest zone, and the production with the non-forest zone, were lower than the 0.05 significance level (2.45^{-30}, 6.08^{-53}, 3.6^{-29}). This means that the null hypothesis (H_0) was rejected and that there is a difference in the mangrove ratios on shrimp farms in the protection, production, and non-forest zone.

3.5.2. Mangrove ratio validation

Julia Hogestijn manually digitized mangroves on 50 randomly selected shrimp farms in the study area using a Geo Eye image that was captured with a spatial resolution of 0.4 m in 2019 (Hogestijn, 2023). The comparison of the relative mangrove cover % estimates based on the 2019 Geo Eye and 2022 SPOT-7 image is displayed in *Figure 11*. A median and mean difference of 21% and 18% between the mangrove ratio estimates of the two images was found. The extrema indicate differences of -63% and 54% respectively (*Figure 11*). The difference between four out of the 50 investigated shrimp farms were indicated to be outliers.
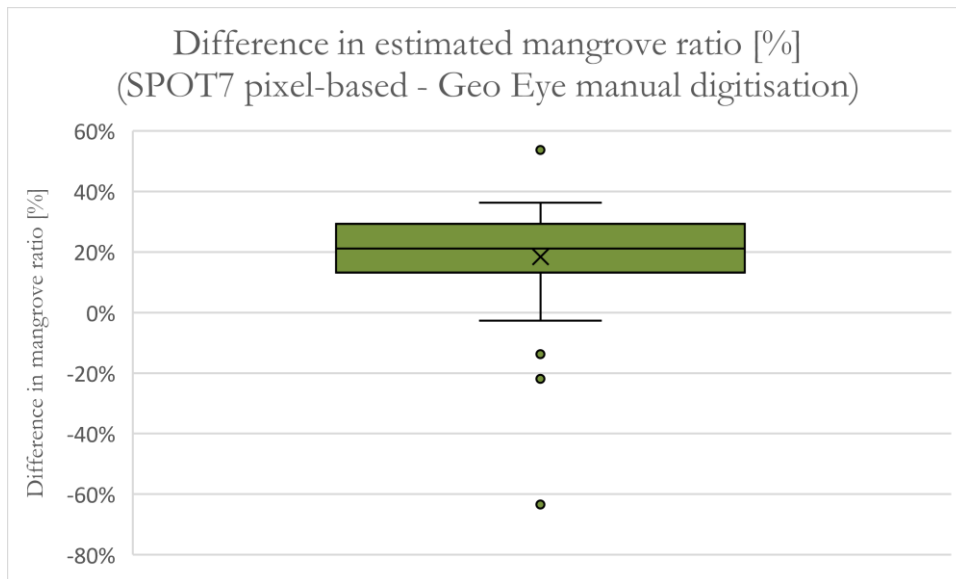
Figure 11. The difference in estimated mangrove ratio [%] calculated by subtracting the area of the manually digitized mangroves of the Geo Eye 2019 image from the pixel-based SPOT-7 2022 mangrove map.

Map 8 illustrates the difference in mangrove cover between the Geo Eye and the SPOT-7 approach with four subsets. Subset A displays a larger mangrove area given by SPOT-7 than by Geo Eye, representing the shrimp farm with the maximum difference of 54% mangrove cover. In contrast, subset B presents a larger mangrove area given by Geo Eye compared to SPOT-7. This subset represents the shrimp farm with the maximum negative difference of -63%.

Map 8. Subsets of the study area comparing mangrove cover based on the Geo Eye and SPOT-7 satellite image. The letter in the upper left corner of each subset acts as an identifier. Where subset A displays reforestation. Subset B displays deforestation. Subset C shows mangrove area estimates on shrimp farms that are close to the calculated

median difference. Subset D presents mangrove rows for the Geo Eye and mangrove patches for the SPOT-7 image.

Subset C of *Map 8* indicates shrimp farms that were indicated by Geo Eye and SPOT-7 to have a relative mangrove cover differing by 23% and 16%, which is close to the median and mean values presented in *Figure 11*. At last subset D illustrates the mangroves mapped with Geo Eye organized as rows, whereas they appear to be one big mangrove patch considering the SPOT-7 classification (*Map 8*). This led to a difference of 33% and 31% between the mangrove ratio estimates for the two shrimp farms observed in subset D.

3.5.3. Farmers perception mangrove ratio

The mangrove ratio computation from the object-based and pixel-based classification was compared to the estimation of shrimp farmers. Several questions from a survey conducted by Vo Quoc Tuan in 2022 focused on the ratio of different land cover classes on shrimp farms in the Cà Mau province. Eleven of the surveyed shrimp farms were fully covered by the SPOT-7 image that was used in this study. The farmer's estimate of these shrimp farms was compared to the relative mangrove cover quantification of the object-based and pixel-based classification. In *Figure 12* the statements concerning the relative mangrove area on the property of the interviewed shrimp farmers are indicated with green bars. The mangrove ratio estimates for shrimp farm number four are similar with 60% estimated by the shrimp farmer, 63% by the object-based, and 60% by the pixel-based approach. This farm displayed the minimum difference between the investigated estimates. The maximum difference was found for shrimp farm three, ten, and eleven, where the owners estimated more mangrove cover than what was computed using the classifications. In contrast, the owner of shrimp farm seven estimated his property to have less mangrove cover than the SPOT-7 mangrove ratio indicates. The owners of shrimp farms one, four, and six stated to have a mangrove ratio of about 60% on their property. This estimate was verified by the classifications. The maximum mangrove cover of 68% was estimated by shrimp farmer number two. This did not correspond with the object-based and pixel-based estimates, which both indicated a mangrove cover of 49%.
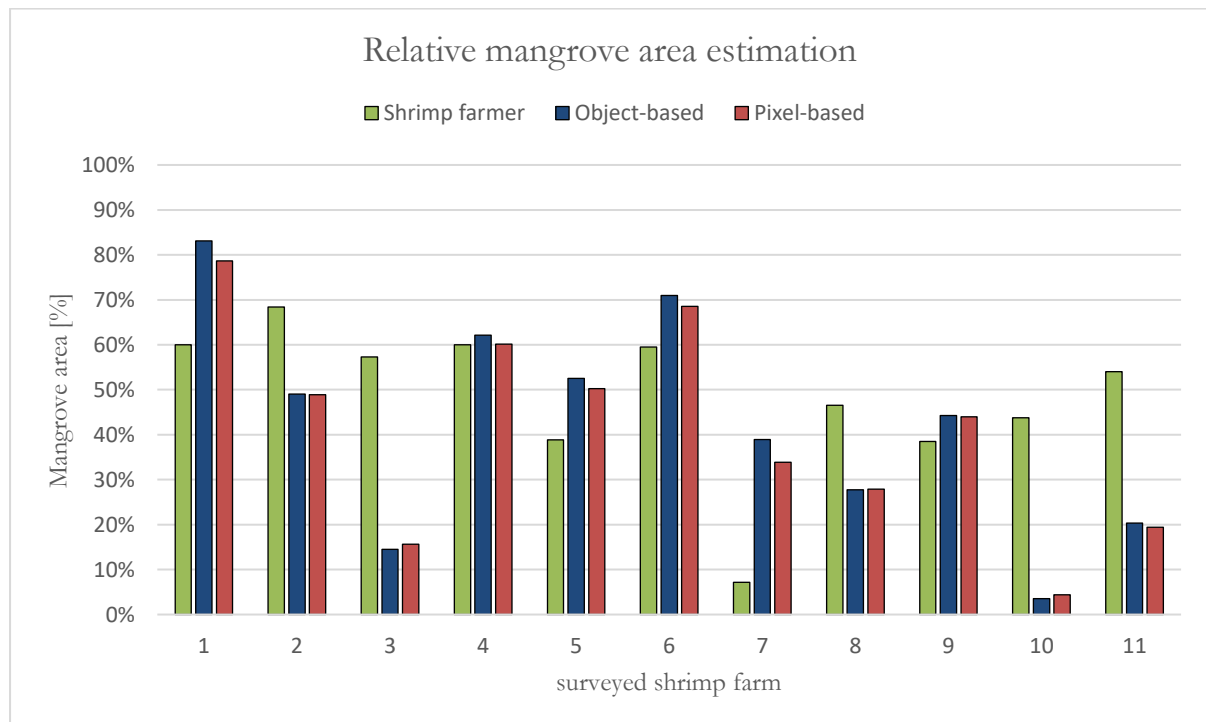
Figure 12. Comparison of the relative mangrove area estimated by shrimp farmers (green), object-based (blue), and pixel-based (red) classification.

Considering the 4% Overall Accuracy computed for the mangrove and non-mangrove class, an error margin of ± 4% from the used median relative mangrove area quantification was applicable for the object-based and pixel-based classification. In this case, shrimp farm one and six exceeded the 60% mangrove threshold even if the error margin was subtracted. All estimates for shrimp farm four range around 60%. This means that considering the ± 4% error range shrimp farm four could have had less or more than 60% relative mangrove cover. All the other shrimp farms were below the critical threshold range of 56% to 64% relative mangrove cover.

4.   DISCUSSION

This chapter discusses the outcomes presented in the Results section. The discussion of the results aims to address this study's objectives and answer the research questions. Moreover, potential research gaps for future research on mangrove monitoring and restoration as well as recommendations on the application and potential improvements of the presented study are going to be debated.

4.1.   Comparison of Object-based and Pixel-based Classification

In this section, the performance of the object- and pixel-based classification is compared and discussed. The comparison answers research question one (RQ1). The focus is on the observation of mangrove shrubs and trees that are listed in the mangrove floristics of the world table presented by Ragavan et al. (2021, p. 40 - 43) that achieve a minimum height of 3 m. Mangroves within the shrimp farm boundary, including the entire property with the ponds as well as the surrounding dikes and land spaces, are considered. In a later section the definition of mangrove as well as the considered area for the mangrove ratio calculation is going to be discussed.

The application of the ten individual replicates of training and validation GTPs resulted in high values with small variation for the Overall Accuracy (OA) in the binary classification of mangrove and non-mangrove land cover. Accordingly, this low sensitivity indicates that there are sufficient training GTPs to produce accurate and reliable object-based and pixel-based classifications.

The classifications into five land cover classes indicated more sensitivity to the individual GTP training and validation sets since the range of investigated accuracies indicated higher variation. Accordingly, the accuracies indicate better or worse results depending on the GTP training and validation dataset replicate used for the accuracy assessment. This trend was observed for the mangrove specific accuracies, namely the mangrove class User Accuracy (UA_m), mangrove class Producer Accuracy (PA_m), and mangrove class Kappa ($Kappa_m$), that focus on the reliability of the map for the mangrove class as well as the Overall Accuracy (OA) and Kappa coefficient, that assess the performance of all five land cover classes. The overall Accuracy (OA) for each of the ten replicated pixel-based accuracy assessments exceed 85%, which indicates the applicability of this approach for the land cover observation (Manandhar et al., 2009). The confusion of the water, vegetation, soil, and infrastructure land cover lead to lower Kappa and Overall Accuracy values for the classifications of all land covers than for the binary mangrove and non-mangrove land cover classification, since these four land cover classes are represented by one class called 'non-mangrove' in the mangrove map.

After the water class with 210 GTPs, the 187 mangrove GTPs represent the second biggest group of GTPs (*Table 3*). This is proportional to the actual land cover in the study area, where water and mangroves dominate. A visual inspection of the SPOT-7 image suggested that the spectral signature of river and channel water compared to aquaculture pond water as well as young sparsely distributed mangroves compared to older and denser mangrove canopies varied (Chen et al., 2017; Wang et al., 2021). The spectral signature also differs depending on the mangrove species (Hati et al., 2021; Prasad et al., 2015). Accordingly, both strata were intensively sampled to capture the spectral variability of water and mangrove cover in the study area. The greater number of training GTPs may result in a more accurate classification of both classes compared to the remaining vegetation, infrastructure, and soil class. The overrepresentation of certain land cover classes with many training GTPs can lead to an

overestimation in the classification. Vice versa this also applies to the underrepresentation of land cover classes (Millard & Richardson, 2015). However, since the water and mangrove coverage dominate the study area, an overrepresentation is unlikely. It was challenging to generate GTPs for the soil class, due to a lack of suitable areas that clearly represent this land cover. Therefore, only 79 soil GTPs are available. The limited number of training GTPs likely leads to a confusion of soil with other land cover. The soil User and Producer Accuracy are lower than for the other land cover classes (*Table 8*). This suggests that the number or proportion of training GTPs influences the classification accuracy of the respective classes. This is verified, considering the study of Mack et al. (2017), which concluded that rarely occurring land cover classes, that are represented by fewer samples than the dominating land coverage, resulted in lower accuracies. A stratification could be used to estimate the proportion of the land cover classes of interest in the study area. Based on the percentage of each class in the entire study area the number of GTPs for the respective class can be adjusted accordingly to avoid bias introduced by over or underrepresentation. Shetty et al. (2021) found that a stratified proportional random sampling favored the classification of the major land use land cover classes. The intensively sampled dominant mangrove and water land cover classes also tended to achieve higher class specific accuracies than residual strata like soil and vegetation, which were represented with fewer GTPs this research (*Table 8* & *Table 10*).

Map 2 illustrates the distribution of the GTPs in the study area. It is noteworthy that the southern part of the production forest and the northern part of the protection forest are not covered with GTPs. Moreover, more GTPs are available for the protection forest, which has a smaller area than the production forest (*Table 3*). Considering the discussed over- and underrepresentation of land cover classes, it could be argued that the production forest is underrepresented due to the smaller number of GTPs. The respective area of the forest zones could be used to calculate the relative area with respect to the total study area to represent the forest zones with a number of GTPs proportional to its relative area in percent. The GTP sampling campaign did not cover the non-forested area and the special-use forest since the focus was on the mangrove mapping of shrimp farms in the production and protection forest. The area outside the forest zones and in the special-use forest are underrepresented. The accuracy for the classification of these areas could not be directly assessed due to the lack of validation GTPs. However, since both unsampled zones are adjacent to the surveyed protection and production forest, the spectral signature of the land cover classes is unlikely to be different over the small distance to their counterparts in the adjacent forest zones. Considering Tobler's first law of geography and the spatial autocorrelation of the adjacent areas' land cover suggests the applicability of the classifier to the unsampled areas (Lv et al., 2017; Tobler, 1970).

The comparison of *Figure 6* and *Figure 7* with *Figure 8* and *Figure 9* illustrates that the distribution of the replicated accuracy and Kappa values is within a smaller range for the pixel-based classification compared to the object-based classification. A trend of higher mean and median values for the assessed accuracies was observed for the pixel-based classification. This indicates the pixel-based classification to be slightly more robust and accurate resulting in a smaller classification error margin. The mangrove-specific accuracies (PA_m, UA_m, $Kappa_m$) indicated a better performance than the generic accuracies that consider all land cover classes. Moreover, the overall accuracy calculated for the mangrove, water, vegetation, soil, and infrastructure class is lower than the overall accuracy that considers the classes mangrove and non-mangrove in *Figure 10*. This indicates that the classification is more accurate for the mangrove class than for the other land cover classes where more classification errors were observed.

The pixel-based classification provides more robust results, as the value range of the examined accuracies is about half as large as in the object-based classification (*Figure 6*, *Figure 7*, *Figure 8* & *Figure 9*). However, the value range of 2% and 3% Overall Accuracy (OA) focusing on the two land cover classes mangrove and non-mangrove in *Figure 10*, indicates a robust performance of the replicated pixel-based and object-

based classifications that use different GTP replicates as training and validation data. The pixel-based classification's median overall accuracy of 96.2%, computed with the ten classification replicates, is slightly higher than the 95.5% of the object-based classification. However, the McNemar test results indicated no significant difference between both approaches classifications. Considering the higher median and smaller value range as well as the simpler and quicker implementation without an object segmentation process that involves testing for suitable scale, compactness and shape parameters, the pixel-based classification is a fair choice for the mangrove observation on shrimp farms. Timewise the application of the Random Forest classifier was quicker for the object-based approach since there are fewer objects to be processed compared to the vast number of pixels. However, considering the entire classification the processing time of both approaches is similar since the time-consuming segmentation process of the object-based approach balances the longer computation using the Random Forest algorithm for each pixel of the pixel-based approach. Capacity wise the object-based classification can be saved as vector data, which requires less storage capacity than the raster file of a pixel-based classification. The difference between the object- and pixel-based classification is very small. This is also indicated by the McNemar test. Both the McNemar test on all land cover GTPs in *Table 6* as well as the McNemar test focusing on the mangrove GTPs in *Table 7* indicate that there is no significant difference between the object-based and pixel-based classification since all x^2 values are below the threshold of 3.84. Due to the 1 degree of freedom, three of the validation GTPs in *Table 6* and four in *Table 7* resulted in a x^2 value of 0, since there was only a difference of 1 between the number of misclassified objects or pixels for the respectively compared classifications.

Concerning the first research question (RQ1) the results indicate that there is no significant difference in the accuracy of mangrove mapping on shrimp farms via the object-based and pixel-based classification. Both approaches were found to be appropriate for the observation of mangroves on a shrimp farm scale with an Overall Accuracy of 95.5% for the object-based and 96.2% for the pixel-based classification. Accordingly, the pixel-based classification performed slightly better than the object-based classification in classifying mangroves from non-mangrove land cover on shrimp farms in the study area. But the difference of a 0.7% higher overall accuracy is marginal.

The visual inspection of the object-based and the pixel-based classification, using *Map 3*, *Map 4*, and *Map 5*, indicates that the pixel-based land cover map is grainier. The pixel-based classification preserves the land cover details on the input data's spatial resolution of 1.5 m, resulting in a pixelated illustration. This can result in the salt and pepper effect, which indicates disrupted land cover patches in pixel-based classifications (Chen et al., 2018). Land cover patches that have too few pixels to be segmented into an object are merged into adjacent objects. Therefore, the object-based land cover map illustrates more continuous land cover patches. However, the segmented objects may be larger than the area of small individual mangrove patches, resulting in mixed objects representing multiple land cover classes. The mean spectral signature of a mixed object may not exactly correspond with the spectral signature of an object containing pixels of one single land cover class. The smoothed spectral properties of objects may be less appropriate for the land cover on shrimp farms since it is more difficult to spectrally separate different land cover classes (Chen et al., 2018).

The mangroves growing in a shrimp farm's pond are mainly organized in rows or as patches (Bosma et al., 2016). Therefore, the object-based classification may be suitable for the monitoring of mangroves in the pond, where mainly continuous rows or patches of mangroves prevail. Employing spatial, textural, and shape properties in addition to the spectral properties of the objects are likely to be beneficial considering the row-like or patchy occurrence of mangroves in shrimp ponds.

Images with a higher spatial resolution than the applied SPOT-7 data may be useful to build objects representing pure land cover classes and preserve the detail of the observed area. The pan-sharpened

SPOT-7 image has a spatial resolution of 1.5 m. Whereas the segmented SPOT-7 image generalizes the land cover with objects of several pixels and not on the individual pixel-size of the pan-sharpened SPOT-7 image. Therefore, the segmented SPOT-7 image illustrates less fine land cover detail than the pan-sharpened SPOT-7 image. Accordingly, the object-based classification may miss mapping land cover on a pixel scale. Since the generated objects, containing several pixels, are the smallest unit considered for an object-based classification, the resulting land cover map illustrates the image on the object level and not with the spatial resolution of the input image. Whereas a pixel-based classification preserves the 1.5 m spatial resolution of the input image since the pixel is the smallest considered unit. Therefore, the pixel-based classification may be more suitable to also detect individual mangrove trees that may grow on the dikes of the shrimp farms or small harvested patches. This approach is more appropriate to monitor mangroves on the entire shrimp farm and not only in the shrimp pond. An individual mangrove tree covering a single pixel may be correctly classified by the pixel-based approach but would be merged into another adjacent object in the object-based approach. Since an object contains several pixels, a single mangrove covered by one pixel cannot be observed by the object-based classification. Satellite remote sensing observations tend to overestimate the mangrove area compared to very high spatial resolution UAV imagery (Hsu et al., 2020). Overestimation depends on the spatial resolution of the data. Images with a finer spatial resolution are likely to represent the mangrove cover more precisely and with less overestimation than sensors with a lower spatial resolution (Hsu et al., 2020). This means that the relative mangrove cover on the shrimp farms estimated via a pixel-based classification, using a SPOT-7 image with a spatial resolution of 1.5 m, maybe more detailed than an object-based approach but still overestimate the actual prevailing mangrove area. Furthermore, the pixel-based approach is more sensitive to observing clearings in the mangrove cover or variations in the canopy density. Accordingly, it is more suitable to map and differentiate the defined mangroves with a minimum height of 3 m from smaller propagules and saplings. This is of interest to map established and healthy mangroves that are more valuable in terms of the ecosystem services they provide, for instance, carbon sequestration and storm surge protection, compared to degraded mangroves or newly planted saplings. Although fine details like clearings and less dense mangrove canopies may not be detected by the object-based approach, it is suitable to map areas that are intended for mangrove land use.

Satellite images with a finer spatial resolution, for instance, GEO Eye imagery, are likely to represent the mangrove cover more accurately and with less overestimation than sensors with a lower spatial resolution like the applied SPOT-7 image (Hsu et al., 2020). The comparison to a manual mangrove digitization using a Geo Eye image with a spatial resolution of 0.4 m indicates a median overestimation of about 21% mangrove cover on shrimp farms for the pixel-based SPOT-7 classification. It must be noted that Hogestijn (2023) did not perform an accuracy assessment for the manual mangrove digitization that bases on the Geo Eye image. When asked concerning the accuracy by the chair Dr. Thomas Groen during her MSc thesis defense, Ms. Hogestijn replied with an estimated accuracy of 90%[3]. Moreover, the Geo Eye and SPOT-7 satellite images were captured three years apart, in 2019 and 2022. Accordingly, the mangrove cover observed on the shrimp farms may have changed during that time. The most significant difference of -63% mangrove cover was observed on a shrimp farm in the production forest where the mangroves most likely were harvested after the Geo Eye image was captured in 2019 (*Figure 11* & *Map 8.B*). But there are also opposite examples. In contrast to deforestation, there are also reforestation efforts. For one shrimp farm in the protection forest, a mangrove ratio of 9% was manually digitized by

---

[3]MSc research exam via Microsoft Teams meeting with the thesis assessment board members (ITC University of Twente, Enschede, The Netherlands) and audience. 31.05.2023.

Ms. Hogestijn for the year 2019. The pixel-based SPOT-7 classification estimated 63% mangrove cover for exactly this shrimp farm, which is illustrated in *Map 8.A*.

The comparison to the Geo Eye mangrove map suggests that the classification, based on the SPOT-7 image with a spatial resolution of 1.5 m, is not able to map the water in between the mangrove rows. Instead of mapping rows of mangroves, as indicated by the manual mangrove mapping, the classification represents mangrove rows as one continuous mangrove patch (*Map 8.D)*. This leads to an overestimation of the mangrove cover by the SPOT-7 pixel-based classification. Hsu et al. (2020) found that satellite remote sensing overestimates mangrove cover compared to UAV images. Overestimations can lead to an incorrect assessment of the mangrove system's ecosystem services and its climate change mitigating function (Hsu et al., 2020). The variability of mangrove area quantifications introduces uncertainty about the deforestation rates, which can lead to low confidence information for the estimation of ecosystem functions and the biodiversity assessment as well as conservation policies (Friess & Webb, 2014). The synchronization of satellite and UAV data is recommended to improve the temporal and spatial resolution of the observation as well as to integrate local stakeholders to collaboratively increase the capability to observe and manage natural resources (Hsu et al., 2020).

In summary, no difference between the accuracy of the object-based and pixel-based classification, using a high spatial-resolution SPOT-7 image covering the study area, was found according to the investigated accuracies and the McNemar test results. Hence, both approaches are applicable to map mangrove cover on mixed mangrove-shrimp farms.

4.2. Comparison of the relative mangrove area on shrimp farms in different forest zones

This section covers the comparison of the mangrove ratio prevailing on shrimp farms in the protection and production forest as well as outside of the forest zones. The discussed results will help to answer the second research question (RQ2): What is the difference in the ratio of mangrove cover on shrimp farms in the protection, production and no forest zones?

Map 3 and *Map 4* suggest that an overall mangrove cover of 48% or 47% prevails in the protection forest zone. The mangrove land cover class is dominant in this forest zone. Whereas mangroves are less abundant in the production forest zone and the not-forested northeastern part of the study area where water dominates the land cover. An overall mangrove cover of 33% occurs in the production forest. This indicates that in the study area, more mangroves are preserved in the forest zones than in the non-forest zone, which presents an overall mangrove cover of 20%. Accordingly, the zonation seems to influence the mangrove prevalence. This trend is confirmed by the analysis of the forest zones' relative mangrove cover on the shrimp farms. *Map 7* and *Map 9* illustrate that the relative shrimp farm mangrove cover in the forest zones is higher than in the not forested area. This is verified by the Mann-Whitney U test, which indicates that there is a statistically significant difference in the mangrove area between the forest zones and the non-forest zone. *Table 9* states that only 25% and 11% of the shrimp farms in the protection and production forest have a relative mangrove cover greater than 64% respectively. Outside of the forest zones, only 7% of the shrimp farms achieved this percentage of mangrove cover. 92% of the shrimp farms outside of the forest zones were found to have less than 56% relative mangrove cover. Although the percentage of shrimp farms belonging to this class is lower in the forest zones, 80% of the production forest's and 62% of the protection forest's shrimp farms have mangrove ratios below the compulsory 60% threshold when the 4% error margin is subtracted (*Table 9*). *Table 11* confirms that the shrimp farms in the protection forest tend to have higher mangrove ratios than the protection forest's shrimp farms.

The Forest Protection Department's database of the shrimp farms' mangrove cover is used to replant mangroves at the properties that have a lack of mangroves. In the protection and production forest, a relative mangrove cover of 60% must be preserved on shrimp farms. However, the financing is challenging since the government assigns a budget of 30 million Vietnamese Dong (VND) per hectare (approximately 1164€) for the plantation of mangrove saplings in the protection forest zone, but only 8 million Vietnamese Dong (VND) per hectare (approximately 310€) are funded to plant mangrove saplings in the production forest zone[4]. The unequal financial support for the mangrove reforestation in the protection and production forest mentioned by the interviewed Forest Management Board technician may partly explain the observation of more shrimp farms with less than 60% mangrove cover in the production forest. Another challenge that was mentioned is that the Ca Mau People's Committee annually decides to fully dedicate the budget to the plantation of mangroves, but not to the protection.

Other than the Forest Management Board, which focuses on a relative mangrove ratio of 60% on the entire shrimp farm stated in Decision 19/QD-UBND from 2010 (Hogestijn, 2023), certification organizations that award labels for organically and ecologically grown shrimp request a mangrove cover of 50% on the aquaculture pond (Joffre et al., 2015; Lai et al., 2022). It appears that the 10% mangrove ratio difference between the pond area and the shrimp farm area accounts for the smaller area of the pond. However, the mangrove ratio reported by the Forest Management Board is considered during eco-label certification audits (Gruber et al., 2020). The reported mangrove ratio on the entire shrimp farm would not be directly applicable for certification organizations' assessment in the pond area. The technical manager of the Forest Protection Department stated that the dikes surrounding the pond are not overgrown with plants since sediment that accumulates in the pond is dug out and dumped on the dikes every two years. This makes it difficult for plants to grow on the dikes, but when visiting mixed mangrove-shrimp farms in March 2023, mangrove propagules and saplings were observed on the edges of shrimp farm dikes. An investigated audit report did not specify the consideration of an error range for the mangrove ratio threshold (Gruber et al., 2020). The technical manager indicated an error margin of 10 to 15% referring to the accuracy of the handheld GPS device. But no accuracy or error margin is considered for the mangrove observation method. This raises the potential for farms with mangrove ratios below the respective threshold to be falsely declared to comply with the regulation. The consideration of an error range, for instance, based on an accuracy assessment as in this study, could support Forest Management Boards and eco-labeling organizations to reduce the risk of erroneously certifying shrimp farms with mangrove ratios ranging slightly below the required threshold values. This would incentivize more sustainable mangrove forest management and ecological shrimp production by improving the certainty that shrimp farms comply with the regulations. The assurance that the shrimp really grew on an ecological farm is of interest to honor the trust that the consumers put into the eco-label of the certification organizations.

Regarding research question two (RQ2), the Mann-Whitney U test revealed a significant difference in the mangrove cover of the investigated zones. Consequently, the relative mangrove cover on the shrimp farms in percent tends to be higher in the protection forest zone than in the production forest. Shrimp farms outside of the forest zones usually achieved a lower mangrove ratio than what was observed within the forest zones. This is indicated by *Map 7* and *Map 9*, which illustrate the relative mangrove area % prevailing on the individual shrimp farms covered by the SPOT-7 image. The results imply the protection forest to have the highest percentage of shrimp farms that achieve a relative mangrove area greater than

---

[4] Zoom meeting with the technical manager of the West Sea Protection Forest Management Board and Prof. Dr. Vo Quoc Tuan (Head of the GIS and remote sensing laboratory, Can Tho University). 14.04.2023.

the 60% threshold for sustainable forest management specified by Decision 19/QD-UBND. In the production forest, the percentage of shrimp farms complying with the set forth mangrove ratio of 60% is smaller than in the protection forest (*Table 9*). The mangrove ratio threshold of 60% does not apply to shrimp farms outside of the forest zones, where shrimp farms with a tendency of a lower relative mangrove area % were observed. However, shrimp farms in the non-forest zone that want to be certified as sustainable shrimp producers must still achieve a mangrove coverage of 50%. Hogestijn (2023) indicated that controversial policies lead to ineffective regulations, which may have resulted in the lack of mangroves on many shrimp farms in the investigated forest zones. On the one hand, the National Decree 773-TTg and the Ca Mau coastal provincial aquaculture plan promoted shrimp farming by demanding the expansion and intensification of shrimp aquacultures. On the other hand, the Vietnamese government decided to implement urgent measures to protect and develop forest areas with an afforestation plan that intended to plant 5 million ha of mangrove forests across the country according to Decision 286/QD-TTG and Decision 661/QD-TTG (Van et al., 2015).

Satellite-based mangrove assessments, such as the one presented in this study, can cover large areas with high accuracy and reduce the frequency of costly mangrove-shrimp farm field surveys. According to the error margin of ± 4%, the shrimp farms with a mangrove ratio ranging from 56 to 64% could either comply with the regulation or be slightly below 60% relative mangrove cover. 14% of the protection forest shrimp farms and 9% of the production forest shrimp farms are within this transition group (*Table 9*). The relative mangrove cover of the shrimp farms that are part of this transition class can be targeted to be closer investigated with the classification of aerial imagery captured by an Unmanned Aerial Vehicle (UAV). Alternatively, a field survey using handheld GPS devices as currently performed by the Forest Management Board could be carried out to investigate the mangrove cover on shrimp farms within the 56% to 64% transition class. According to the technical manager of the West Sea Protection Forest Management Board, a field survey takes about two hours per shrimp farm[5]. A maximum of four shrimp ponds can be surveyed per day. This would result in a manually mapped mangrove cover estimate. The error range of the handheld GPS device could be considered, but there is no estimation of the survey method's accuracy.

In terms of the third research objective and question (RO3 & RQ3), the shrimp farm's mangrove ratio, estimated by the respective operating shrimp farmer, tended to divert from the ratio computed with the classifications (*Figure 12*). The farmer's perception equally overestimated (5 shrimp farms) and underestimated (5 shrimp farms) the mangrove cover. Only the mangrove ratio estimation of one out of eleven shrimp farmers matched with the object-based and pixel-based classification. It suggests that the ground-based assessment of the mangrove cover's proportion relative to the shrimp farm area is challenging. This makes it difficult for shrimp farmers who want to comply with the regulations to determine and achieve the threshold of 60% mangrove cover.

4.3.   Definition of mangroves on shrimp farms

First, this section discusses the definition of the area where mangrove cover is monitored on the investigated shrimp farm. Then the definition of what is considered as mangrove in the observation is discussed.

---

[5] Zoom meeting with the technical manager of the West Sea Protection Forest Management Board and Prof. Dr. Vo Quoc Tuan (Head of the GIS and remote sensing laboratory, Can Tho University). 14.04.2023.

4.3.1. Monitoring area

Hogestijn (2023) pointed out that organizations and administrative bodies use different scopes to monitor mangroves on shrimp farms. Either the mangrove ratio in the shrimp pond or the mangrove ratio on the shrimp farm is considered. Since certification labels focus on ecological shrimp production the mangrove ratio on the aquaculture pond is considered (Joffre et al., 2015; Lai et al., 2022). The Forest Management Board on the other hand assesses the mangrove ratio on the entire shrimp farm (Hogestijn, 2023). The consideration of the mangrove ratio in the shrimp pond would likely result in a higher mangrove ratio for the monitored shrimp farm since the aquaculture pond is dominated by mangroves and water. Whereas besides the pond, shrimp farms have areas covered by infrastructure, soil, and non-mangrove vegetation. Accordingly, considering the mangrove ratio in the shrimp ponds could give a wrong impression of the mangrove cover in the forest zones.

The observation of a mangrove ecosystem and its functions on a landscape scale may make more sense in terms of sustainable mangrove forest management than downscaling the scope to the extent of aquaculture ponds. Therefore, the consideration of the mangrove ratio on the entire shrimp farm area may be more appropriate since the land use change from mangrove to aquaculture pond as well as the conversion of mangrove to infrastructure or agriculture is monitored. The observation of mangrove ratios in shrimp ponds would narrow down the scope of the mangrove monitoring and ignore the conversion from mangrove to non-mangrove land use in the forest zone. Since the forest zones include the entire landscape and not solely the aquaculture ponds, the relative mangrove cover % should be investigated on the shrimp farm's total area. Hence, the Forest Management Board's approach of assessing mangroves on the entire shrimp farm area is reasonable for mangrove preservation purposes. This approach gives a stronger incentive to conserve mangroves than the mangrove monitoring limited to the pond area.

Vietnamese experts proposed to consider an even larger monitoring scale on landscape level instead of farm level to improve the connectivity between the tidal estuarine system and the mangroves as well as enabling small shrimp farms to comply (Joffre et al., 2015). This approach would shift the mangrove conservation responsibility from individual farmers to the shrimp farming community, which could motivate collective mangrove management but potentially also lead to disputes between the shrimp farmers. The intended interaction of mangroves with fluvial and tidal processes, envisioned by the Vietnamese experts, would be beneficial, but the shrimp farms are embanked with dikes and only allow limited water exchange with the sluices (Lai et al., 2022). Accordingly, space for mangroves on riverbanks or de-embanked shrimp farms, that allow a natural fluvial and tidal water flow, would be necessary. The feasibility of a mangrove buffer zone along the rivers, like the coastal mangrove belt of the Mekong Delta, could be considered to facilitate mangrove rehabilitation (Wölcke et al., 2016). However, space is limited, and it is unlikely that individual farmers in the community voluntarily abandon their shrimp farm for the landscape scale mangrove conservation. The definition of reasonable landscape areas to monitor the mangroves would also be challenging and necessary for the proposed approach of the Vietnamese experts (Joffre et al., 2015). Therefore, the implementation of a landscape scale mangrove monitoring is currently not applicable.

4.3.2. Mangrove definition

The definition of mangrove, mangrove forest, and mangrove ecosystem is crucial for the observation and mapping of mangroves with remote sensing. Ellison et al. (2020) state that "Mangroves are a taxonomically diverse group of ±70 tree, shrub and fern species (in at least 25 genera and 19 families)" (Ellison et al., 2020, p. 2). Whereas according to Mukherjee et al. (2014), a mangrove can be an individual woody plant of the three main genera *Acrostichum*, *Avicennia*, and *Rhyzophora* growing on tropical and subtropical coasts. The stated mangrove plants and their associated organisms can form a mangrove

forest community or mangal. A mangrove ecosystem consists of the mangal, and the abiotic factors associated with it (Mukherjee et al., 2014). Regarding the preservation of the valuable services and functions of mangrove ecosystems, it would be most appropriate to conserve entire mangrove forest communities that contain mangrove species as well as associated organisms. Mangrove monocultures are less productive and resilient than a healthy biodiverse mangrove ecosystem (Quarto, 2012). The mortality rate of mangrove propagules on monocultures tends to be higher than on sites that allow the natural colonization of mangrove seedlings of pioneer species like *Avicennia alba* and *Sonneratia alba* (Ellison et al., 2020). Moreover, Ellison et al. (2020) found that naturally recolonized mangrove areas achieved higher biodiversity of mangrove species as well as fauna than adjacent constructed shorelines. For a sustainable and successful mangrove ecosystem rehabilitation the recreation of the natural hydrology may be more beneficial than manually planting mangrove saplings (Quarto, 2012). Natural recruitment of propagules from nearby mangrove systems that are connected via waterways is necessary for the recolonization (Ellison et al., 2020).

Natural regeneration of *Rhyzophora* and *Bruguiera* was observed within 200 m of the study area's waterways like the Cửa Lớn River and its tributaries (Van et al., 2015). Wilson (2010) observed a natural regeneration of mangroves on shrimp farms with suitable conditions where pond dikes were breached to reintroduce tidal flow. Within 39 months the mangrove cover grew sufficiently to be detectable with remote sensing (Wilson, 2010). The dikes and sluices of the shrimp farms limit the natural tidal and alluvial recolonization of mangroves due to the restriction of the water flow. Therefore, natural mangrove rehabilitation in the studied mixed mangrove-shrimp farm systems seems to be challenging.

Although experts also consider a mono-specific mangrove stand as a mangrove ecosystem, it is desirable to aim for biodiverse mangrove ecosystems that host a variety of species (Mukherjee et al., 2014). The restoration of the faunal composition, structure, and natural processes via colonization by non-planted species on artificial mangrove plantations may take years (Van et al., 2015). The timber harvest of *Rhyzophora apiculata* on mixed mangrove shrimp farm systems leads to a 10 to 12 years rotation of grown trees being replaced with newly planted mangrove saplings (Van et al., 2015). This suggests that the recovery of permanent, biodiverse mangrove forests as well as the provided ecosystem services and functions on shrimp farms, is not likely. The current approach of replanting mangrove propagules on shrimp farms supports the creation of integrated mangrove monocultures but may not result in the rehabilitation of a biodiverse mangrove ecosystem. Quarto (2012) states that mainly *Rhyzophora spp.* propagules are planted without considering the environmental conditions at the restoration site. The plantation of *Rhyzophora* monocultures is tempting for the local community due to the economically added value of the timber products (Ha et al., 2014). Firewood and charcoal from harvested *Rhyzophora* can be sold on local markets or exported to Japan and Korea (Ha et al., 2014; Quarto, 2012). Although the plantation of *Avicennia* may benefit the pond's fertility and pH regulation the plantation of *Rhyzophora* is preferred because it is tolerant to inundation and easy to plant (Bosma et al., 2016). Cà Mau has a long mangrove plantation history. Already the French colonialists replanted *Rhyzophora apiculata* for charcoal and tannin production since it is the most economic species (Van et al., 2015). Also, the following large-scale reforestation programs after the Vietnam War and the introduction of integrated mangrove shrimp farm systems rather aimed to increase timber production, to meet the demand of the growing population, than to restore the functions and services of healthy mangrove ecosystems. *Rhyzophora apiculata* was used due to its ease and timber utility, which lead to the development of mangrove-shrimp farming systems with *R. apiculata* becoming the typical land use (Van et al., 2015).

4.3.3. Mangrove management

The engagement of the local community and progress monitoring is important for the long-term success of restoration projects (Ellison et al., 2020). Therefore, approaches like the Community-based Ecological Mangrove Restoration (CBEMR) aim to restore more naturally functional and biodiverse mangrove ecosystems than the often applied capital and labor-intensive manual plantation of monocultures (Quarto, 2012). The lack of funding for the protection and preservation of mangroves was expressed by the interviewed expert of the West Sea Protection Forest Management Board. Funding is available for the replantation of *Rhyzophora* saplings but not for the conservation of the existing and newly planted mangroves. Since Vietnamese policies prioritize mangrove restoration for the mitigation of climate change and the achievement of sustainable coastal development, targets for mangrove restoration are determined on national and provincial levels (Pham et al., 2022). This indicates that mangrove replantation or afforestation is favored, and the preservation of existing mangrove ecosystems in zones where the harvest is allowed may be neglected. This is problematic since there is low or medium restoration potential in most provinces because coastal erosion and coastal squeeze cause unfavorable conditions for mangrove restoration (Pham et al., 2022). Considering the currently applied restoration policies and practices the continued dominance of *Rhyzophora* monocultures in the study area is likely. According to the interviewed forest manager, there must be 6,000 mangroves per hectare to be considered as a mangrove forest that provides important ecosystem services. Trees of the *Rhyzophora* and *Avicennia* genus are counted on a sampling plot of 100 m² to upscale and estimate if the investigated patch of land achieves the mangrove forest status. However, a variety of species and plants may be considered as mangroves or part of a mangrove forest. For instance, the *Nypa fructicans* palm tree is listed as mangrove plant species (Mukherjee et al., 2014). The fern mangrove *Acrostichum* is mentioned as mangrove genera but not stated in the consensus list of mangrove plant species (Mukherjee et al., 2014). The definition of mangrove can lead to alternating results of surveys and inventory maps, depending on if a holistic view of the plants in a mangrove ecosystem or merely mangrove trees of certain species are considered. The variety of functions and services of a mangrove ecosystem bases on the interaction of diverse flora and fauna as well as the interacting spheres, namely the biosphere, hydrosphere, lithosphere, and atmosphere (Aprilia et al., 2022). The interconnection of the spheres via the flux of energy and matter, in the form of the carbon, water, nitrogen, phosphorous, and sulfur cycle, is fundamental to the function of mangrove ecosystems (Aprilia et al., 2022; Maulana et al., 2017). This suggests that a variety of plants as listed by Mukherjee et al. (2014) and Ragavan et al. (2021) could be considered for the mangrove monitoring since the interaction of mangrove forest communities' diverse fauna and flora enhance the valuable ecosystem services.

4.4. Potential improvements and recommendations

This section first discusses limitations and possibilities for improvements of the presented research. Subsequently, recommendations for the mangrove monitoring on shrimp farms are given.

4.4.1. Limitations and potential improvements

The pre-processing of the applied satellite remote sensing SPOT-7 image was kept to a minimum due to time limitations as well as to make it quickly replicable for local stakeholders with limited GIS and remote sensing background, for instance, the staff of the Forest Management Board. The satellite image pre-processing involved cloud and cloud shadow screening and masking instead of the application of an additional atmospheric correction because the SPOT-7 image was delivered radiometrically and atmospherically corrected by the provider. Previous studies applied additional atmosphere corrections, for instance the ATCOR-2 software was used by Vo et al. (2013) to perform an atmospheric correction of a

SPOT-5 image in the Cà Mau province, Vietnam. Another study on Vietnamese mangroves applied the Fast Line-of-sight Atmospheric Analysis of Spectral Hypercubes (FLAASH) for the atmospheric correction procedure (Pham et al., 2019a). The results of the studies by Bektas Balcik & Karakacan Kuzucu (2016) and Siregar et al. (2018) suggest the applicability of FLAASH as atmospheric correction of SPOT-7 imagery prior to supervised land cover and land use classifications. The application of an additional atmospheric correction and its effect on the performance of the supervised classification of mangroves on a shrimp farm scale could be the subject of future studies.

After the GTP quality assessment the requirements and assumptions for the GTPs were adjusted to avoid neglecting 199 GTPs. Mainly soil GTPs would have been neglected. However, the loss of mangrove GTPs presumably would affect the binary classification into mangrove and non-mangrove the most. Accordingly, it would be interesting to compare the accuracy and robustness of the binary classification applied in this study, which used the adjusted GTP dataset, with a binary classification using the GTP dataset that neglects the 199 GTPs, which did not comply with the initially considered requirements.

The GTPs were divided into 70% training and 30% validation data, which is commonly used in modelling and classification tasks. The Overall Accuracy for the classifications of mangrove and non-mangrove land cover in *Figure 10* indicated little variability for the ten individual GTP replicates. Accordingly, the classification was robust and accurate using 70% of the GTPs to train the classifier. This raises the interest in how the proportion of training to validation GTPs affects the robustness and accuracy of the classification. This can be studied using less GTPs to train the data, for instance, with an equal split into 50% training and 50% validation GTPs, to test if there is a difference in the robustness and accuracy using different proportions for the GTP training and validation dataset. In case that classifications that use less GTPs are similarly robust and accurate, a smaller number of GTPs could be sampled to reduce the time and cost of field surveys.

Talukdar et al. (2020) performed a Random Forest classification using 200 decision trees. Applying a vast number of decision trees results in a better accuracy for image processing but increases the computation time (Talukdar et al., 2020). Considering the time-consuming process of calculating 200 decision trees, this study used the pre-setting of 50 decision trees suggested by eCognition. Future research could investigate and compare the effect of the number of decision trees, for instance, 50, 100, 150, and 200 trees, on the accuracy of the image classification.

Considering the long computation time to generate classification replicates for both the object-based and pixel-based approaches, this study performed the classification and accuracy assessment with ten individual training and validation GTP datasets for both approaches. In future research a larger sample population of 30 replicates of the GTP training and validation datasets could be generated to enable the performance of statistical tests for the assessment of the robustness as well as the difference between the performance of the object-based and pixel-based classifier.

This study's segmentation process applied a single segmentation level. Multiple segmentation levels can improve the segmentation and benefit the OBIA that bases on the segmented objects. The laborious set-up of multiple segmentation levels could result in higher segmentation accuracy. This potentially could improve the object-based classification accuracy. Considering this, the application of multiple segmentation levels could have made a difference for the comparison between the object-based and pixel-based approach.

In future research, the importance of the various inputs to the Random Forest classifier can be assessed with the ggplot 'variable importance' tool in R or Python (Sharma, 2022). This can simplify the model and ensure that only the bands that add important information are considered in the classification process.

The GTPs sampled during the 22nd and 23rd of March 2023 were applied to train and validate the SPOT-7 image captured on the 25th July 2022. In the optimal case the GTPs are sampled during the same date that the remote sensing image is captured. However, the GTPs sampled by the colleagues from Can Tho

University during the field campaign from the 21st to the 25th July 2022 were not applicable, due to the insufficient number of GTPs. Moreover, the GPS location noted for the GTPs stated the position of the surveyor, but not the surveyed land cover. Therefore, the field sampling campaign was organized and conducted to generate an applicable GTP dataset. It was assumed that the mangrove cover does not change significantly during the time span between the GTP field sampling and image caption. The quality assessment only found few mismatches of the 2023 GTPs to the 2022 SPOT-7 image. The mismatches were annotated with a note stating the land use change from 2022 to 2023 and neglected from the quality assessed GTP dataset.

Since the GTPs were sampled in 2023, they were not applicable as training and validation data for the classification and accuracy assessment of the Geo Eye satellite image from 2019 used by Hogestijn (2023). Future research could perform pixel-based and object-based classification with a higher spatial resolution image like the Geo Eye captured in the year of the GTP sampling campaign to investigate the differences in the relative mangrove cover estimation using the same machine learning classifiers and data of the same year. This could study the effect of the spatial resolution on a potential over-estimation of the mangrove area, without the disturbing effect of land cover change over time, as observed for the Geo Eye 2019 to SPOT-7 2022 comparison.

Shrimp farms that are not fully covered because they are located at the SPOT-7 image's border or have parts that were neglected as no data value because they were covered by the cloud and cloud shadow mask could be excluded from the map and analysis. Since only shrimp farms with a minimum size of 1 ha were observed in this study many farms that are not fully covered by the SPOT-7 input data for the classifications are already ignored. However, to guarantee the integrity of the mangrove observation a screening of incompletely covered shrimp farms could be performed to avoid considering such farms in the analysis. Moreover, shrimp farms with an area smaller than 1 ha could be surveyed with UAV data to provide detailed and precise information on the mangrove proportion.

The trees in mixed mangrove-shrimp farm systems are mainly mangroves. However, there is the chance that another type of plant, for instance, banana palms or mango trees for food supply, could be planted by the farmers on their property. This could lead to confusion of non-mangrove plants with mangroves, which would result in a mangrove overestimation on shrimp farms with fruit trees in the study area. During an excursion to mixed mangrove shrimp farms, only dragon fruit cactus was observed, which is unlikely to resemble the spectral signature of lush mangrove canopy.

4.4.2. Recommendations

This study's satellite-based mangrove observation covers shrimp farms in an area of about 76,350 km². This study's GTP field sampling campaign was performed within 2 days. After the processing of the data, the resulting classification enables the observation of the mangrove cover on 1,677 shrimp farms in the study area. The mapping of mangrove cover with a high spatial resolution builds the base for following calculations of biomass and carbon storage estimations. Quantifying the carbon stored in the mangroves, enhances communicating the importance of the mangroves' carbon sequestration and function. The classified mangrove maps may be used as input data for a model to report the carbon stock within the study area. Biophysical characteristics of the mangroves, for instance, the Leaf Area Index (LAI), the above-ground biomass, and carbon stock could be computed with allometric models (Andalibi et al., 2021; Kamal et al., 2022). Since most of the carbon is stored in the soil of mangrove systems, it is important to consider a model that accounts for the mangrove soil carbon sequestration (Campbell et al., 2022). Prof. Dr. Nguyen Van Cong expressed an interest in the LAI, above-ground biomass, and carbon

stock of the observed mangrove-shrimp farm systems during a meeting at Can Tho University 6. However, considering the risk of satellite-based mangrove area overestimation the SPOT-7 estimates with a spatial resolution of 1.5 m are likely to not represent the mangroves' biomass and carbon stock as realistically as the dense point clouds captured by a UAV or very high spatial resolution (30 cm) MAXAR WorldView data (Hsu et al., 2020; Lassalle & de Souza Filho, 2022).

Considering the expenditure of time, capturing UAV data for about 1,677 shrimp farms in this area is not reasonable. A hybrid monitoring approach could make use of the large coverage of satellite remote sensing data and the accuracy of very high spatial resolution UAV data. First, the classification of mangroves with high spatial resolution satellite imagery covering a large area could be performed. Based on the mangrove classification and the error margin indicated by the accuracy assessment, shrimp farms with a mangrove ratio of 60% ± the error range could be indicated to minimize the number of shrimp farms that are closer investigated with UAV field surveys. The accurate observation of the mangrove cover with a UAV can clarify the status of the mangrove ratio on shrimp farms. The QField application could be used for the collection of GTPs for the mangrove classification and accuracy assessment of the satellite remote sensing as well as the UAV data. A QField manual that was developed for the GTP sampling in the study area is attached in *Appendix A*. The proposed hybrid approach could provide a transparent and accurate mangrove observation while reducing the surveying and particularly the processing time of the UAV data. In April 2023, the head of Can Tho University's GIS and remote sensing laboratory, Prof. Dr. Vo Quoc Tuan, held a UAV training session for the Biển Tây Protection Forest Management Board. Collaborations like that may help to adopt more transparent and accurate mangrove monitoring and management. The application of the proposed hybrid monitoring approach could be considered for the annual mangrove inventory monitoring of the Protection Forest Management Board. Further research as well as training and tutorials on the GIS and remote sensing methods of the envisaged hybrid monitoring approach, may be necessary to facilitate its application. The dry period during the Northeast monsoon from December to April is recommended for annual GTP field surveys and UAV flights since less intense wind and precipitation are more suitable sampling and flight conditions (Groenewold et al., 2015).

The study area is subject to strict legal constraints since it borders the West Sea, which leads into international waters in the Gulf of Thailand. Accordingly, the strict flight regulations in the study area complicate the provision of UAV flight permits by the authorities. Loosening the flight regulations would allow researchers and forest managers to test the applicability and accuracy of UAV-based mangrove observations and allow a comparison to the results of this study. The studies of Yang et al. (2022) and Tong et al. (2023) demonstrate the application of unmanned aerial vehicle (UAV) with a high spatial resolution of less than 10 cm to map mangrove biophysical parameters like height as well as the canopy area and volume using a canopy height model. Canopy and species characteristics are valuable information for the monitoring and quantification of mangroves above ground carbon using a UAV (Li et al., 2019). UAV data offers to observe mangroves on shrimp farms more precisely and detailed than satellite remote sensing data as the SPOT-7 image applied in this study. However, Yang et al. (2022) state that a maximum mangrove area of 0.5 ha was investigated within one day. Considering that only shrimp farms of a minimum area of 1 ha were mapped in this study, capturing UAV data with that high spatial detail would take at least 2 days for the smallest of the 1,677 shrimp farms within the study area. An area of up to 200 ha can be covered with a rotary-wing UAV during one sampling day. In terms of spatial coverage, the application of a fixed-wing UAV could be of interest since it can cover a larger area and offers a longer flight time than a rotary-wing UAV (Amarasingam et al., 2022). However, the horizontal

---

6 Meeting with Prof. Dr. Nguyen Van Cong (Dean of the College of Environment and Natural Resources) and Prof. Dr. Vo Quoc Tuan (Head of the GIS and remote sensing laboratory), Can Tho University, Vietnam. 06.03.2023.

takeoff and landing of a fixed-wing UAV is challenging in the study area's mixed mangrove-shrimp farm environment and less user-friendly than a rotary-wing UAV, which can vertically take off and land on small open spaces (Amarasingam et al., 2022). Vertical Take-off and Landing (VTOL) UAVs combine the deployment benefit of rotary-wing UAVs' vertical take-off and landing with the spatial coverage of fixed-wing UAVs (Zhao & Li, 2022). Within a flight time of 110 minutes a VTOL UAV may cover an area of 1200 ha in one flight (DeltaQuad, 2023). Besides all the benefits of a VTOL mapping UAV, like the DeltaQuad Pro #MAP, such remote sensing platforms may not be affordable or applicable without appropriate training for the Vietnamese Forest Management Boards (DeltaQuad, 2023).

The proposed hybrid monitoring system could support the production of the annual national forest cover statistic by the Forest Protection Department mentioned by Hogestijn (2023). An annual observation of the relative mangrove area on the shrimp farms may be applicable to monitor the development of replanted mangrove saplings as well as the harvest of grown mangroves for timber, firewood, or charcoal production. A time span of five years from planted mangrove saplings to grown trees was stated in the expert interview. The human-induced depletion or harvest of mangroves is a more rapid process than the growth of trees. Therefore, an annual time scale is more important to detect the loss of mangroves than the gain achieved via reforestation. A mosaic of optical remote sensing imagery can gap-fill cloud-covered pixels and enable an annual mangrove classification and mapping of the respective Forest Management Board's survey area. Norway's International Climate and Forests Initiative (NICFI) satellite data program offers analyze-ready mosaics with a spatial resolution of 4.77 m for non-commercial and non-profit use (Planet Labs PBC., 2022a, 2023). Bunting et al. (2023) applied NICFI monthly mosaics to monitor mangrove loss across Africa with an estimated overall accuracy of 92%. Monthly NICFI mosaics are available for tropical countries including Vietnam (Planet Labs PBC., 2022a). The application of monthly NICFI mosaics captured during the dry period from December to April could be interesting for the mangrove monitoring of the Biển Tây Protection Forest Management Board (Groenewold et al., 2015). Further research on the applicability on shrimp farm level is necessary, due to the lower spatial resolution (4.77 m) compared to the 1.5 m of the SPOT-7 image used in this study. The GTPs that were generated for this study could be used to classify and perform an accuracy assessment of a Planet Super Dove image that captured the study area on the 22nd of July 2022, three days before the analyzed SPOT-7 image (Airbus, 2022; Planet Labs PBC., 2022b). The comparison of both satellite images' accuracy could investigate the applicability of different spatial resolutions for the observation of mangrove cover on shrimp farms.

In the case that the cloud-covered pixels cannot be compensated for with a monthly or annual mosaic, that involves satellite remote sensing images captured during the observation month or year of interest, active radar remote sensing could be considered to substitute the missing data to enable the annual monitoring. Active Synthetic Aperture Radar (SAR) data could be of interest to account for cloud cover-induced data gaps in optical remote sensing data since radar remote sensing can penetrate through clouds. This is especially of interest during the months of the cloudier wet season from May to November (Groenewold et al., 2015). Pham et al. (2019) reviewed several studies that exemplified the application of radar remote sensing for the monitoring of mangroves. However, high spatial resolution and active radar remote sensing data come at a cost (Pham et al., 2019). Obtaining data is expensive and therefore may not be accessible to local stakeholders like the Forest Management Boards.

Alternatively, observation gaps of shrimp farms where cloud cover or cloud shadow hinder the mangrove mapping optical remote sensing imagery, like the applied SPOT-7 image, could be compensated via UAV field surveys. The flexible application of UAVs may offer a more cost-efficient alternative to map mangroves on a small spatial scale.

The future publication of annual mangrove maps and shrimp farm mangrove ratios could support the shrimp farmers who seem to be challenged by estimating the relative mangrove cover on their properties. The availability of information on the mangrove status could help shrimp farmers manage and preserve the mangrove cover on their farms accordingly to achieve the required mangrove ratio thresholds. Additionally, an awareness-raising campaign that conveys the importance of the valuable mangrove ecosystem services could be organized. Particularly shrimp farmers with a lack of mangrove cover on their property could be aimed for with the information and awareness raising sessions. The involvement of the district and commune-level People's Committee and Forest Management Boards in the awareness-raising campaign is important to reach local stakeholders. The cooperation and engagement of local communities and stakeholders is fundamental for the successful implementation of conservation and restoration measures. Many restoration projects do not address the reason causing mangrove loss (Quarto, 2012). Besides shrimp farming and forestry there are only limited sources of income for the population in the study area. However, the benefits of integrating healthy and productive mangroves on the shrimp farm for the local community must be clarified to raise the individual responsibility for mangrove conservation. The example of Mui Ca Mau National Park shows that eco-tourism could represent another means of income and support the mangrove conservation in the study area (Kien et al., 2017). But the study area is declared as a zone where tourists are not allowed to travel, which prevents this alternative source of income.

The technical manager of the West Sea Protection Forest Management Board expressed the necessity of training in GIS and remote sensing to support the Forest Management Board's staff improve their skills[7]. He proposed that teaching institutes could organize training sessions on remote sensing methods for the Forest Management Board since there is a demand in many units. The development of a manual that instructs the execution of a pixel-based classification and a subsequent accuracy assessment, as presented by this study, could serve as teaching material for the Forest Management Board. Acting by developing educational materials and organizing training sessions with interested technical managers and surveyors would support the monitoring and management of natural resources in the study area. The tutorial in *Appendix A* aims to convey a field sampling method using open-source software. Developing and sharing more educational material as well as organizing training sessions to gain practical experience with GIS and remote sensing software is desirable to support the mangrove conservation and reforestation efforts of the local stakeholders.

Mangroves of the genera *Avicennia* and *Rhyzophora* dominate in Vietnam (Veettil et al., 2019). The harvest of grown mangroves combined with the plantation of *Rhyzophora* on the study area's shrimp farms by the Forest Management Board may gradually lead to a further loss of mangrove species diversity. The compound effect of the anthropogenically driven decline of mangrove biodiversity as well as large-scale human interventions into the hydrology that alter the sediment flux via dams and channels impact the Mekong Delta. Additionally, erosion and climate change-induced sea level rise pose a threat to the region. This could lead from the equilibrium state during the Holocene through a tipping point to a less desirable species configuration of the mangrove forests and ultimately to a collapse of the Mekong Delta in the Anthropocene (Renaud et al., 2013). The monitoring of mangrove species dynamics in the study area via a remote sensing time series could indicate long-term changes in the prevailing species composition. The studies of Cao et al. (2018) and Wang et al. (2018a) used machine learning algorithms on remote sensing data for the classification of mangrove species. The application of a remote sensing-based mangrove

---

[7] Zoom meeting with the technical manager of the West Sea Protection Forest Management Board and Prof. Dr. Vo Quoc Tuan (Head of the GIS and remote sensing laboratory, Can Tho University). 14.04.2023.

species classification in a future study could provide insights into the spatial and temporal development of the study area's mangrove species composition. The application of the SPOT-7 image used in this study and the resulting mangrove map could be further processed to classify mangrove species in the study area. This could reveal valuable information on the mangrove species composition in the study area and test the potential influence of the manual plantation of *Rhyzophora* on the diversity and dominance of mangrove species. Especially a comparison of the special use forest's species composition with the mangrove species occurring on the integrated mangrove-shrimp farm systems in the protection and production forest could evaluate the effect of the currently applied mangrove management practices on the biodiversity and productivity of the mangrove communities.

5. CONCLUSION

This study presented the land cover classification of a pan-sharpened SPOT-7 satellite image and its application for the observation of mangrove ratios on shrimp farms in the study area. The first research aim was to compare the accuracy of the object-based and pixel-based classification. The study's results indicate that there is no statistically significant difference between the accuracy of both applied classification approaches. The accuracy assessment using the validation GTPs shows that the two approaches map mangroves with an overall accuracy of 96%. The second research aim was to analyze the mangrove cover on shrimp farms in the observed forest management zones. In the protection forest, a higher percentage of shrimp farms was found to have sufficient mangrove cover (>60%) than in the production forest. However, considering the error margin of 4% the number of shrimp farms complying with this sustainability criterion is still low in both forest zones with only 25% and 11% of the shrimp farms respectively. This is even less in the non-forest zone (7%) where the regulation is not in force. The third research aim focused on the assessment of discrepancies between ground-based and satellite-based mangrove ratio estimates. Considering the mangrove ratios calculated from the object-based and pixel-based classification as reference values, the farmers' ground-based perception tended to over or underestimate the relative mangrove cover on the shrimp farms.

Very high spatial resolution satellite remote sensing or UAV imagery may provide more detailed and accurate mangrove observations on a finer spatial scale to avoid the overestimation of the mangrove cover. A hybrid monitoring approach involving the classification of mangroves with high spatial resolution satellite data, covering a large area, combined with the application of a UAV, to accurately capture and investigate the mangrove cover on shrimp farms that are indicated with mangrove ratios ± the error range of the satellite remote sensing mangrove classification, is recommended. Additionally, the classification of mangrove species could give insights into the mangrove species composition prevailing in the study area's forest zones. The current mangrove harvest and replantation of *Rhyzophora* benefits the timber production on mixed mangrove monoculture shrimp farm systems but does not establish or protect the valuable services and functions of productive, biodiverse mangrove ecosystems.

6.   ETHICAL CONSIDERATION

This section focuses on the ethical processing and implication of the qualitative information obtained during the interview as well as the geodata that was sampled and used for this research. Furthermore, the potential consequences of the research results on the shrimp farmers in the study area are considered.

The qualitative information obtained from the questionnaire and interview was kept confidential. The interviewee, who voluntarily participated, was anonymized in this thesis. The notes and record of the interview are securely stored and protected from disclosure to third parties.

A forest manager accompanied the students during the GTP field survey and explained the purpose of the research to the owners of the examined shrimp farms. To avoid threatening liberties or private information of the individuals encountered on the shrimp farms, it was taken care of that no person was captured on the images that represent the respectively sampled land cover class. Moreover, the sensitive land cover data is securely stored and protected from disclosure to third parties.

Since the resulting maps of this research indicate the mangrove cover on shrimp farms in the study area, the land use habits and practices of individual shrimp farmers in the local community could be influenced. For example, shrimp farmers that do not comply with the mangrove cover regulations in the protection and production forest, risk losing their land use rights. Many shrimp farms are family businesses that depend on the land use rights in terms of revenue as well as accommodation. Except for the forestry and aquaculture sector there are not many alternative sources of income in the study area. Accordingly, non-compliance with the regulations could result in the loss of housing and financial stability for individuals and families in the study area. This could have ripple effects on the entire local community. However, shrimp farmers that establish their aquaculture on land in the protection and production forest sign a contract that states the regulations and requirements for the land use rights. Therefore, the shrimp farmers agreed to respect the regulations and preserve 60% mangrove cover on their shrimp farm. To test the compliance with this regulation, the Forest Management Board puts a lot of effort into the mangrove monitoring. Nonetheless, the laborious monitoring of the Forest Management Board only detects about three cases of community-level violations annually, although a survey by Truong et al. (2021) indicates that about 50% of the investigated households cleared the mangrove cover to an extent that exceeds the regulated level. Consequently, the approaches studied in this research offer a more transparent and efficient mangrove observation that could improve the current monitoring performed by the Forest Management Board. A more transparent mangrove assessment using remote sensing imagery could incentivize a more efficient ecosystem restoration and contribute to more sustainable aquacultures. As a result, the ecosystem services of a healthy mangrove forest would support and benefit the human, faunal and floral community in the study area.

LIST OF REFERENCES

Airbus. (n.d.). *SPOT Imagery User Guide DEFENCE AND SPACE Intelligence Organisation of the SPOT 6 & SPOT 7 Imagery User Guide.*

Airbus. (2022). *Satellite pour l'observation de la terre (SPOT 7) image of the study area in Nam Can district, Vietnam 8°43'35.00''N, 104°54'6.00''E.*

Alongi, D. M. (2018). *Blue Carbon Coastal Sequestration for Climate Change Mitigation.* Springer Science.

Amarasingam, N., Ashan Salgadoe, A. S., Powell, K., Gonzalez, L. F., & Natarajan, S. (2022). A review of UAV platforms, sensors, and applications for monitoring of sugarcane crops. In *Remote Sensing Applications: Society and Environment* (Vol. 26). Elsevier B.V. https://doi.org/10.1016/j.rsase.2022.100712

Andalibi, L., Ghorbani, A., Moameri, M., Hazbavi, Z., Nothdurft, A., Jafari, R., & Dadjou, F. (2021). Leaf area index variations in ecoregions of ardabil province, iran. *Remote Sensing, 13*(15). https://doi.org/10.3390/rs13152879

Aprilia, D., Arifiani, K. N., Dianti, D., Cahyaningsih, A. P., Kusumaningrum, L., Sarno, S., Rahim, K. A. B. A., & Setyawan, A. D. (2022). Review: Biogeochemical process in mangrove ecosystem. *International Journal of Bonorowo Wetlands, 10*(2). https://doi.org/10.13057/bonorowo/w100205

Baumgartner, U., & Nguyen, T. H. (2017). Organic certification for shrimp value chains in Ca Mau, Vietnam: a means for improvement or an end in itself? *Environment, Development and Sustainability, 19*(3), 987–1002. https://doi.org/10.1007/s10668-016-9781-z

Behera, M. D., Barnwal, S., Paramanik, S., Das, P., Bhattyacharya, B. K., Jagadish, B., Roy, P. S., Ghosh, S. M., & Behera, S. K. (2021). Species-level classification and mapping of a mangrove forest using random forest—utilisation of aviris-ng and sentinel data. *Remote Sensing, 13*(11). https://doi.org/10.3390/rs13112027

Bektas Balcik, F., & Karakacan Kuzucu, A. (2016). Determination of land cover/land use using spot 7 data with supervised classification methods. *International Archives of the Photogrammetry, Remote Sensing and Spatial Information Sciences - ISPRS Archives, 42*(2W1), 143–146. https://doi.org/10.5194/isprs-archives-XLII-2-W1-143-2016

Bosma, R. H., Nguyen, T. H., Siahainenia, A. J., Tran, H. T. P., & Tran, H. N. (2016). Shrimp-based livelihoods in mangrove silvo-aquaculture farming systems. *Reviews in Aquaculture, 8*(1), 43–60. https://doi.org/10.1111/raq.12072

Bouma, T. J., van Belzen, J., Balke, T., Zhu, Z., Airoldi, L., Blight, A. J., Davies, A. J., Galvan, C., Hawkins, S. J., Hoggart, S. P. G., Lara, J. L., Losada, I. J., Maza, M., Ondiviela, B., Skov, M. W., Strain, E. M., Thompson, R. C., Yang, S., Zanuttigh, B., … Herman, P. M. J. (2014). Identifying knowledge gaps hampering application of intertidal habitats in coastal protection: Opportunities & steps to take. *Coastal Engineering, 87*, 147–157. https://doi.org/10.1016/j.coastaleng.2013.11.014

Bunting, P., Hilarides, L., Rosenqvist, A., Lucas, R. M., Kuto, E., Gueye, Y., & Ndiaye, L. (2023). Global Mangrove Watch: Monthly Alerts of Mangrove Loss for Africa. *Remote Sensing, 15*(8), 2050. https://doi.org/10.3390/rs15082050

Campbell, A. D., Fatoyinbo, T., Charles, S. P., Bourgeau-Chavez, L. L., Goes, J., Gomes, H., Halabisky, M., Holmquist, J., Lohrenz, S., Mitchell, C., Moskal, L. M., Poulter, B., Qiu, H., Resende De Sousa, C. H., Sayers, M., Simard, M., Stewart, A. J., Singh, D., Trettin, C., …

Lagomasino, D. (2022). A review of carbon monitoring in wet carbon systems using remote sensing. In *Environmental Research Letters* (Vol. 17, Issue 2). IOP Publishing Ltd. https://doi.org/10.1088/1748-9326/ac4d4d

Cao, J., Leng, W., Liu, K., Liu, L., He, Z., & Zhu, Y. (2018). Object-Based mangrove species classification using unmanned aerial vehicle hyperspectral images and digital surface models. *Remote Sensing, 10*(1). https://doi.org/10.3390/rs10010089

Chen, B., Xiao, X., Li, X., Pan, L., Doughty, R., Ma, J., Dong, J., Qin, Y., Zhao, B., Wu, Z., Sun, R., Lan, G., Xie, G., Clinton, N., & Giri, C. (2017). A mangrove forest map of China in 2015: Analysis of time series Landsat 7/8 and Sentinel-1A imagery in Google Earth Engine cloud computing platform. *ISPRS Journal of Photogrammetry and Remote Sensing, 131*, 104–120. https://doi.org/10.1016/J.ISPRSJPRS.2017.07.011

Chen, N. (2020). Mapping mangrove in Dongzhaigang, China using Sentinel-2 imagery. *Journal of Applied Remote Sensing, 14*(01), 1. https://doi.org/10.1117/1.jrs.14.014508

Chen, Y., Zhou, Y., Ge, Y., An, R., & Chen, Y. (2018). Enhancing land cover mapping through integration of pixel-based and object-based classifications from remotely sensed imagery. *Remote Sensing, 10*(1). https://doi.org/10.3390/rs10010077

Das, S., Hazra, S., Giri, S., Das, I., Chanda, A., Akhand, A., & Maity, S. (2017). Light absorption characteristics of chromophoric dissolved organic matter (CDOM) in the coastal waters of northern Bay of Bengal during winter season. *Indian Journal of Geo Marine Sciences, 46*(05), 884–892.

Dawod, A. Y., & Sharafuddin, M. A. (2021). Assessing mangrove deforestation using pixel-based image: A machine learning approach. *Bulletin of Electrical Engineering and Informatics, 10*(6), 3178–3190. https://doi.org/10.11591/eei.v10i6.3199

DeltaQuad. (2023). *DeltaQuad Pro #MAP*. https://www.deltaquad.com/vtol-drones/map/

Doughty, C. L., & Cavanaugh, K. C. (2019). Mapping coastal wetland biomass from high resolution unmanned aerial vehicle (UAV) imagery. *Remote Sensing, 11*(5). https://doi.org/10.3390/rs11050540

Drăguţ, L., Csillik, O., Eisank, C., & Tiede, D. (2014). Automated parameterisation for multi-scale image segmentation on multiple layers. *ISPRS Journal of Photogrammetry and Remote Sensing, 88*, 119–127. https://doi.org/10.1016/j.isprsjprs.2013.11.018

Drăguţ, L., Tiede, D., & Levick, S. R. (2010). ESP: A tool to estimate scale parameter for multiresolution image segmentation of remotely sensed data. *International Journal of Geographical Information Science, 24*(6), 859–871. https://doi.org/10.1080/13658810903174803

Duarte, C. M., Losada, I. J., Hendriks, I. E., Mazarrasa, I., & Marbà, N. (2013). The role of coastal plant communities for climate change mitigation and adaptation. In *Nature Climate Change* (Vol. 3, Issue 11, pp. 961–968). https://doi.org/10.1038/nclimate1970

el Mahrad, B., Newton, A., Icely, J. D., Kacimi, I., Abalansa, S., & Snoussi, M. (2020). Contribution of remote sensing technologies to a holistic coastal and marine environmental management framework: A review. *Remote Sensing, 12*(14). https://doi.org/10.3390/rs12142313

Ellison, A. M., Felson, A. J., & Friess, D. A. (2020). Mangrove Rehabilitation and Restoration as Experimental Adaptive Management. *Frontiers in Marine Science, 7.* https://doi.org/10.3389/fmars.2020.00327

Estoque, R. C., Myint, S. W., Wang, C., Ishtiaque, A., Aung, T. T., Emerton, L., Ooba, M., Hijioka, Y., Mon, M. S., Wang, Z., & Fan, C. (2018). Assessing environmental impacts and change in Myanmar's mangrove ecosystem service value due to deforestation (2000–2014). *Global Change Biology, 24*(11), 5391–5410. https://doi.org/10.1111/gcb.14409

European Space Agency (ESA). (n.d.). *SPOT 7 Instruments.* Retrieved January 6, 2023, from https://earth.esa.int/eogateway/missions/spot-7

Friess, D. A., Thompson, B. S., Brown, B., Amir, A. A., Cameron, C., Koldewey, H. J., Sasmito, S. D., & Sidik, F. (2016). Policy challenges and approaches for the conservation of mangrove forests in Southeast Asia. *Conservation Biology : The Journal of the Society for Conservation Biology*, *30*(5), 933–949. https://doi.org/10.1111/cobi.12784

Friess, D. A., & Webb, E. L. (2014). Variability in mangrove change estimates and implications for the assessment of ecosystem service provision. *Global Ecology and Biogeography*, *23*(7), 715–725. https://doi.org/10.1111/geb.12140

GISGeography. (2022a, May 26). *OBIA – Object-Based Image Analysis (GEOBIA).* https://gisgeography.com/obia-object-based-image-analysis-geobia/

GISGeography. (2022b, May 28). *Spectral Signature Cheatsheet - Spectral Bands in Remote Sensing.* https://gisgeography.com/spectral-signature/

Goldberg, L., Lagomasino, D., Thomas, N., & Fatoyinbo, T. (2020). Global declines in human-driven mangrove loss. *Global Change Biology*, *26*(10), 5844–5855. https://doi.org/10.1111/gcb.15275

Google Earth. (2023). *Cau Mau province 9°5'0"N, 105°8'0"E, elevation 4 ft.* http://www.google.com/earth/

Groenewold, S. A., Stive, M. J. F., Van De Giesen, N. C., Stoop, B., Bouziotas, D., Hanssen, J., Dunnewolt, J., & Postma, M. (2015). *Integrated Coastal Management in the Province Ca Mau-Vietnam. An Integrated Research to the Coastal and Water Resource Management Issues.* https://repository.tudelft.nl/islandora/object/uuid:021a36a7-f7ce-406f-9e62-605e8de8ec6f/datastream/OBJ1/download

Gruber, E., Cuong, L. V., & Nguyen, H. T. (2020). *Surveillance 2 Audit Report - Final.* https://myasc.asc-aqua.org/netapp/FileHandler.ashx?id=9FCDF19E-65EA-4ACD-A35D-B340B627DCD4

Guo, M., Li, J., Sheng, C., Xu, J., & Wu, L. (2017). A review of wetland remote sensing. In *Sensors (Switzerland)* (Vol. 17, Issue 4). MDPI AG. https://doi.org/10.3390/s17040777

Guo, X., Ye, J., & Hu, Y. (2022). Analysis of Land Use Change and Driving Mechanisms in Vietnam during the Period 2000–2020. *Remote Sensing*, *14*(7). https://doi.org/10.3390/rs14071600

Gupta, K., Mukhopadhyay, A., Giri, S., Chanda, A., Datta Majumdar, S., Samanta, S., Mitra, D., Samal, R. N., Pattnaik, A. K., & Hazra, S. (2018). An index for discrimination of mangroves from non-mangroves using LANDSAT 8 OLI imagery. *MethodsX*, *5*, 1129–1139. https://doi.org/10.1016/j.mex.2018.09.011

Ha, T. T. P., van Dijk, H., & Visser, L. (2014). Impacts of changes in mangrove forest management practices on forest accessibility and livelihood: A case study in mangrove-shrimp farming system in Ca Mau Province, Mekong Delta, Vietnam. *Land Use Policy*, *36*, 89–101. https://doi.org/10.1016/j.landusepol.2013.07.002

Ha, T. T. T., van Dijk, H., & Bush, S. R. (2012). Mangrove conservation or shrimp farmer's livelihood? The devolution of forest management and benefit sharing in the Mekong Delta, Vietnam. *Ocean and Coastal Management*, *69*, 185–193. https://doi.org/10.1016/j.ocecoaman.2012.07.034

Hati, J. P., Samanta, S., Rani Chaube, N., Misra, A., Giri, S., Pramanick, N., Gupta, K., Datta Majumdar, S., Chanda, A., Mukhopadhyay, A., & Hazra, S. (2021). Mangrove classification using airborne hyperspectral AVIRIS-NG and comparing with other spaceborne hyperspectral

and multispectral data. *Egyptian Journal of Remote Sensing and Space Science*, *24*(2), 273–281. https://doi.org/10.1016/j.ejrs.2020.10.002

Havice, E., & Iles, A. (2015). Shaping the aquaculture sustainability assemblage: Revealing the rule-making behind the rules. *Geoforum*, *58*, 27–37. https://doi.org/10.1016/j.geoforum.2014.10.008

Hijmans, R., Rojas, E., Cruz, M., O'Brien, R., & Barrantes, I. (n.d.). *DIVA-GIS. Spatial Data Download. Country: Vietnam. Subject: Administrative areas (GADM).* Retrieved June 8, 2023, from https://biogeo.ucdavis.edu/data/diva/adm/VNM_adm.zip

Hock, L. K., & Su, Y. T. (2020). Climate change mitigation and adaptation: role of mangroves in Southeast Asia. In W. Leal Filho, A. M. Azul, L. Brandli, P. G. Özuyar, & T. Wall (Eds.), *Climate Action* (pp. 224–236). Springer International Publishing. https://doi.org/10.1007/978-3-319-95885-9

Hogestijn, J. (2023). *The Effectiveness of Policy Implementation in the Forest Management Zones in Ca Mau, Vietnam.* ITC University of Twente.

Horstman, E. M., Dohmen-Janssen, C. M., Narra, P. M. F., van den Berg, N. J. F., Siemerink, M., & Hulscher, S. J. M. H. (2014). Wave attenuation in mangroves: A quantitative approach to field observations. *Coastal Engineering*, *94*, 47–62. https://doi.org/10.1016/j.coastaleng.2014.08.005

Hsu, A. J., Kumagai, J., Favoretto, F., Dorian, J., Martinez, B. G., & Aburto-Oropeza, O. (2020). Driven by drones: Improving mangrove extent maps using high-resolution remote sensing. *Remote Sensing*, *12*(23), 1–18. https://doi.org/10.3390/rs12233986

Huang, Z., Tian, Y., Zhang, Q., Huang, Y., Liu, R., Huang, H., Zhou, G., Wang, J., Tao, J., Yang, Y., Zhang, Y., Lin, J., Tan, Y., Deng, J., & Liu, H. (2022). Estimating mangrove above-ground biomass at Maowei Sea, Beibu Gulf of China using machine learning algorithm with Sentinel-1 and Sentinel-2 data. *Geocarto International.* https://doi.org/10.1080/10106049.2022.2102226

Jhonnerie, R., Siregar, V. P., & Nababan, B. (2017). Comparison of Random Forest Algorithm Which Implemented on Object and Pixel Based Classification For Mangrove Land Cover Mapping. *Applied Science and Technology*, *1*(1), 293–302. http://www.estech.org

Jhonnerie, R., Siregar, V. P., Nababan, B., Prasetyo, L. B., & Wouthuyzen, S. (2015). Random Forest Classification for Mangrove Land Cover Mapping Using Landsat 5 TM and Alos Palsar Imageries. *Procedia Environmental Sciences*, *24*, 215–221. https://doi.org/10.1016/j.proenv.2015.03.028

Jiang, Y., Zhang, L., Yan, M., Qi, J., Fu, T., Fan, S., & Chen, B. (2021). High-resolution mangrove forests classification with machine learning using worldview and uav hyperspectral data. *Remote Sensing*, *13*(8). https://doi.org/10.3390/rs13081529

Joffre, O. M., Bosma, R. H., Bregt, A. K., van Zwieten, P. A. M., Bush, S. R., & Verreth, J. A. J. (2015). What drives the adoption of integrated shrimp mangrove aquaculture in Vietnam? *Ocean and Coastal Management*, *114*, 53–63. https://doi.org/10.1016/j.ocecoaman.2015.06.015

Juhls, B., Paul Overduin, P., Hölemann, J., Hieronymi, M., Matsuoka, A., Heim, B., & Fischer, J. (2019). Dissolved organic matter at the fluvial-marine transition in the Laptev Sea using in situ data and ocean colour remote sensing. *Biogeosciences*, *16*(13), 2693–2713. https://doi.org/10.5194/bg-16-2693-2019

Kamal, M., Hidayatullah, M. F., Mahyatar, P., & Ridha, S. M. (2022). Estimation of aboveground mangrove carbon stocks from WorldView-2 imagery based on generic and species-specific allometric equations. *Remote Sensing Applications: Society and Environment*, *26*. https://doi.org/10.1016/j.rsase.2022.100748

Kamal, M., & Phinn, S. (2011). Hyperspectral data for mangrove species mapping: A comparison of pixel-based and object-based approach. *Remote Sensing*, *3*(10), 2222–2242. https://doi.org/10.3390/rs3102222

Kavzoglu, T. (2017). Object-Oriented Random Forest for High Resolution Land Cover Mapping Using Quickbird-2 Imagery. *Handbook of Neural Computation*, 607–619. https://doi.org/10.1016/B978-0-12-811318-9.00033-8

Kien, P. A., Tuan, V. A., & Trung, N. T. (2017). Development of sustainable ecotourism at Ramsar site Mui Ca Mau. *Van Hien University Journal of Science*, *5*(2), 201–211. https://tckh.vhu.edu.vn/Resources/Docs/SubDomain/tckh/Phung%20Anh%20Kien,%20Vu%20Anh%20Tuan,%20Nguyen%20Tan%20Trung%20-%20Development%20of%20sustainable%20ecotourism%20at%20Ramsar%20site%20Mui%20Ca%20Mau.pdf

Klemas, V. (2013). Using Remote Sensing to Select and Monitor Wetland Restoration Sites: An Overview. *Journal of Coastal Research*, *29*(4), 958–970. https://doi.org/10.2307/23486563

Lai, Q. T., Tuan, V. A., Thuy, N. T. B., Huynh, L. D., & Duc, N. M. (2022). A closer look into shrimp yields and mangrove coverage ratio in integrated mangrove-shrimp farming systems in Ca Mau, Vietnam. *Aquaculture International*, *30*(2), 863–882. https://doi.org/10.1007/s10499-021-00831-1

Lassalle, G., & de Souza Filho, C. R. (2022). Tracking canopy gaps in mangroves remotely using deep learning. *Remote Sensing in Ecology and Conservation*, *8*(6), 890–903. https://doi.org/10.1002/rse2.289

Li, Z., Zan, Q., Yang, Q., Zhu, D., Chen, Y., & Yu, S. (2019). Remote estimation of mangrove aboveground carbon stock at the species level using a low-cost unmanned aerial vehicle system. *Remote Sensing*, *11*(9). https://doi.org/10.3390/rs11091018

Liu, C., Frazier, P., & Kumar, L. (2007). Comparative assessment of the measures of thematic classification accuracy. *Remote Sensing of Environment*, *107*(4), 606–616. https://doi.org/10.1016/j.rse.2006.10.010

Luo, Y. M., Huang, D. T., Liu, P. Z., & Feng, H. M. (2016). An novel random forests and its application to the classification of mangroves remote sensing image. *Multimedia Tools and Applications*, *75*(16), 9707–9722. https://doi.org/10.1007/s11042-015-2906-9

Luom, T. T., Phong, N. T., Anh, N. T., Tung, N. T., Tu, L. X., & Duong, T. A. (2021). Using fine-grained sediment and wave attenuation as a new measure for evaluating the efficacy of offshore breakwaters in stabilizing an eroded muddy coast: Insights from ca mau, the mekong delta of vietnam. *Sustainability (Switzerland)*, *13*(9). https://doi.org/10.3390/su13094798

Lv, Z., Zhang, P., & Benediktsson, J. A. (2017). Automatic object-oriented, spectral-spatial feature extraction driven by Tobler's first law of geography for very high resolution aerial imagery classification. *Remote Sensing*, *9*(3). https://doi.org/10.3390/rs9030285

Mack, B., Leinenkugel, P., Kuenzer, C., & Dech, S. (2017). A semi-automated approach for the generation of a new land use and land cover product for Germany based on Landsat time-series and Lucas in-situ data. *Remote Sensing Letters*, *8*(3), 244–253. https://doi.org/10.1080/2150704X.2016.1249299

Mahmoudi, F. T., & Karami, A. (2020). Quantitative Assessment of Transformation Based Satellite Image Pan-sharpening Algorithms. *Journal of Electrical and Computer Engineering Innovations*, *8*(2), 161–168. https://doi.org/10.22061/JECEI.2020.7191.367

Manandhar, R., Odehi, I. O. A., & Ancevt, T. (2009). Improving the accuracy of land use and land cover classification of landsat data using post-classification enhancement. *Remote Sensing*, *1*(3), 330–344. https://doi.org/10.3390/rs1030330

Massó i Alemán, S., Bourgeois, C., Appeltans, W., Vanhoorne, B., de Hauwere, N., Stoffelen, P., Heughebaert, A., & Dahdouh-Guebas, F. (2010). The "Mangrove Reference Database and Herbarium." *Plant Ecology and Evolution*, *143*(2), 225–232. https://doi.org/10.5091/plecevo.2010.439

Maulana, E., Wulan, T. R., Wahyunungsih, D. S., Ibrahim, F., Putra, A. S., & Putra, M. D. (2017). Geoecology identification using landsat 8 for spatial planning in north Sulawesi Coastal. *Indonesian Journal of Geography*, *49*(2), 212–217. https://doi.org/10.22146/ijg.13189

Maurya, K., Mahajan, S., & Chaube, N. (2021). Remote sensing techniques: mapping and monitoring of mangrove ecosystem—a review. In *Complex and Intelligent Systems* (Vol. 7, Issue 6, pp. 2797–2818). Springer International Publishing. https://doi.org/10.1007/s40747-021-00457-z

Millard, K., & Richardson, M. (2015). On the importance of training data sample selection in Random Forest image classification: A case study in peatland ecosystem mapping. *Remote Sensing*, *7*(7), 8489–8515. https://doi.org/10.3390/rs70708489

Mukherjee, N., Sutherland, W. J., Khan, M. N. I., Berger, U., Schmitz, N., Dahdouh-Guebas, F., & Koedam, N. (2014). Using expert knowledge and modeling to define mangrove composition, functioning, and threats and estimate time frame for recovery. *Ecology and Evolution*, *4*(11), 2247–2262. https://doi.org/10.1002/ece3.1085

Muller-Karger, F. E., Hestir, E., Ade, C., Turpie, K., Roberts, D. A., Siegel, D., Miller, R. J., Humm, D., Izenberg, N., Keller, M., Morgan, F., Frouin, R., Dekker, A. G., Gardner, R., Goodman, J., Schaeffer, B., Franz, B. A., Pahlevan, N., Mannino, A. G., … Jetz, W. (2018). Satellite sensor requirements for monitoring essential biodiversity variables of coastal ecosystems. *Ecological Applications*, *28*(3), 749–760. https://doi.org/10.1002/eap.1682

Muoi, L. Van, Srilert, C., Dang Tri, V. P., & Pham Van, T. (2022). Spatial and temporal variabilities of surface water and sediment pollution at the main tidal-influenced river in Ca Mau Peninsular, Vietnamese Mekong Delta. *Journal of Hydrology: Regional Studies*, *41*. https://doi.org/10.1016/j.ejrh.2022.101082

Nguyen, H., Harper, R. J., & Dell, B. (2023). Examining local community understanding of mangrove carbon mitigation: A case study from Ca Mau province, Mekong River Delta, Vietnam. *Marine Policy*, *148*. https://doi.org/10.1016/j.marpol.2022.105398

Nguyen, H. Q., Tran, D. D., Luan, P. D. M. H., Ho, L. H., Loan, V. T. K., Anh Ngoc, P. T., Quang, N. D., Wyatt, A., & Sea, W. (2020). Socio-ecological resilience of mangrove-shrimp models under various threats exacerbated from salinity intrusion in coastal area of the Vietnamese Mekong Delta. *International Journal of Sustainable Development and World Ecology*, *27*(7), 638–651. https://doi.org/10.1080/13504509.2020.1731859

Nguyen, H. T. T., Doan, T. M., Tomppo, E., & McRoberts, R. E. (2020). Land use/land cover mapping using multitemporal sentinel-2 imagery and four classification methods-A case study from Dak Nong, Vietnam. *Remote Sensing*, *12*(9). https://doi.org/10.3390/RS12091367

Nguyen, P., Rodela, R., Bosma, R., Bregt, A., & Ligtenberg, A. (2018). An Investigation of the Role of Social Dynamics in Conversion to Sustainable Integrated Mangrove-Shrimp Farming in Ben Tre Province, Vietnam. *Singapore Journal of Tropical Geography*, *39*(3), 421–437. https://doi.org/10.1111/sjtg.12238

Pham, L. T. H., & Brabyn, L. (2017). Monitoring mangrove biomass change in Vietnam using SPOT images and an object-based approach combined with machine learning algorithms. *ISPRS Journal of Photogrammetry and Remote Sensing*, *128*, 86–97. https://doi.org/10.1016/j.isprsjprs.2017.03.013

Pham, L. T. H., Vo, T. Q., Dang, T. D., & Nguyen, U. T. N. (2019). Monitoring mangrove association changes in the Can Gio biosphere reserve and implications for management. *Remote Sensing Applications: Society and Environment*, *13*, 298–305. https://doi.org/10.1016/j.rsase.2018.11.009

Pham, M. H., Do, T. H., Pham, V.-M., & Bui, Q.-T. (2020). *Mangrove forest classification and aboveground biomass estimation using an atom search algorithm and adaptive neuro-fuzzy inference system*. https://doi.org/10.1371/journal.pone.0233110

Pham, T. D., Xia, J., Ha, N. T., Bui, D. T., Le, N. N., & Tekeuchi, W. (2019). A review of remote sensing approaches for monitoring blue carbon ecosystems: Mangroves, sea grasses and salt marshes during 2010–2018. *Sensors (Switzerland)*, *19*(8). https://doi.org/10.3390/s19081933

Pham, T. D., Yokoya, N., Bui, D. T., Yoshino, K., & Friess, D. A. (2019). Remote sensing approaches for monitoring mangrove species, structure, and biomass: Opportunities and challenges. *Remote Sensing, 11*(3). https://doi.org/10.3390/rs11030230

Pham, T. T., Vien, N. N., & Vo, Q. T. (2022). Opportunities and challenges for mangrove restoration in the Mekong Delta: Status, policies and stakeholder outlook. In *Opportunities and challenges for mangrove restoration in the Mekong Delta: Status, policies and stakeholder outlook*. Center for International Forestry Research (CIFOR). https://doi.org/10.17528/cifor/008610

Phinn, S. R., Stow, D. A., Franklin, J., Mertes, L. A. K., & Michaelsen, J. (2003). Remotely sensed data for ecosystem analyses: Combining hierarchy theory and scene models. *Environmental Management, 31*(3), 429–441. https://doi.org/10.1007/s00267-002-2837-x

Planet Labs PBC. (2022a). *NICFI Satellite Data Program Frequently Asked Questions*. https://assets.planet.com/docs/NICFI_General_FAQs.pdf

Planet Labs PBC. (2022b, July 22). *SuperDove (PSD.SD) image of the study area in Nam Can district, Vietnam 8°43'35.00"N, 104°54'6.00"E*. https://www.planet.com/

Planet Labs PBC. (2023). *Norway's International Climate and Forests Initiative Satellite Data Program*. https://www.planet.com/nicfi/

Polidoro, B. A., Carpenter, K. E., Collins, L., Duke, N. C., Ellison, A. M., Ellison, J. C., Farnsworth, E. J., Fernando, E. S., Kathiresan, K., Koedam, N. E., Livingstone, S. R., Miyagi, T., Moore, G. E., Nam, V. N., Ong, J. E., Primavera, J. H., Salmo, S. G., Sanciangco, J. C., Sukardjo, S., … Yong, J. W. H. (2010). The loss of species: Mangrove extinction risk and geographic areas of global concern. *PLoS ONE, 5*(4). https://doi.org/10.1371/journal.pone.0010095

Prasad, K. A., Gnanappazham, L., Selvam, V., Ramasubramanian, R., & Kar, C. S. (2015). Developing a spectral library of mangrove species of Indian east coast using field spectroscopy. *Geocarto International*, *30*(5), 580–599. https://doi.org/10.1080/10106049.2014.985743

Quarto, A. (2012). Ecological mangrove restoration: re-establishing a more biodiverse and resilient coastal ecosystem with community participation. In D. J. Macintosh, R. Mahindapala, M. Markopoulos, & International Union for Conservation of Nature and Natural Resources (IUCN) (Eds.), *Sharing lessons on mangrove restoration : proceedings and a call for action from an MFF Regional Colloquium, 30-31 August 2012, Mamallapuram, India* (pp. 277–290).

Ragavan, P., Kathiresan, K., Kumar, S., Nagarajan, B., Jayaraj, R. S. C., Mohan, P. M., Sachithanandam, V., Mageswaran, T., & Rana, T. S. (2021). Biogeography of the Mangrove Ecosystem: Floristics, Population Structure, and Conservation Strategies. In R. P. Rastogi, D. K. Gupta, & M. Phulwaria (Eds.), *Mangroves: Ecology, Biodiversity and Management* (pp. 33–61). Springer Nature Singapore Pte Ltd. https://doi.org/https://doi.org/10.1007/978-981-16-2494-0

Reif, M. K., & Theel, H. J. (2017). Remote sensing for restoration ecology: Application for restoring degraded, damaged, transformed, or destroyed ecosystems. *Integrated Environmental Assessment and Management*, *13*(4), 614–630. https://doi.org/10.1002/ieam.1847

Renaud, F. G., Syvitski, J. P. M., Sebesvari, Z., Werners, S. E., Kremer, H., Kuenzer, C., Ramesh, R., Jeuken, A. D., & Friedrich, J. (2013). Tipping from the Holocene to the Anthropocene: How threatened are major world deltas? In *Current Opinion in Environmental Sustainability* (Vol. 5, Issue 6, pp. 644–654). https://doi.org/10.1016/j.cosust.2013.11.007

Rhyma, P. P., Norizah, K., Hamdan, O., Faridah-Hanum, I., & Zulfa, A. W. (2020). Integration of normalised different vegetation index and Soil-Adjusted Vegetation Index for mangrove vegetation delineation. *Remote Sensing Applications: Society and Environment*, *17*. https://doi.org/10.1016/j.rsase.2019.100280

Ridha, S. M., & Kamal, M. (2021). *An object-based approach for vegetation and non-vegetation discrimination using WorldView-2 image*. 38. https://doi.org/10.1117/12.2619373

Ruwaimana, M., Satyanarayana, B., Otero, V., Muslim, A. M., Muhammad Syafiq, A., Ibrahim, S., Raymaekers, D., Koedam, N., & Dahdouh-Guebas, F. (2018). The advantages of using drones over space-borne imagery in the mapping of mangrove forests. *PLoS ONE*, *13*(7). https://doi.org/10.1371/journal.pone.0200288

Satellite Imaging Corporation. (2022). *Planetscope - Dove Satellite Constellation (3m)*. https://www.satimagingcorp.com/satellite-sensors/other-satellite-sensors/dove-3m/

Sharma, M. (2022). *Comparison of low-cost methods for vegetation mapping using object based analysis of UAV imagery: A case study for the greater Côa Valley, Portugal*. ITC University of Twente.

Shetty, S., Gupta, P. K., Belgiu, M., & Srivastav, S. K. (2021). Assessing the effect of training sampling design on the performance of machine learning classifiers for land cover mapping using multi-temporal remote sensing data and google earth engine. *Remote Sensing*, *13*(8). https://doi.org/10.3390/rs13081433

Shi, T., Liu, J., Hu, Z., Liu, H., Wang, J., & Wu, G. (2016). New spectral metrics for mangrove forest identification. *Remote Sensing Letters*, *7*(9), 885–894. https://doi.org/10.1080/2150704X.2016.1195935

Siregar, V. P., Prabowo, N. W., Agus, S. B., & Subarno, T. (2018). The effect of atmospheric correction on object based image classification using SPOT-7 imagery: A case study in the Harapan and Kelapa Islands. *IOP Conference Series: Earth and Environmental Science*, *176*(1). https://doi.org/10.1088/1755-1315/176/1/012028

Son, N. T., Chen, C. F., Chang, N. bin, Chen, C. R., Chang, L. Y., & Thanh, B. X. (2015). Mangrove mapping and change detection in ca mau peninsula, vietnam, using landsat data and object-based image analysis. *IEEE Journal of Selected Topics in Applied Earth Observations and Remote Sensing*, *8*(2), 503–510. https://doi.org/10.1109/JSTARS.2014.2360691

Talukdar, S., Singha, P., Mahato, S., Shahfahad, Pal, S., Liou, Y. A., & Rahman, A. (2020). Land-use land-cover classification by machine learning classifiers for satellite observations-A review. In *Remote Sensing* (Vol. 12, Issue 7). MDPI AG. https://doi.org/10.3390/rs12071135

Tobler, W. R. (1970). A Computer Movie Simulating Urban Growth in the Detroit Region. In *Geography* (Vol. 46).

Tong, S. S., Pham-Duc, B., Phan, T. H., Bui, V. T., Le, V. C., Pham, T. L., & Tong, T. H. A. (2023). Investigation of estuarine mangrove ecosystem changes using unmanned aerial vehicle images: Case study in Xuan Thuy National Park (Vietnam). *Regional Studies in Marine Science*, *62*. https://doi.org/10.1016/j.rsma.2023.102910

Tran, H., Tran, T., & Kervyn, M. (2015). Dynamics of land cover/land use changes in the Mekong Delta, 1973-2011: A Remote sensing analysis of the Tran Van Thoi District, Ca Mau Province, Vietnam. *Remote Sensing*, *7*(3), 2899–2925. https://doi.org/10.3390/rs70302899

Tran, T. V, Reef, R., & Zhu, X. (2022). A Review of Spectral Indices for Mangrove Remote Sensing. In *Remote Sensing* (Vol. 14, Issue 19). MDPI. https://doi.org/10.3390/rs14194868

Trang, N. T. Q., Quang, T. le, Ai, T. T. H., Giang, N. V., & Hoa, P. V. (2016). Object-Based vs. Pixel-Based Classification of Mangrove Forest Mapping in Vien An Dong Commune, Ngoc Hien District, Ca Mau Province Using VNREDSat-1 Images. *Advances in Remote Sensing*, *05*(04), 284–295. https://doi.org/10.4236/ars.2016.54022

Trimble Inc. (n.d.). *Tutorial-Sample Statistics and Accuracy Assessment*. Retrieved June 13, 2023, from https://support.ecognition.com/hc/en-us/articles/360016128300-Tutorial-Sample-Statistics-and-Accuracy-Assessment-Tool

Trimble Inc. (2020). *ESP II: Automated Estimation of Scale Parameter (ESP2) Tool* . https://support.ecognition.com/hc/en-us/articles/360016278880--ESP-II-Automated-Estimation-of-Scale-Parameter-ESP2-Tool

Truong, D. T., Vo, Q. T., & Pham, K. N. (2021). Does the devolution of forest management help conserve mangrove in the Mekong Delta of Viet Nam? *Land Use Policy*, *106*. https://doi.org/10.1016/j.landusepol.2021.105440

Truong, T. D., & Do, L. H. (2018). Mangrove forests and aquaculture in the Mekong river delta. *Land Use Policy*, *73*, 20–28. https://doi.org/10.1016/J.LANDUSEPOL.2018.01.029

Valderrama-Landeros, L., Flores-de-Santiago, F., Kovacs, J. M., & Flores-Verdugo, F. (2018). An assessment of commonly employed satellite-based remote sensors for mapping mangrove species in Mexico using an NDVI-based classification scheme. *Environmental Monitoring and Assessment*, *190*(1). https://doi.org/10.1007/s10661-017-6399-z

Van, T. T., Wilson, N., Thanh-Tung, H., Quisthoudt, K., Quang-Minh, V., Xuan-Tuan, L., Dahdouh-Guebas, F., & Koedam, N. (2015). Changes in mangrove vegetation area and character in a war and land use change affected region of Vietnam (Mui Ca Mau) over six decades. *Acta Oecologica*, *63*, 71–81. https://doi.org/10.1016/j.actao.2014.11.007

Veettil, B. K., Ward, R. D., Quang, N. X., Trang, N. T. T., & Giang, T. H. (2019). Mangroves of Vietnam: Historical development, current state of research and future threats. In *Estuarine, Coastal and Shelf Science* (Vol. 218, pp. 212–236). Academic Press. https://doi.org/10.1016/j.ecss.2018.12.021

Virdis, S. G. P. (2014). An object-based image analysis approach for aquaculture ponds precise mapping and monitoring: A case study of Tam Giang-Cau Hai Lagoon, Vietnam. *Environmental Monitoring and Assessment*, *186*(1), 117–133. https://doi.org/10.1007/s10661-013-3360-7

Vo, Q. T. (2022). *Survey of shrimp farms in Ca Mau province (unpublished data)*. GIS and remote sensing laboratory, Can Tho University.

Vo, Q. T., Kuenzer, C., Vo, Q. M., Moder, F., & Oppelt, N. (2012). Review of valuation methods for mangrove ecosystem services. In *Ecological Indicators* (Vol. 23, pp. 431–446). https://doi.org/10.1016/j.ecolind.2012.04.022

Vo, Q. T., Oppelt, N., Leinenkugel, P., & Kuenzer, C. (2013). Remote sensing in mapping mangrove ecosystems - an object-based approach. *Remote Sensing*, *5*(1), 183–201. https://doi.org/10.3390/rs5010183

Wang, D., Song, C., Zhang, B., Chen, J., Luo, A., Wang, X., Wu, S., & Ye, Y. (2021). Deciphering dissolved organic matter from freshwater aquaculture ponds in Eastern China based on optical and molecular signatures. *Process Safety and Environmental Protection*, *155*, 122–130. https://doi.org/10.1016/J.PSEP.2021.09.025

Wang, D., Wan, B., Qiu, P., Su, Y., Guo, Q., Wang, R., Sun, F., & Wu, X. (2018). Evaluating the performance of Sentinel-2, Landsat 8 and Pléiades-1 in mapping mangrove extent and species. *Remote Sensing, 10*(9). https://doi.org/10.3390/rs10091468

Wang, D., Wan, B., Qiu, P., Su, Y., Guo, Q., & Wu, X. (2018). Artificial mangrove species mapping using Pléiades-1: An evaluation of pixel-based and object-based classifications with selected machine learning algorithms. *Remote Sensing, 10*(2). https://doi.org/10.3390/rs10020294

Wang, L., Yan, J., Mu, L., & Huang, L. (2020). Knowledge discovery from remote sensing images: A review. In *Wiley Interdisciplinary Reviews: Data Mining and Knowledge Discovery* (Vol. 10, Issue 5). Wiley-Blackwell. https://doi.org/10.1002/widm.1371

Wasniewski, A., Hoscilo, A., Zagajewski, B., & Moukétou-Tarazewicz, D. (2020). Assessment of sentinel-2 satellite images and random forest classifier for rainforest mapping in Gabon. *Forests, 11*(9). https://doi.org/10.3390/f11090941

White, L., Brisco, B., Dabboor, M., Schmitt, A., & Pratt, A. (2015). A collection of SAR methodologies for monitoring wetlands. In *Remote Sensing* (Vol. 7, Issue 6, pp. 7615–7645). MDPI AG. https://doi.org/10.3390/rs70607615

Wilson, N. (2010). *Biomass and Regeneration of Mangrove vegetation in Kien Giang Province, Vietnam.*

Wölcke, J., Albers, T., Roth, M., Vorlaufer, M., & Korte, A. (2016). *Integrated coastal protection and mangrove belt rehabilitation in the Mekong Delta - Pre-feasibility study for investments in coastal protection along 480 kilometers in the Mekong Delta.*

Xuan, B. B., Sandorf, E. D., & Ngoc, Q. T. K. (2021). Stakeholder perceptions towards sustainable shrimp aquaculture in Vietnam. *Journal of Environmental Management, 290.* https://doi.org/10.1016/j.jenvman.2021.112585

Yang, Y., Liang, X., Wang, B., Xie, Z., Shen, X., Sun, X., & Zhu, X. (2022). Biophysical parameters retrieval of mangrove ecosystem using 3D point cloud descriptions from UAV photographs. *Ecological Informatics, 72.* https://doi.org/10.1016/j.ecoinf.2022.101845

Zhao, T., & Li, W. (2022). Design Configuration and Technical Application of Rotary-Wing Unmanned Aerial Vehicles. *Mechatronics and Intelligent Transportation Systems, 1*(1), 69–85. https://doi.org/10.56578/mits010108

Zhu, X., Meng, L., Zhang, Y., Weng, Q., & Morris, J. (2019). Tidal and meteorological influences on the growth of invasive Spartina alterniflora: Evidence from UAV remote sensing. *Remote Sensing, 11*(10). https://doi.org/10.3390/rs11101208

APPENDICES

Appendix A

In this section of the appendices the tutorial developed for training the Ground Truth Point (GTP) sampling is given. The presented workflow using QGIS and the QField application was applied during the GTP field survey in the study area.

Tutorial on setting up a QGIS Project, using QField for field data collection and transfer data to and from QField

Author: Finn Münch, March 2023

The main objective of this tutorial is to expose you to an innovative data collection method for spatially explicit field data (with coordinates!). This tutorial is designed for QGIS users. After having finished this tutorial, you will be able to:

- Set up the Qfield application on your mobile phone and connect it to your laptop where QGIS is installed.
- Start a new QGIS project
- Transfer data from the computer to the mobile phone to allow map display for orientation and navigation.
- Manually digitize and enter data (Ground Truth Points) in the field.
- Downloading the field data from the mobile phone to the computer

The context of this tutorial is a study on land cover assessment in an integrated shrimp farm-mangrove system in Năm Căn district, Cà Mau Province, Vietnam.

Some background:

Although mangroves provide valuable ecosystem services, a severe mangrove forest degradation caused by the establishment of, and cultivation practices on shrimp farms is observed in Vietnam. The land use contracts require the shrimp farmers to maintain 60% mangrove cover on their property. However, the Vietnamese forest management authorities as well as certification organisations lack accurate methods for the observation and quantification of mangroves on shrimp farm scale. A remote sensing-based mangrove monitoring has great potential to provide more accurate, transparent, and regular observations.

To map and classify land cover on farm level, rather high-resolution satellite imagery is required. This study uses a sub-set of a pan-sharpened SPOT-7 image (1.5 m) and a base map downloaded from Google Earth (0.5 m).

The Ground Truth Points (GTPs) to be generated during the sampling campaign (done by you) are going to be used to classify a subset of a SPOT-7 satellite image. The resulting land cover map will allow extracting the mangrove area and assessing the ratio of mangrove area to the total shrimp farm area. The accuracy assessment that accompanies the map provides quality information that is important for policy makers and sustainability certification.

Random sampling is not possible in the highly fragmented mangrove area. Also travelling in the area is challenging and time consuming. Therefore, a clustered sampling approach will be used. To make sure that all the GTPs are well distributed over the study area, randomly 50 farm areas were selected where the clusters of GTP will be taken.

WARNING: Set up an organized directory structure to store the data for your field survey project!

To develop this tutorial, a variety of projects was used to create the examples given in this tutorial. Therefore, the directory paths and file names vary and are not applicable to your individual projects.

To allow multiple individuals collecting data in the field, each student or student group gets an identification letter (e.g. group A). That name should then come back in the folder name to avoid overwriting data later on.

Therefore, create in your computer a folder called "NamCan_GTPs_A" if you are group A, or "NamCan_GTPs_B" if you are group B and so on. This would result for instance, in this simple path directory 'C:\Users\finnm\Desktop\NamCan_GTPs_A' on my PC.

Next, create the following subfolders within the 'NamCan_GTPs_A' folder:

- a subfolder called "Data" to store the relevant data that you use in your QGIS project.
- a subfolder called "QField_Import_NC"
- a subfolder called "QField_Export_NC"

Then create a new QGIS project in the 'NamCan_GTPs_A' folder and name it "NamCan_GTPs_" and again add the your respective group identifier for instance, "A". In this case it would result in the QGIS project name "NamCan_GTPs_A".

Start QGIS, start a new project and set the coordinate system to 'VN-2000 / UTM zone 48N – EPSG:3405' if your study area is in Vietnam.

Now that your computer has a logic folder structure, and you have started QGIS, it is time to take the first steps.

1. Add a basemap to the 'XYZ Tiles' of your QGIS project

Often, it is convenient to use google satellite imagery. You can set it as your basemap as follows:

1.1. **Right click** on 'XYZ Tiles' and select 'New Connection…'.
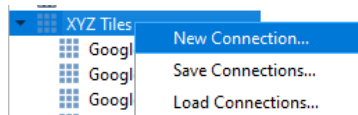
1.2. **Define** the name of the basemap, for instance, 'Google Satellite', in the 'Name' section.

1.3. **Copy** and print the following URL link https://www.google.cn/maps/vt?lyrs=s@189&gl=cn&x={x}&y={y}&z={z} into the 'URL' section.

1.4. **Click** 'OK' to add the 'Google Satellite' basemap to the 'XYZ Tiles'.

A description on how to add a variety of basemaps can be found on the following website https://opensourceoptions.com/blog/how-to-add-google-satellite-imagery-and-google-maps-to-qgis/ .

1.5. Add the 'Google Satellite' XYZ Tile as Layer to your Project by **right clicking** on it and selecting 'Add Layer to Project'.
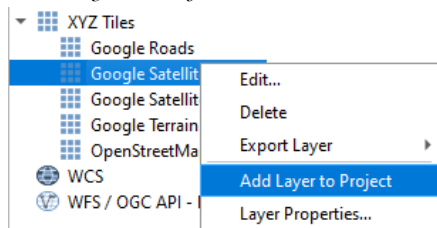
2. Export the google satellite imagery to a GeoTIFF (.tif) file

2.1. **Right click** on the added '*Google Satellite*' layer and **click** 'Export' 'Save As…'.
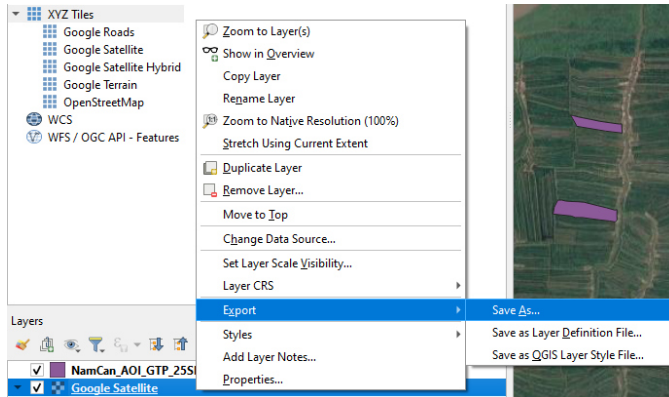
2.2. **Uncheck** the '*Create VRT*' box.
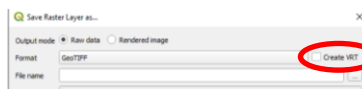
2.3. **Click** the box with the 3 dots next to the '*File name*' box to define the output location and file name of the GeoTIFF.
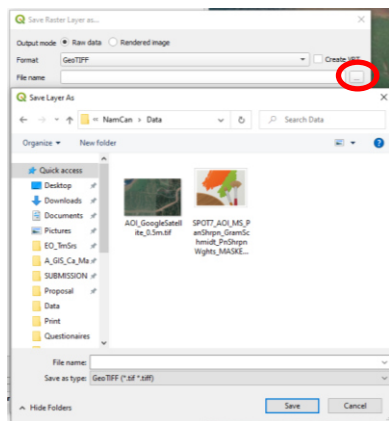
2.4. Select the output Coordinate Reference System *(CRS).*
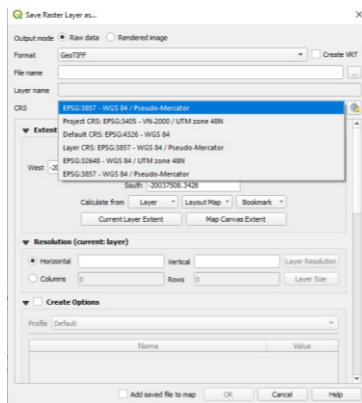
2.5. Select the Extent either from a layer in your project '*Calculate from Layer*' or from the '*Map Canvas Extent*'.
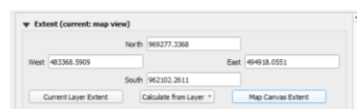
2.6. Define the Resolution. Depending on the '*CRS*' that you chose, the spatial dimensions of the map can be in different units. Since the selected '*CRS*' bases on a UTM projection the unit is given in meters m. In the '*Resolution (current: layer)*' section you can **define** the spatial resolution of the output GeoTIFF. In this tutorial a pixel size of 0.5 m is defined.

2.7. At last, click okay to start the export of the GeoTIFF (*.tif*) file. You can see the progress of the export on the ground bar of QGIS.
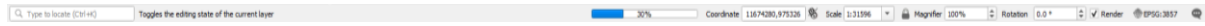
2.8. Once the Layer is successfully exported, a green notification will pop up on the top of the map canvas. The raster layer, in this case called 'TEST.tif', will be added as new layer to the project.
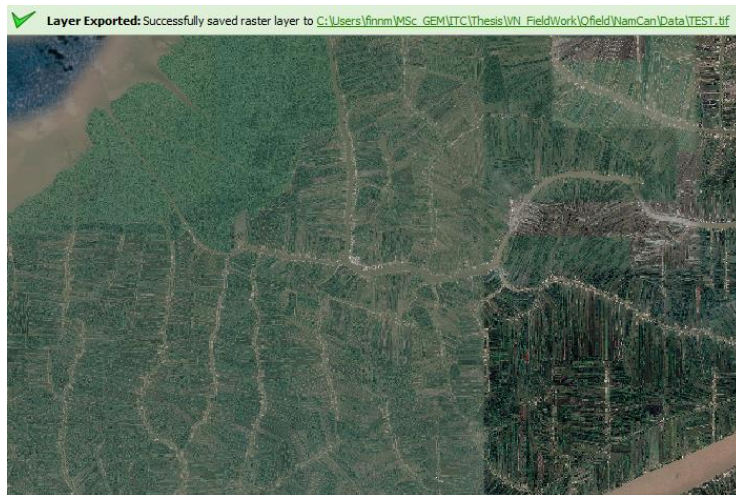
2.9. Now you can remove the '*Google Satellite*' XYZ Tile by **right clicking** on the layer and **selecting** 'Remove Layer…'. **Click** '*OK*' in the pop up window to confirm to remove the layer.
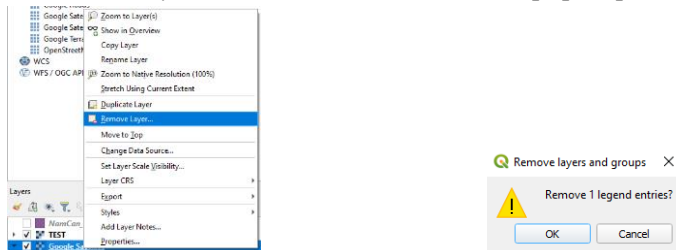
3. Install the Qfield plugin.

3.1. **Click** on '*Plugins*' and then select '*Manage and Install Plugins…*'.
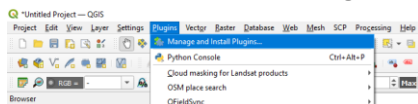
3.2. **Type** '*Qfield*' into the search bar and press enter to search for the plugin.
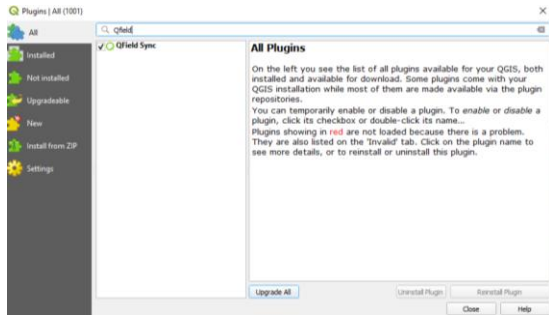
3.3. **Select** '*Qfield*' and install the plugin. If this plugin is already installed you can reinstall it. If there is an update available, as it is the case in the illustration below, you can upgrade the plugin to the current version.
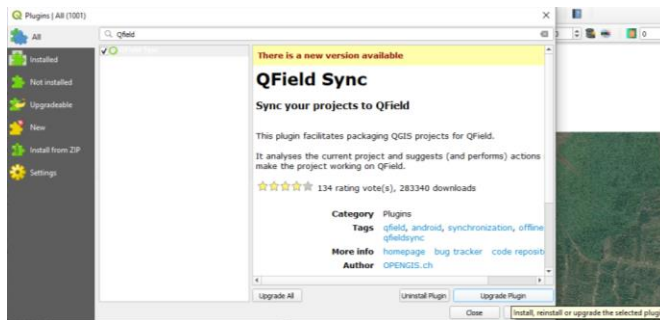
3.4. After successfully installing the '*QField*' plugin, three new buttons called '*Package for QField*', '*Synchronize from QField*', and '*Configure Current Project*' are displayed on the top bar of QGIS.
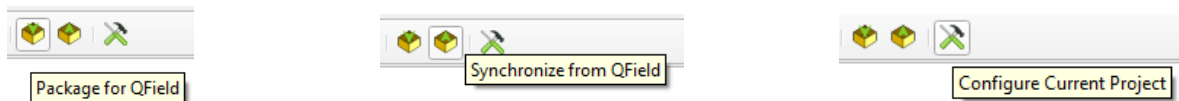
4. Create a point shapefile '.shp' for the landcover sampling survey

4.1. **Click** on '*Layer*', '*Create Layer*', '*New Shapefile Layer…*' to create a new point shapefile.
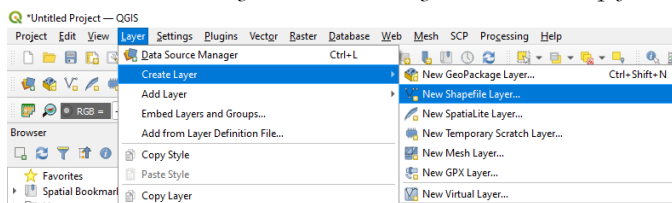
4.2. Browse to the destination folder and **define** the '*File name*' of the new shapefile layer, for instance, "*TEST_GPTs*" by **clicking** on the box with the 3 dots. Finally **click** the '*Save*' button.
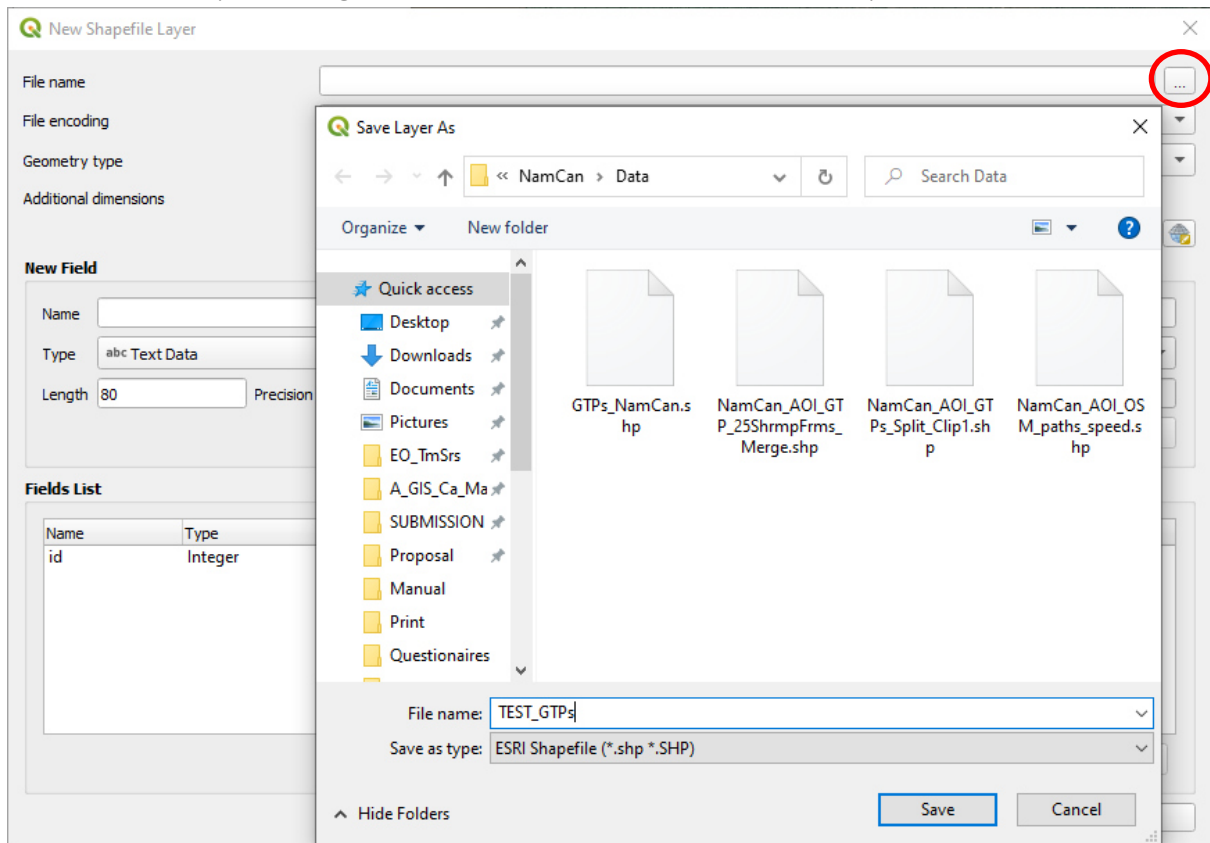
4.3. **Select** '*Point*' as '*Geometry type*'.
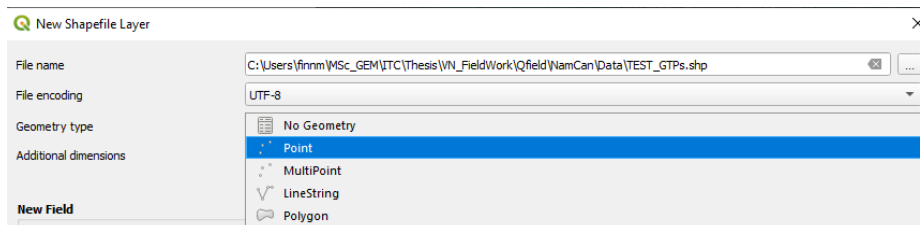
4.4. Select the Coordinate Reference System for instance, "*EPSG:3405 - VN-2000 / UTM Zone 48N*".
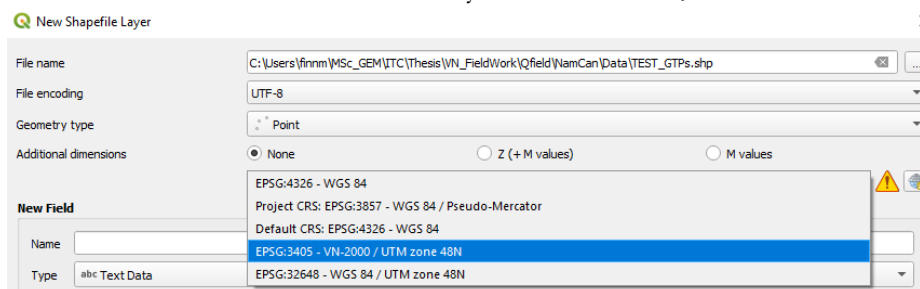
4.5. Now you can **add new fields** to the attribute table of the layer. For example, add a field called '*Class*'. Since we know already in advance the land cover classes that we will observe in the field, we can create a

drop-down list with the options for these classes. We will do this later.
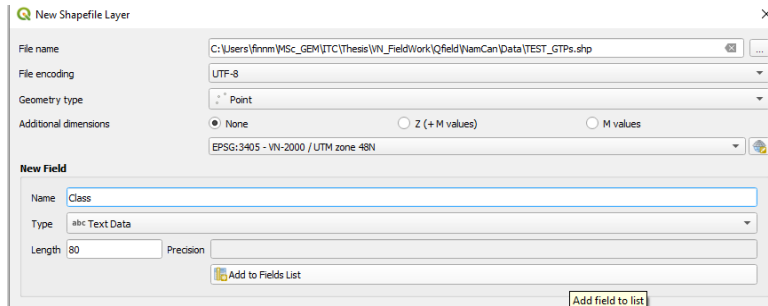
Add a field of the type '*Date*' to represent the date of the observation. **Add** a field of the type '*Text Data*' that will represent the link to the photo of the observed point. Make sure to define a sufficient length, for example 255, to prevent issues with the length of the image name. **Add** a field of the type '*Text Data*' that will represent the code of the observation.

You can also add the fields after you created the new shapefile layer. **Right click** on the new layer and **select** '*Properties*'. Then **browse** to the '*Fields*' section. **Click** on '*Toggle editing mode*' and then '*New Field*'. **Define** the name of the field for instance, "*Date*" and set up the Type to be '*Date*'. Press '*OK*' to create the new field.
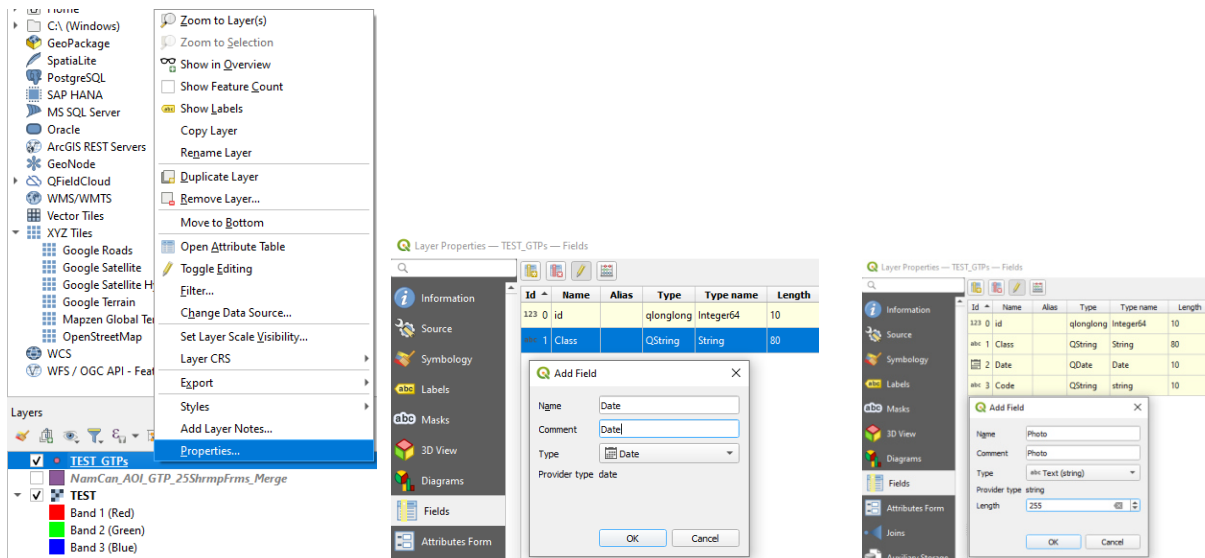
Click on '*Toggle editing mode*' again to stop editing and save the changes by **pressing** '*OK*' in the "*Stop Editing*" pop-up window.
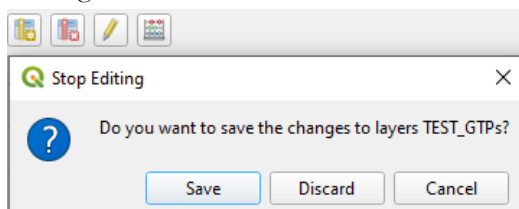
4.6. After you created the new fields, you can create a drop down menu for a particular field if you like. In this tutorial, we will do this for the field 'class' which will contain the land cover classes that we are going to observe in the field and which you need to see in your QField application.

Browse to the '*Attribute Form*' section to set up the fields. **Click** on the field called '*Class*' and select "*Value Map*" as '*Widget type*'.
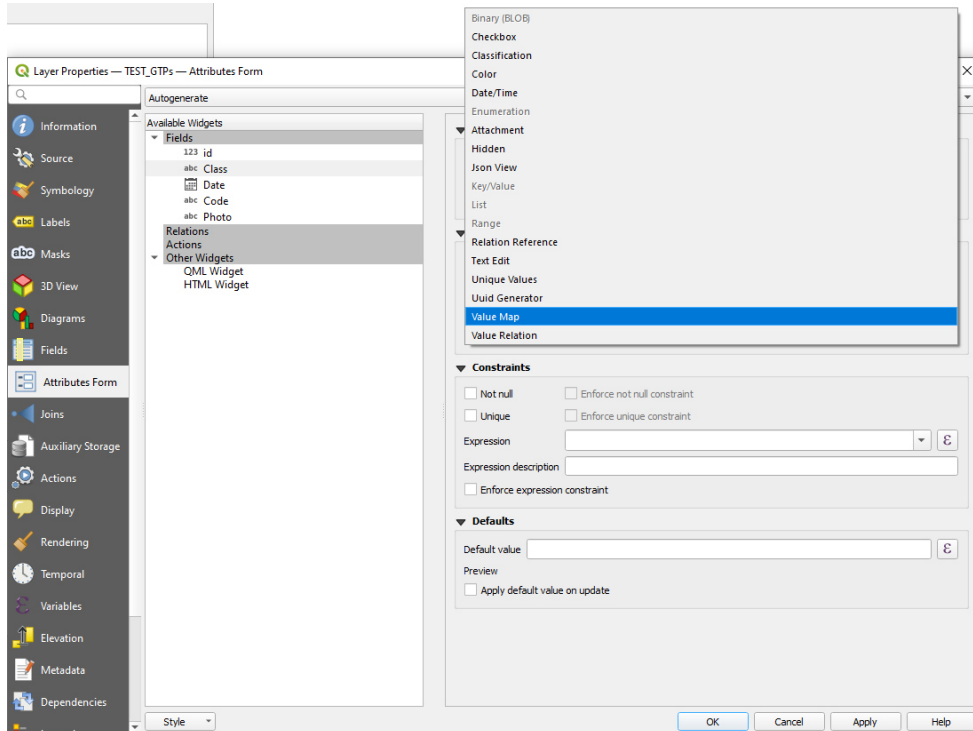
Then **define** the land cover classes you intend to observe, for instance,: "*Mangrove*" and "*Water*". This will generate the options in the drop down menu to select the respective land cover type later in QField. You can also use "*Text Edit*" as '*Widget type*' if you intend to manually type the land cover type for each observation in the field.

Then **check** the '*Not Null*' and '*Enforce not null constraints*' checkboxes to force that this field must be filled out during the field observations.

Next **click** on the field called '*Date*'. Scroll down to the '*Default*' section and **type** "now()" into the '*Default value*' field. This will automatically generate the observation date when a new record is created.
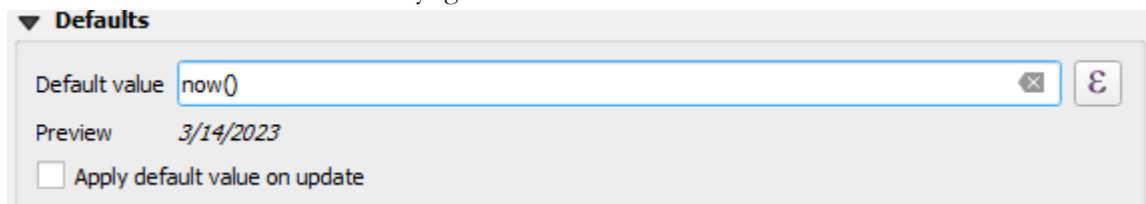
Then **click** on the field called '*Code*' to **check** the '*Not Null*' and '*Enforce not null constraints*' checkboxes to force that this field must be filled out during the field observations.
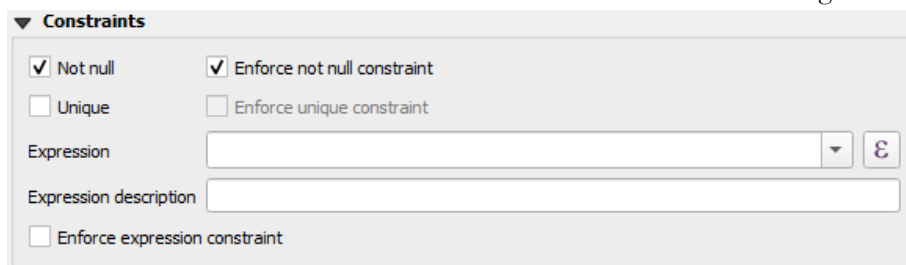
Then **click** on the field called '*Photo*' and **set** the '*Widged type*' to "Attachment". In the '*Constraints*' section check the "*Not null*" and "*Enforce not null constraint*" checkboxes to enforce that a photo of the observation

must be taken. After setting up all fields **click** the '*Apply*' button and then on '*OK*'.
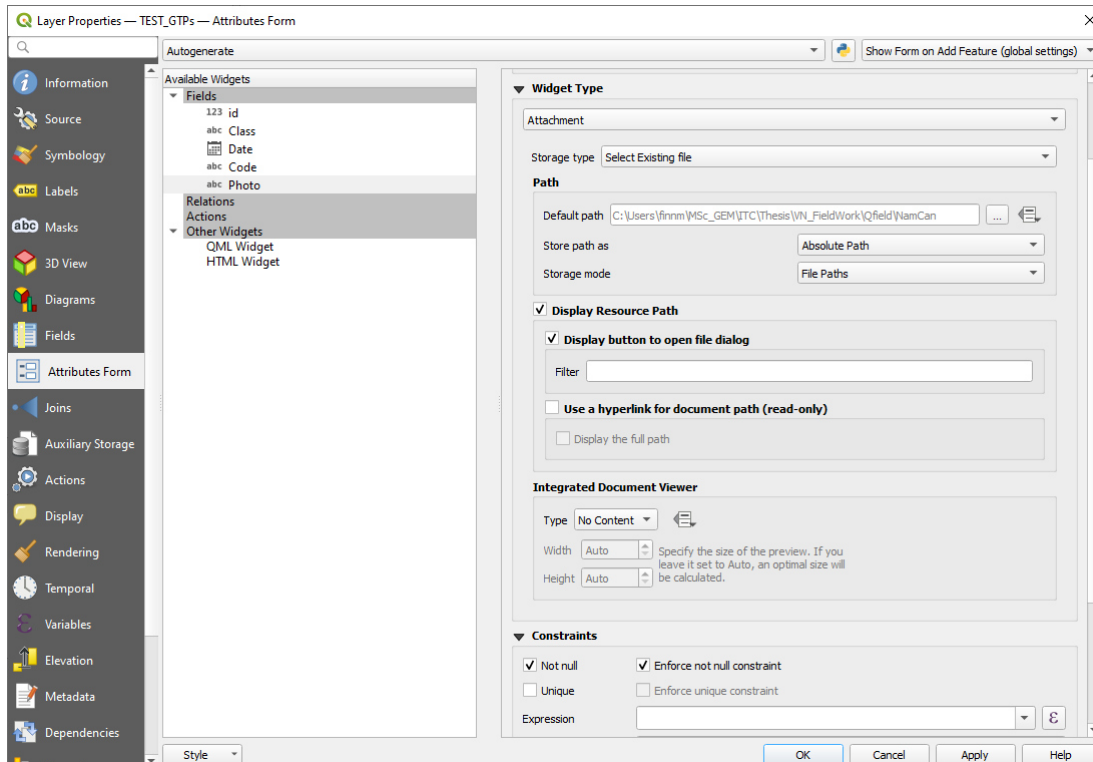
5. Export the QGIS project and its files

After adding all layers that support your field survey, for instance, a road network shapefile or shrimp farm boundaries, to your QGIS project make sure to **save** (**CTRL + S**) it. Now that all edits are saved you can package the project and its files to a QField import folder.

5.1. **Click** on the '*Package for QField*' button.

5.2. A window stating '*WARNINGs*' with error messages may pop up. These errors need to be fixed first. Often it has to do with unsaved changes when you were setting up all the fields or with inconsistencies in

the coordinate system. If there is no '*ERROR*' displayed you can proceed by **clicking** '*Next*'.
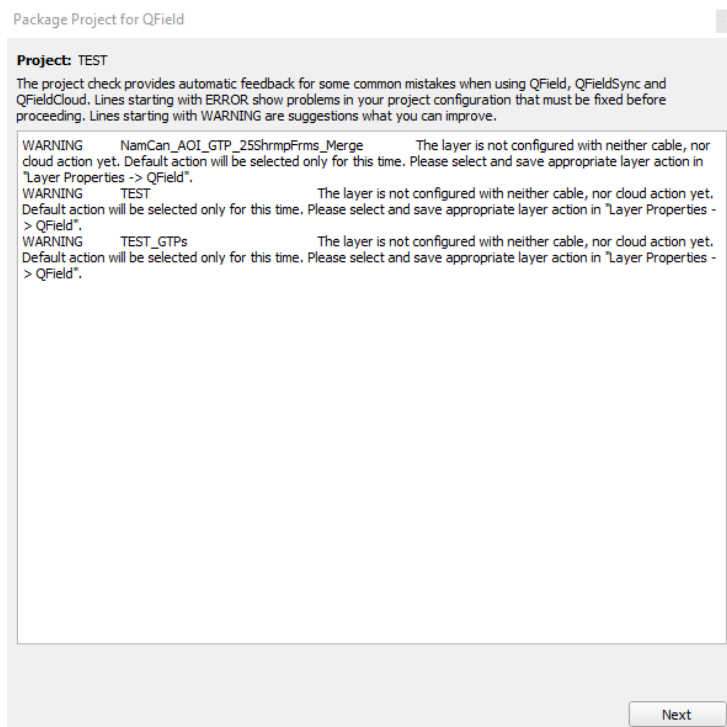
5.3. Create a new directory to store the import data for QField.

5.4. **Deselect** all '*Directories*' in the '*Advanced*' section and then **browse** to your newly created import directory where you intend to store the project and its data. **Click** '*Select Folder*'.
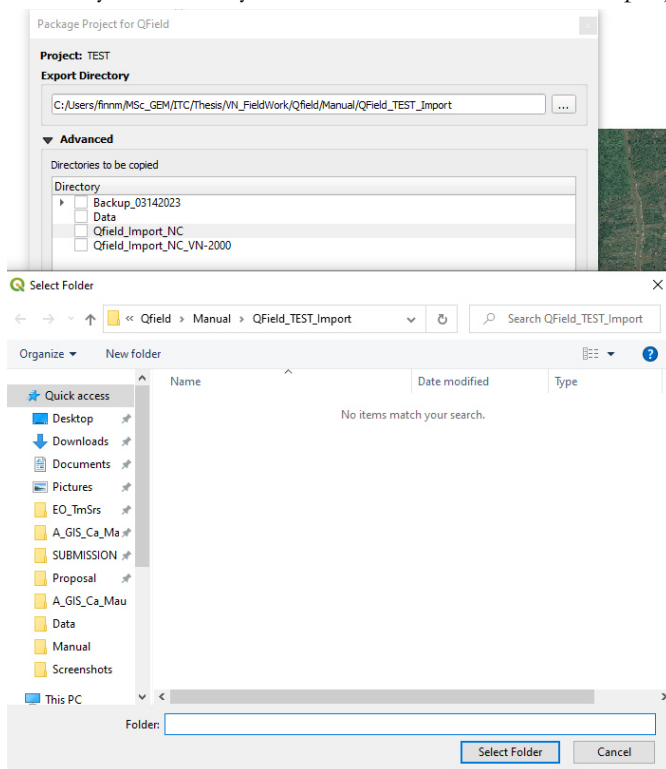
5.5. **Click** '*Create*'. This may take a bit of time. You can observe the progress of the project creation.
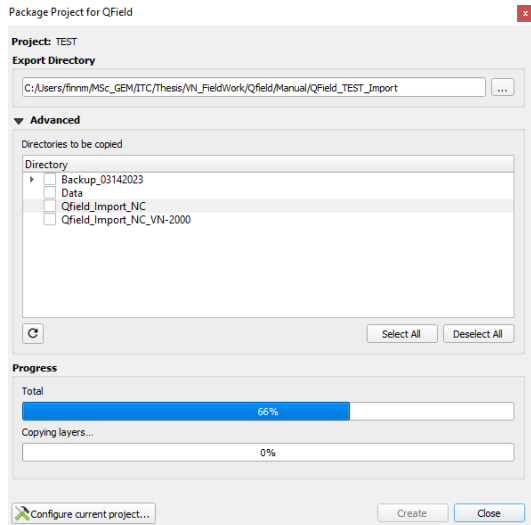
5.6. **Click** '*OK*' to confirm the coordinate system conversion from 'EPSG:32648 – WGS 84 / UTM zone 48N' to 'EPSG:3405 – VN-2000 / UTM zone 48N'.
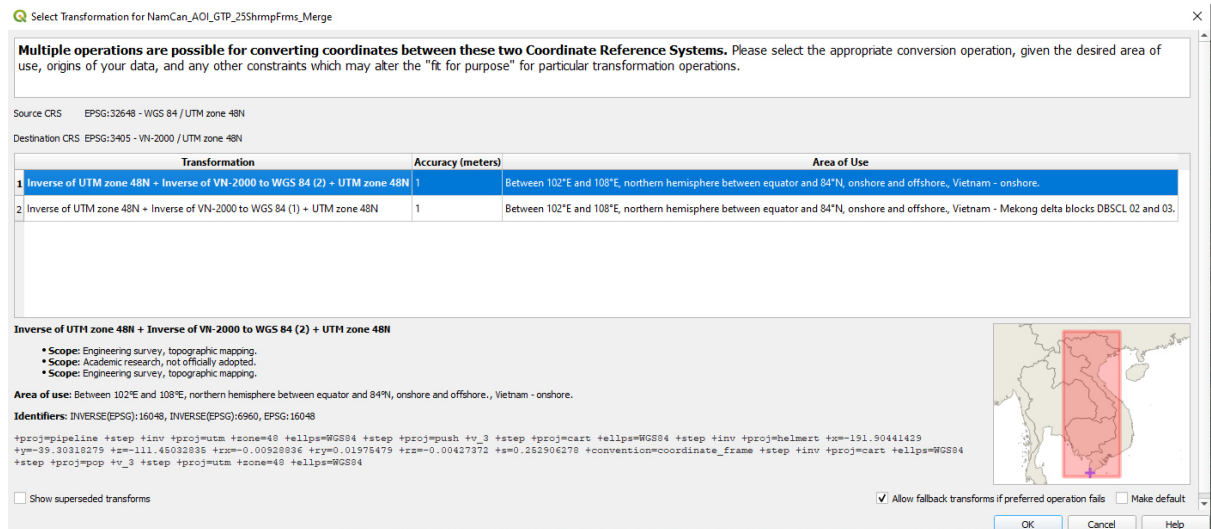
5.7. At last, a green notification will appear under the top tool bar indicating the successful creation of the QGIS project. Moreover, the next step, copying this folder to your QField device, is indicated.

6. Transfer the QField import folder to your mobile device

6.1. **Connect** your mobile QField device via cable to your PC.
6.2. **Create** a folder called "*QField*" on your mobile device.
6.3. **Copy** the "*QField_Import*" folder from your PC to the '*QField*' directory on your mobile QField device.

Setting up and using the QField Application on your mobile phone

1. Set up the QField Project

1.1. **Download** the '*QField*' application from the App Store https://apps.apple.com/us/app/qfield-for-qgis/id1531726814 for IOS and from the Google Play Store https://play.google.com/store/apps/details?id=ch.opengis.qfield&gl=US&pli=1 for Android to the device.

1.2. **Connect** your mobile phone with a cable to your PC. If you use an Android device, **click** on the pop-up window of your phone's top bar or search for "USB Preferences" in your phone's settings.
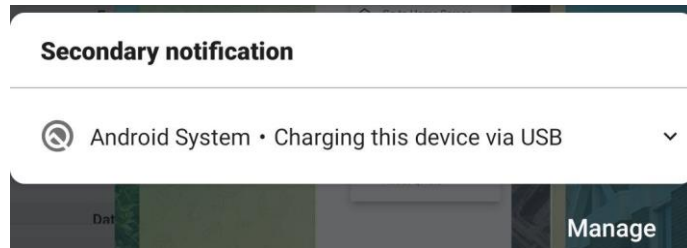
Then **select** '*File Transfer*' in the '*USE USB FOR*' section.
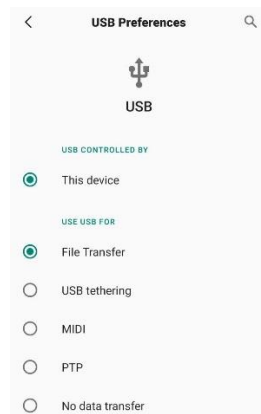
Create a new folder (**CTRL + SHIFT + N**) called '*QField*' on your phone.

Copy the Import folder with your individual identification letter to your phone. For instance, if your identification is "A" you copy (**CTRL + C**) the folder called '*Qfield_Import_NC_A*' and paste (**CTRL + V**) it into the new folder on your phone.
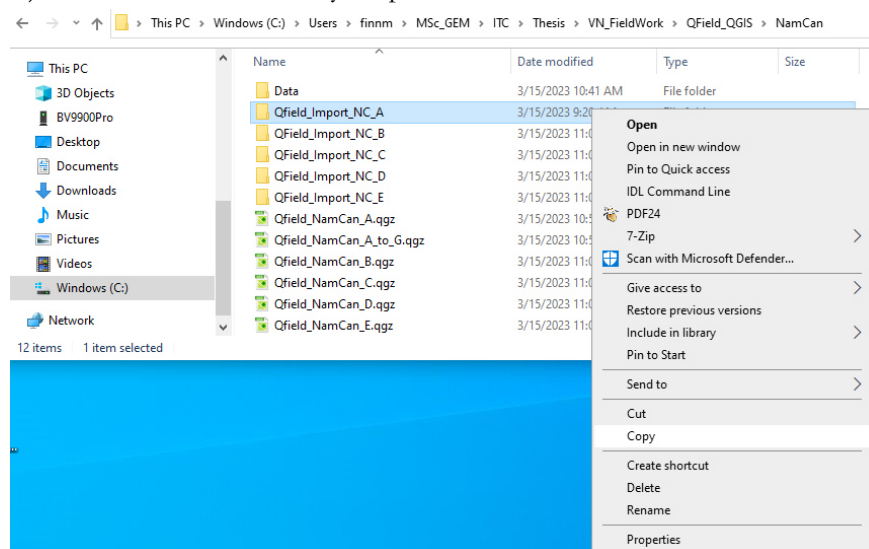
1.3.   **Start**   the   '*QField*'   application   and   **click**   on   '*Open   local   file*'.

1.4. **Press** the green and white plus button on the lower right corner of the screen and select '*Import project from*   *folder*'.
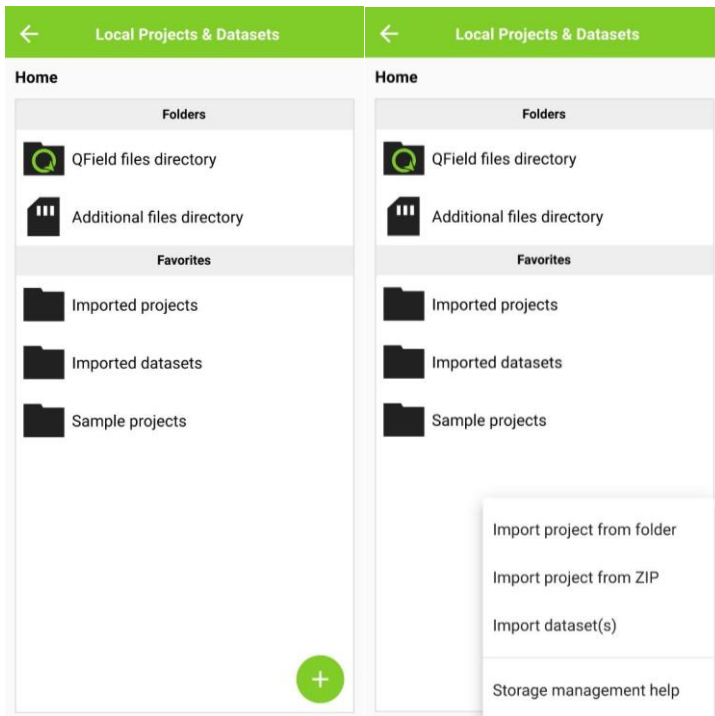
1.5. **Browse** to the '*QField*' folder where the import folder is stored on the device, click '*USE THIS FOLDER*' and then press '*ALLOW*' to grant QField the access. Depending on the size of the project

loading the data into QField can take some time.
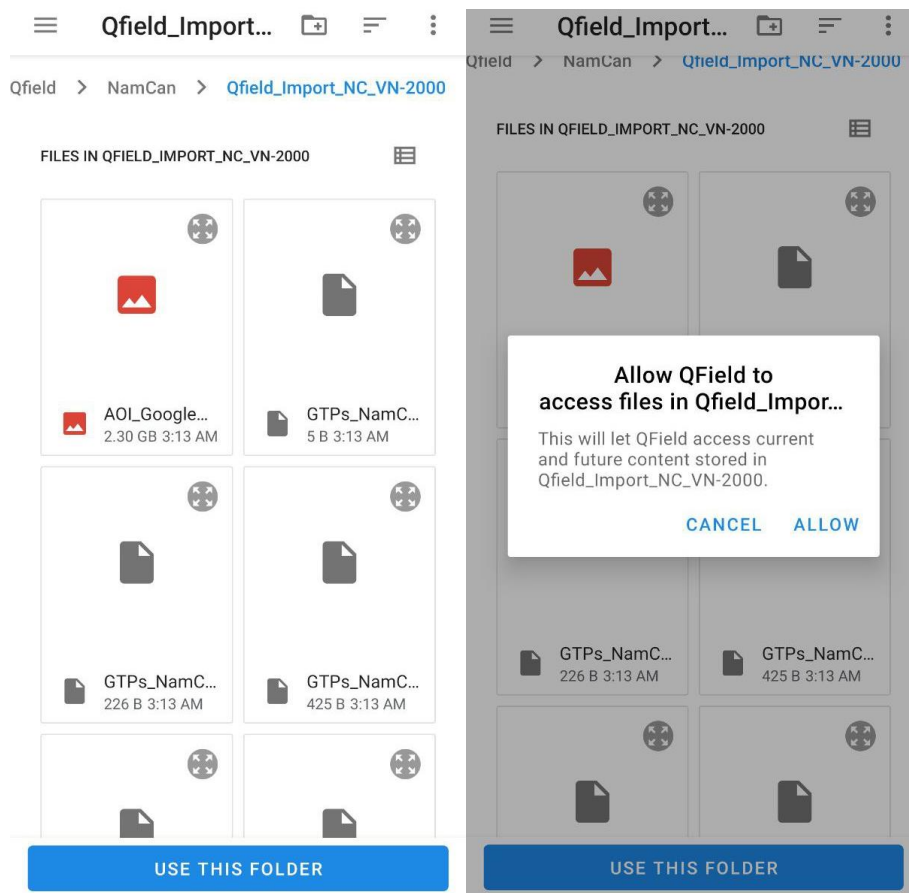
1.6. **Open** the '*QField*' project by **clicking** on the Project file name in this case '*Qfield_NamCan_VN-2000_qfield*'.
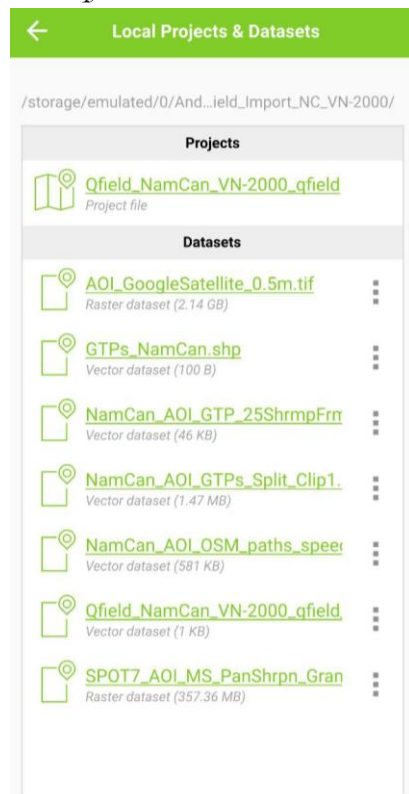
In case that you already opened the Project of interest before, you can directly start it from the QField home screen by clicking on the respective Project name, for instance, '*Qfield_NamCan_VN-2000_qfield*', which is indicated as '*Last session*'
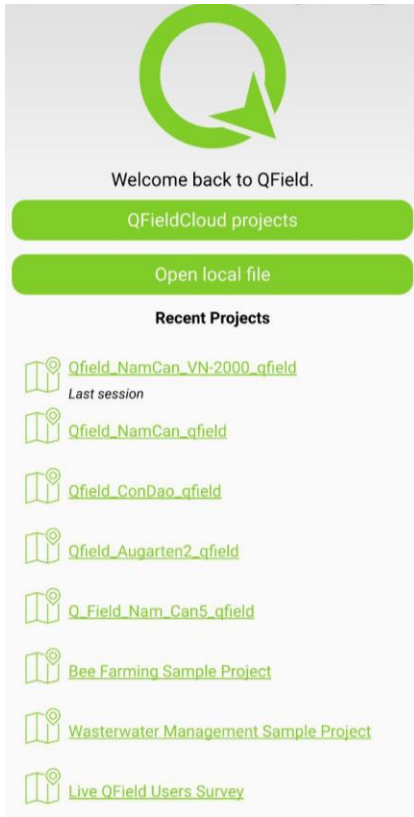
2. QField functions

Press the ▤ button on the top left corner to see the available layers of the QField Project.
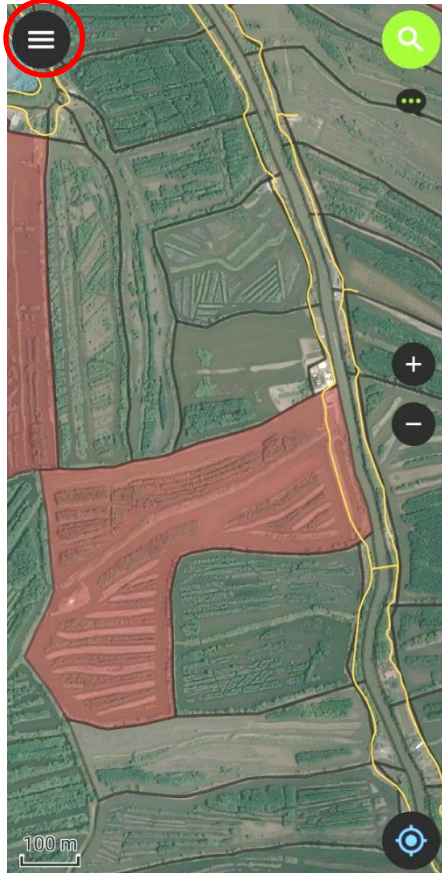
2.1. **Click** on one layer and hold for about 2 seconds to see the edit function for the selected layer. You can display or not display it on the map by checking or unchecking the box called '*Show on map*'.
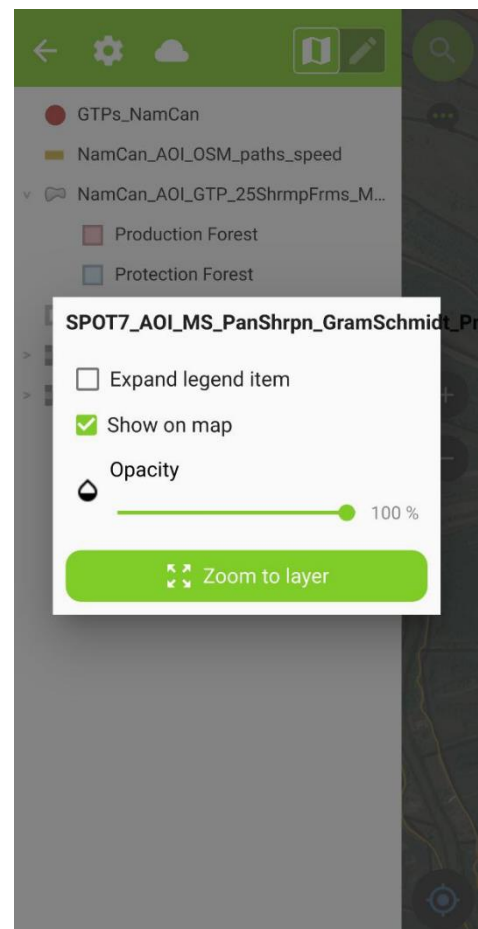
Moreover, you can adjust the opacity of the layers to adjust its transparency with the green slidebar, or '*Zoom to layer*' by clicking the respective green button. Once you are in the study area, don't use the '*Zoom to layer*' function as this will zoom out to the full extent of the layer and cost time too zoom in to the right level of detail again.

When zoomed out sufficiently you will notice some irregular black areas. These are areas that were cloud-covered and these have been masked out. We should avoid positioning the GTP in these masked out area and make sure that a GTP is located in a pixel that clearly represents a particular type of land cover.

Changing between different map layers as background goes easiest by switching the '*Show on map*' function on and off. If you switch off the layer called '*NamCan_AOI_GTP_25ShrmpFrms_Merge*' you can more clearly see the raster satellite images without the transparent red or blue color of this layer. This is useful to select the land cover. Alternatively the '*Opacity*' can be set to 50% with the green slide bar to have more transparent polygons showing close to normal colors while still indicating the shrimp farms of interest.

2.2. Now, let's start adding field data. **Click** on the layer called '*GTPs_NamCan*' and then **press** the button with the pencil in the top right corner to change this layer from 'browse mode' to 'digitize   mode'.
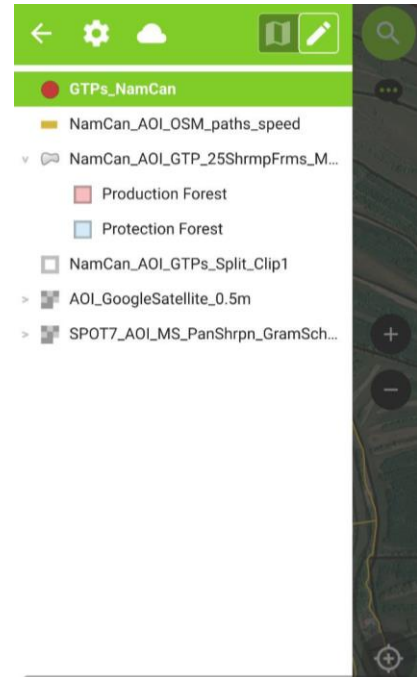

2.3. You can navigate, zoom in and out on the map with your fingers. You can also control the zoom with the plus and minus   button.
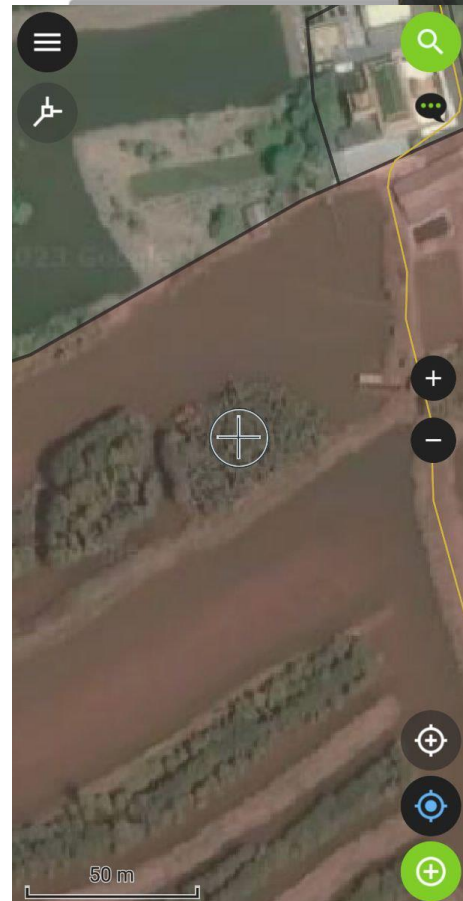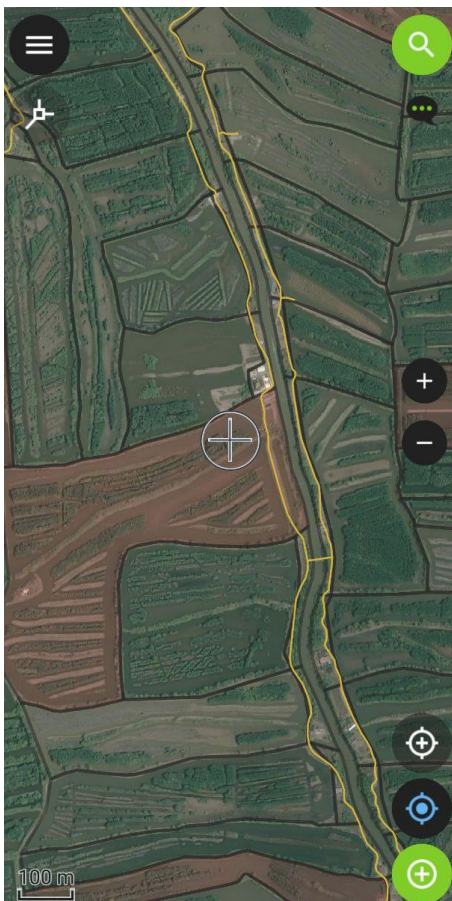
2.4. You can automatically zoom and lock to your cursor to the device's current location by clicking on the upper most button of the lower right corner . The button will switch to blue and have a box around it. To unlock the cursor from your device's position press the button again. The central button switches on or off that the canvas follows the device's location. The central button will appear blue when it is switched on. Press the button again to switch the follow canvas mode off.

The lowest button ⊕ in the bottom right corner adds a new point at the location of the cursor, for instance, on pixels covering mangroves. We will use that later.
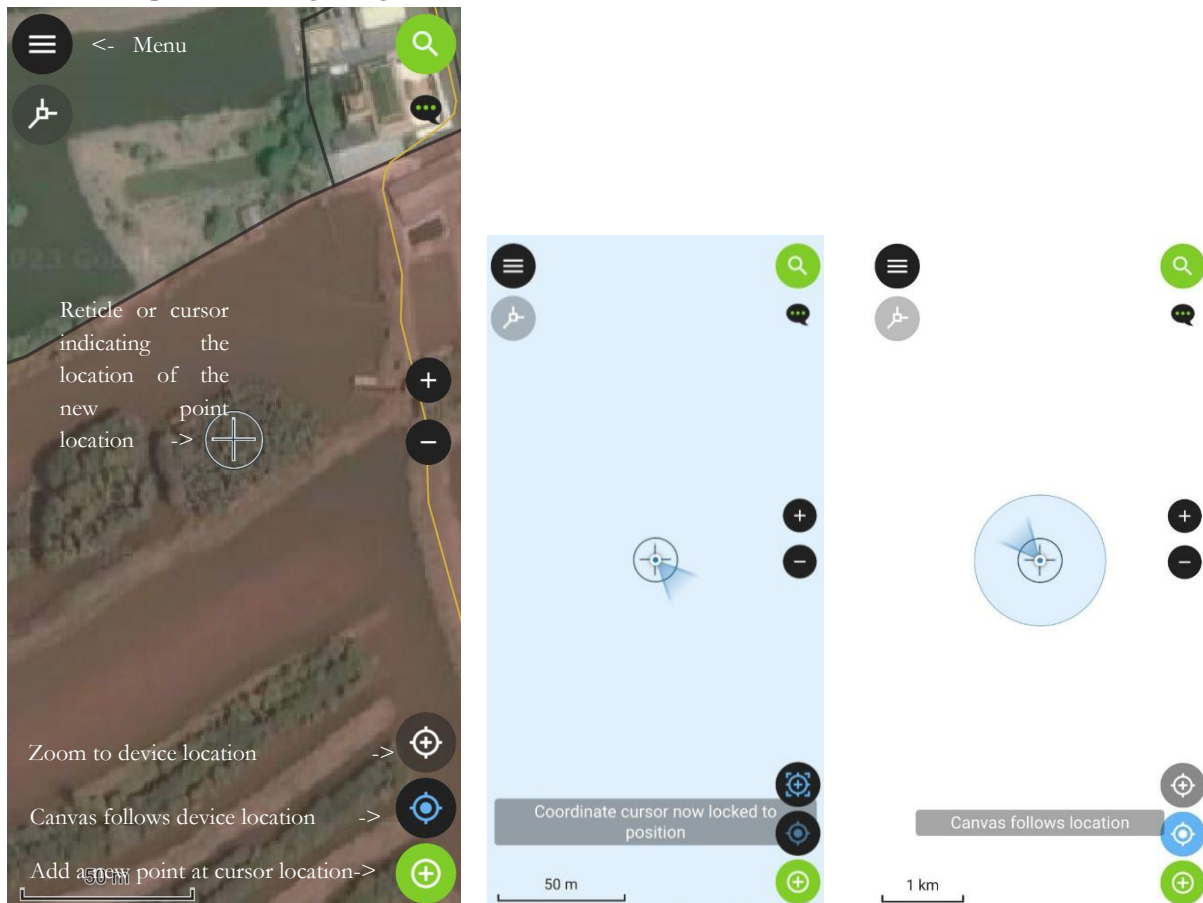
The layer '*AOI_GoogleSatellite_0.5m*' is ideal for recognizing and identification of land cover on an image. However, we want to avoid selecting GTPs on mixed pixels in the SPOT-7 image. Therefore, use the layer called '*SPOT-7*' as background image when entering a GTP.

Press the layer '*GoogleSatellite_0.5m*' for two seconds and uncheck the '*Show on map*' box. Now you can check while using the '*SPOT-7*' as background image if the GTP is located well within the respective land cover type with a buffer of at least one pixel of the same land cover around it.

In general, at farm level the land cover types may occupy a rather narrow or small area, like strips of mangroves, the water in between or the dykes on the farm. So, within a small distance you can probably take a number of GTPs in different land cover types. However, it should be avoided that points of the same land cover class are positioned too close to each other in the same land cover unit. Therefore, make sure they are at least at a distance of 100 m apart from each other.

2.5. **Click** the **green button** ⊕ in the bottom right corner to create a new point. The '*Add Feature on GTPs_NamCan*' window will appear. **Select** the land cover that you are currently observing from the dropdown menu of the '*Class*' section, in this case '*Mangrove*'. **Press** on the camera 📷 in the '*Photo*' section to take an image to the observed land cover class.

Scroll down to the '*Comment*' section to add a comment if you observe something noteworthy describing the point (optional). For instance, you could write a remark on the density and age of the observed mangroves.
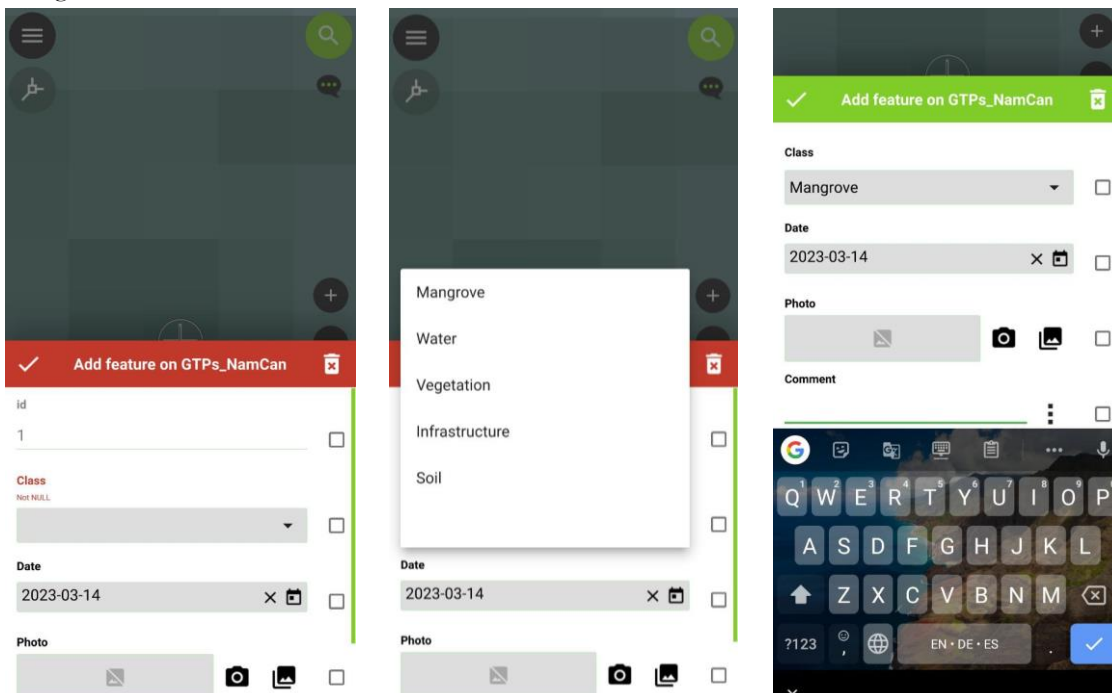
Note (in the comment box) if it is pond or river water when creating a '*Water*' GTP as the water quality and colour of the water may influence the classification. Note what kind of vegetation it is if you generate '*Vegetation*' land cover points that is not mangrove. Note what type of infrastructure you are observing,

for example a shed, bridge, or path, when you create an '*Infrastructure*' GTP. Finally **click** on the checkmark ✅ in the upper left corner of the '*Add feature on GTPs_NamCan*' box to save the point. The new point and a label with its ID will appear on the map.

2.6. In case you want to edit an existing point, you can **click** on the point and **select** the respective point, in this case '*Mangrove*' from the active '*GTP_NamCan*' layer. Then edit whatever is necessary.
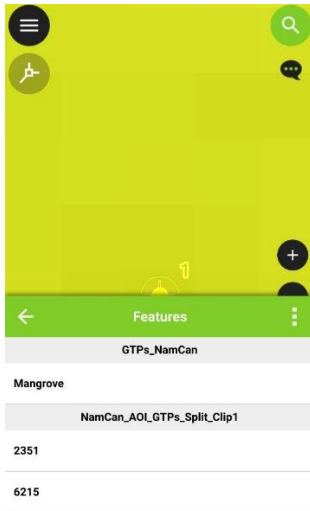
2.7. You can adjust the attributes of the point or have a look at the menu to edit the selected point. The buttons for these functions are displayed on the green top bar of the attribute table. In the worst case you can delete the point by clicking on the menu button ⋮ on the outmost right side of the green bar.
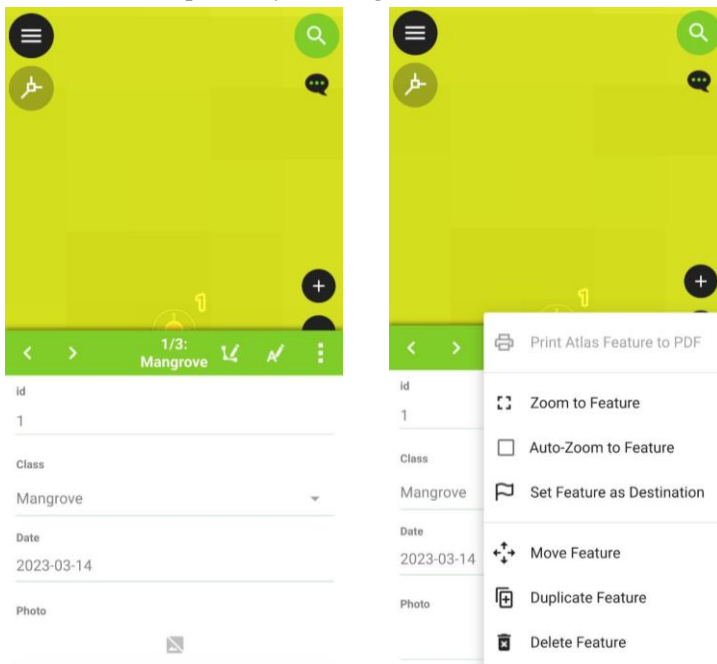

Important note: The ID of a ground control point is automatically set. It was noted that using the '*Move Feature*' function or the '*vertice tool*' creates errors in the automated numbering. Therefore, If you are not satisfied with the location or attribute of the created point, **click** on ⋮ and **delete** it with the 🗑 '*Delete Feature*' option on the menu's ground. Then **create** a new point. This avoids errors in the automated id, since relocating the point with the vertex tool results in an increment of the point's id. Therefore, do not use the '*Move Feature*' function or the '*vertice tool*'!

2.7. In a farm area, **generate** one point for each land cover class (Mangrove, Water, Vegetation, Infrastructure, and Soil) on each red or blue indicate shrimp farm of interest. The aimed number of points for each shrimp farm is indicated in the table below. In case not every land cover class is represented on the investigated shrimp farm try to compensate the missing land cover class on an adjacent shrimp farm or along the way. Additionally create one '*Water*' land cover points in the river or channel close to the investigated shrimp farm, since the spectral signature is likely to differ from the water in the shallower shrimp ponds. The ideal sampling point scenario for each shrimp farms is given in the following table:

Class	Points
Mangrove	2
Water (shrimp pond)	1
Water (river or channel)	1
Vegetation	1
Infrastructure	1
Soil	1

Take care that the points are located at least 4 pixel sizes (6 m) apart from each other to avoid mixed pixels. You can either count the pixels or measure the distance with the '*Measure Tool*'. Click on the Menu button in the top left corner and then click the settings button to select the '*Measure Tool*'.

2.8. After creating the 7 points switch back into '*browse mode*' by **clicking** on ▣.
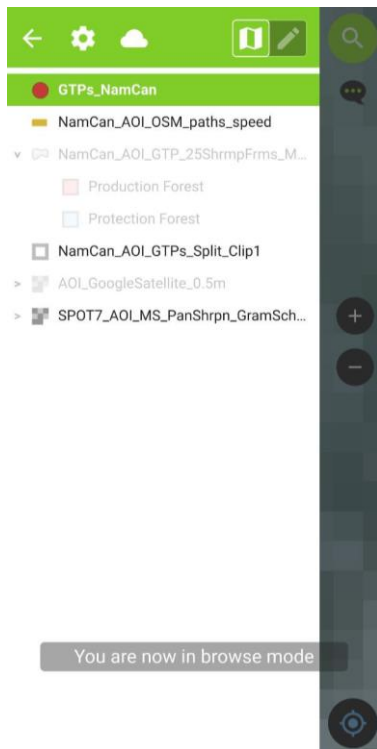
Now you can close the QField app and go to the next area of interest. Two shrimp farms of interests are always located next to each other to reduce the travel time in the study area. After you sampled one shrimp farm cluster, which includes two shrimp farms, ride with your motorbike to the next shrimp farm cluster.

3. Transfer the QField data to your PC

3.1. In case you do not have it yet, **create** a directory called "*QField_Export*" with your respective identifier on your PC. For instance, the name of the folder for the person with the identifier "A" would be "*QField_Export_A*". Otherwise use the one that you made at the start.

3.2. **Connect** your mobile QField device to your PC. If you use an Android device, **click** on the pop-up window of your phone's top bar or search for "USB Preferences" in your phone's settings.
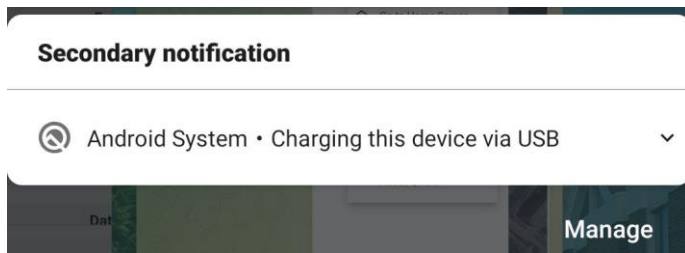
Then **select** '*File Transfer*' in the '*USE USB FOR*' section.
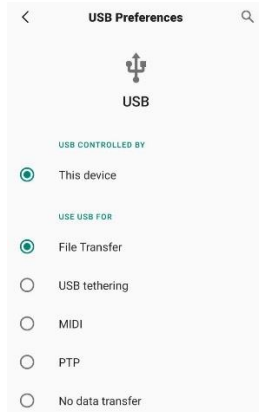
3.3. In the QField app you can have a look at the directory path where your project is stored. **Click** on ⚙️
and then on '*Open Project Folder*'. Now you can see the directory where the Project Folder is stored as well
as the folder's content ('*Folders*', '*Projects*', and '*Datasets*').
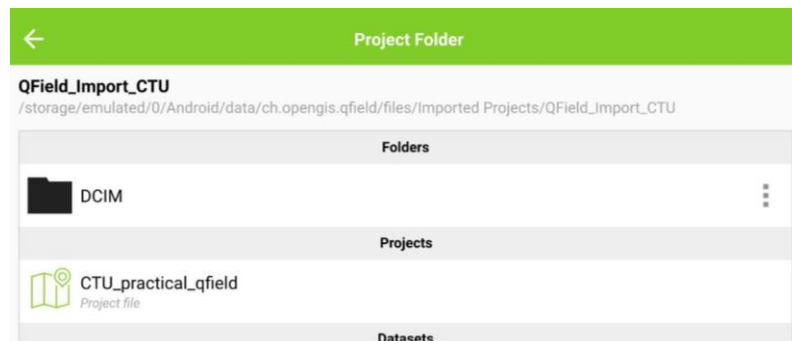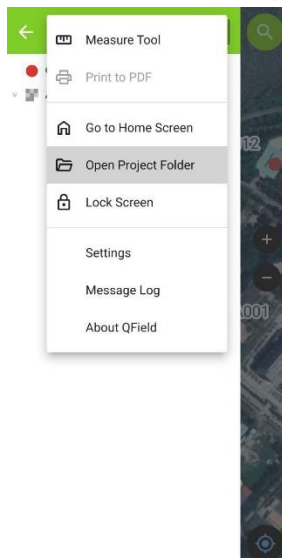
3.4. **Browse** with your PC to the indicated QField Project directory of the connected QField device, in
this case "This PC\BV9900Pro\Internal shared storage\Android\data\ch.opengis.qfield\files\Imported
Projects\QField_Import_CTU".

Select (**CTRL + A**) the entire content of the Project Folder and **copy** (**CTRL + C**) the content.
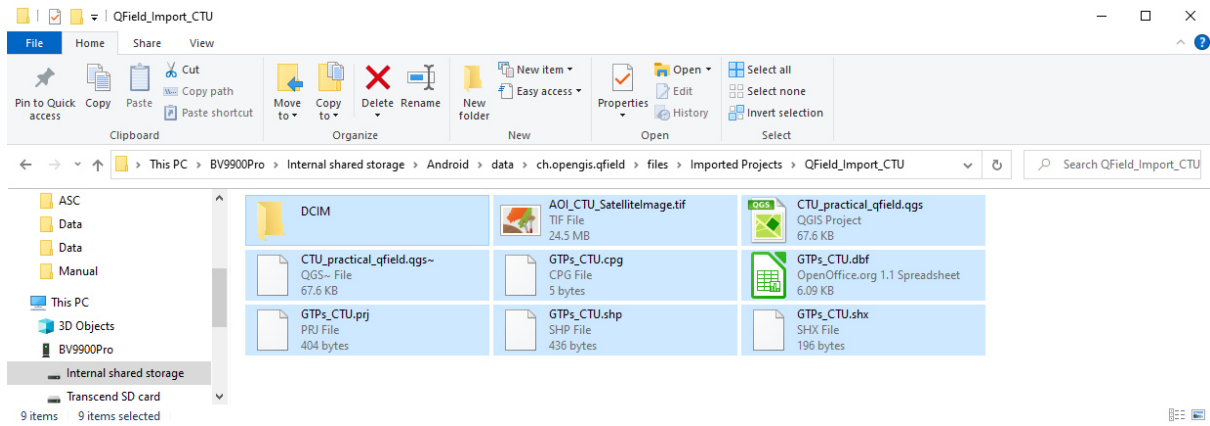

3.5. **Browse** to the newly created '*QField_Export*' directory on your PC and **paste** (**CTRL + V**) the copied files into this folder.
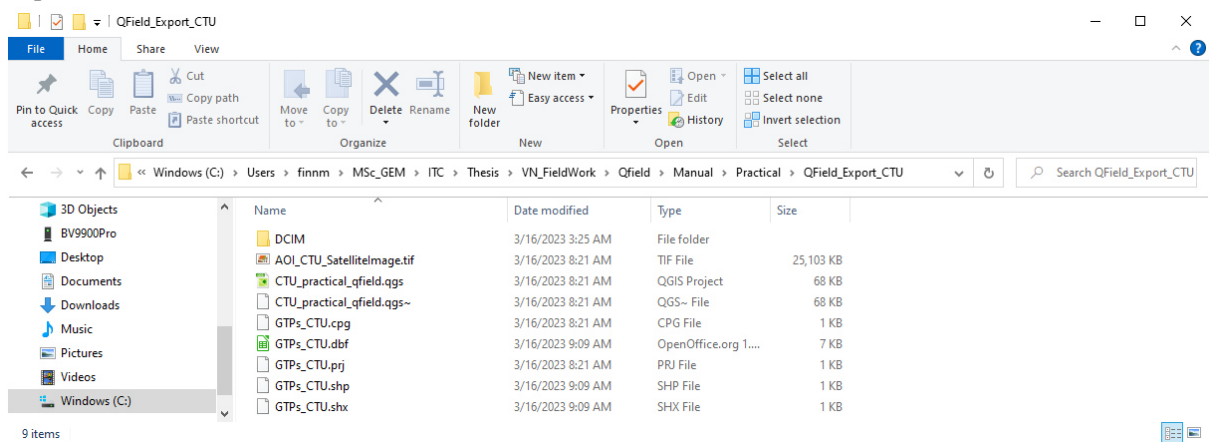
4. Synchronise the QField project from your mobile device with your QGIS project on your PC

4.1. **Open** the " Qfield_NamCan_A.qgz" QGIS project with your respective identifier, in this case "A". **Click** on the '*Synchronise from QField*' button in your PC's QGIS project.
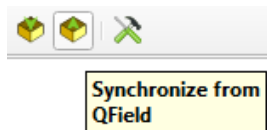
4.2. Deselect or **uncheck** all directories in the '*Advanced*' section and then **click** ⬚ to **browse** to the folder where your QFleld_Export folder that contains your GTPs and **click** '*Select Folder*'.
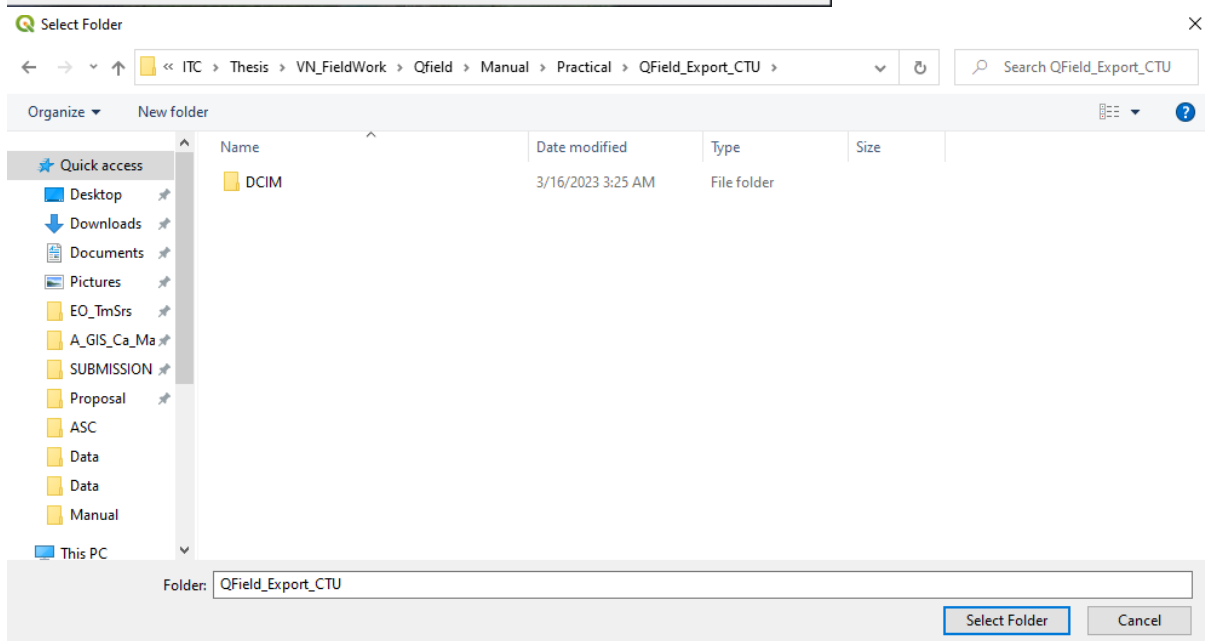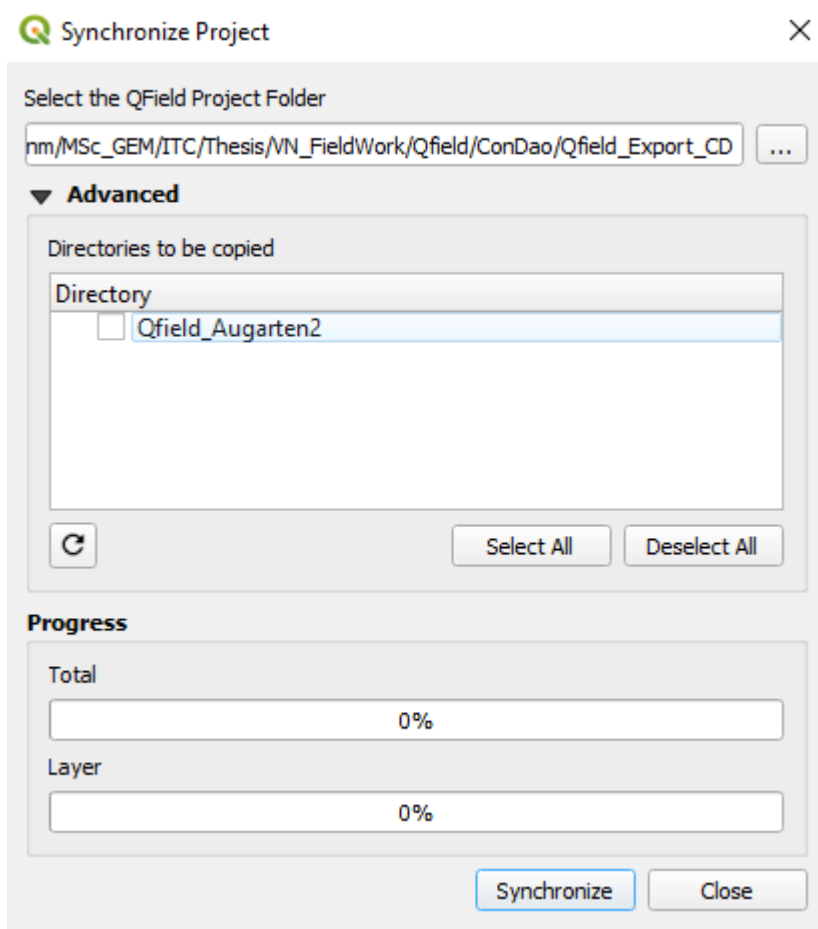
At last **click** '*Synchronize*'. You can observe the Progress of the synchronization.

4.3. Ones the data is synchronized the GTPs taken during the field survey are displayed in your QGIS project.

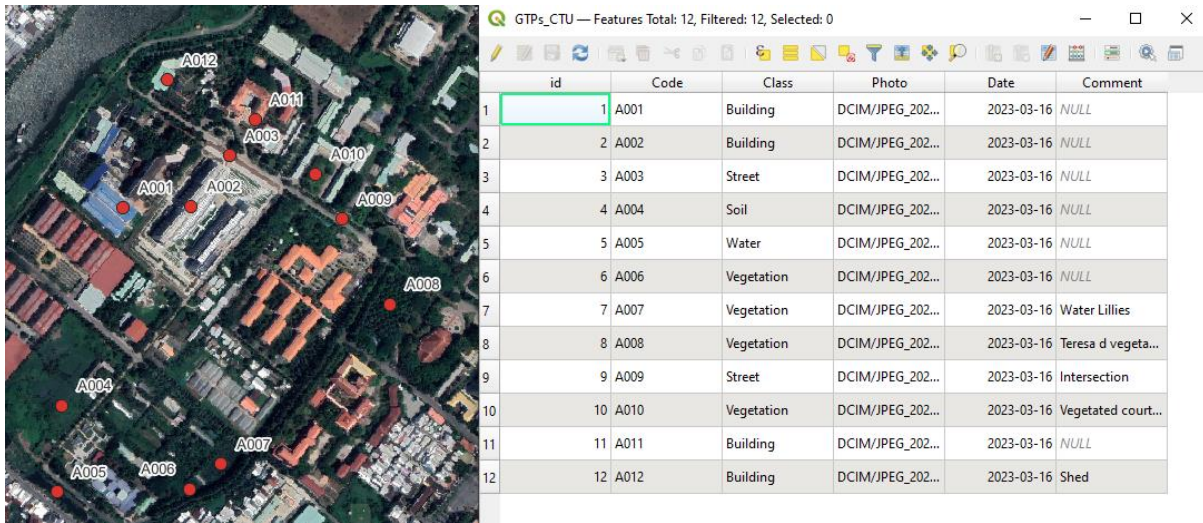4.4. To display the images you took during the field survey **right click** on your point shapefile layer and **select** properties. **Click** on the '*Attributes Forms*' section and select the field '*Photo*'. **Select** '*image*' from the '*Type*' drop down menu in the subsection '*Integrated Document Viewer*' of the '*Widget Type*' section. Then **adjust** the width to 400 and the height to 300 px. Verify the changes by **clicking** the '*Apply*' button on the ground of the window and close the Properties window.
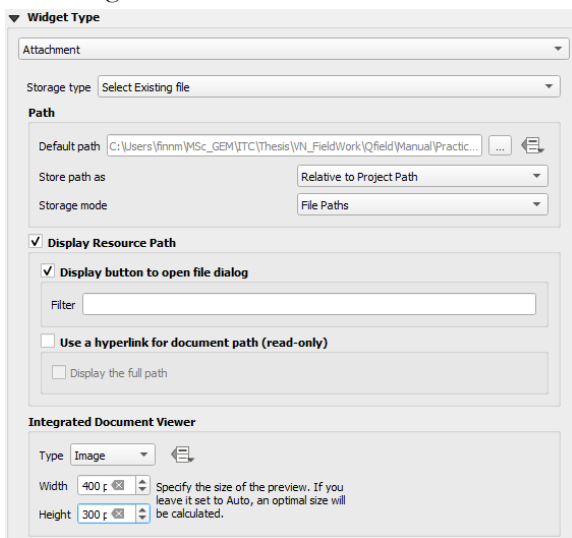
4.5. Use '*Identify Features*' to **select** a feature of interest.
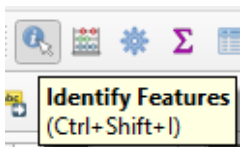
4.5. **Right click** on the feature '*Photo*' and **select** '*View Feature Form…*'.
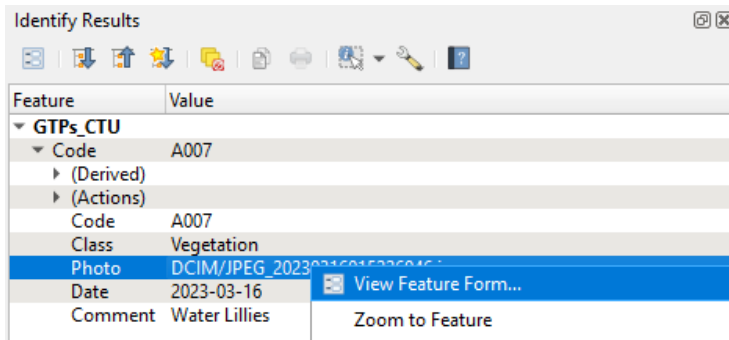
The attributes including the image taken at the selected point are displayed.
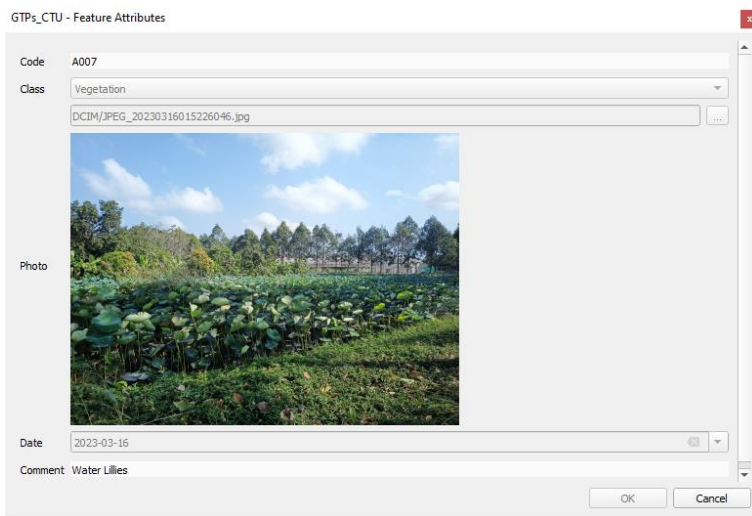
Appendix B

The entity of collected Ground Truth Points (GTPs) sampled by the Vietnamese students with the QField application is illustrated in *Table 10*.

Table 10. Ground Truth Points (GTPs) collected by the students for each land cover class.

Land cover Class	GTPs
Mangrove	216
Water	217
Vegetation	129
Infrastructure	111
Soil	106
Total	**778**

Appendix C

Object-based mangrove to shrimp farm ratio

Map 9. Relative mangrove area on the shrimp farms in percent according to the object-based classification (Airbus, 2022).

Table 11. Count [n] of shrimp farms for the relative mangrove cover class in the four forest zones for the object-based and pixel-based approach. Relative count of shrimp farms in the forest zones per square kilometer [n/km^2].

Forest Zone	Area [km^2]	< 1% [n]	< 1% [n/km^2]	1 to 46 %	1 to 46 % [n/km^2]	46 to 56 %	46 to 56 % [n/km^2]	56 to 64 %	56 to 64 % [n/km^2]	64 to 99 %	64 to 99 % [n/km^2]	99 to 100%	99 to 100% [n/km^2]
Special-use forest	10,088	0	0	0	0	0	0	0	0	11	0.40	7	0.69
Protection forest	21,116	2	0.09	207	9.61	102	4.59	69	2.18	125	5.87	0	0
Production forest	43,757	20	0.43	680	15.53	128	2.99	90	1.55	118	2.86	0	0
Not forestry	11,477	11	0.96	108	8.71	6	0.52	2	0	9	0.78	0	0
Total	86,439	33	0.38	995	11.51	236	2.73	161	1.86	263	3.04	7	0.08

Table 12. Count [n] of shrimp farms with less than 56%, between 56 to 64%, and more than 64% mangrove cover for the Protection, Production, and No Forest zones.

		Object-based		
		< 56% mangrove cover	56 to 64% mangrove cover	>64% mangrove cover
Pixel-based	< 56% mangrove cover	1264	0	0
	56 to 64% mangrove cover	0	161	0
	>64% mangrove cover	0	0	252

Appendix D

This Appendix section contains the notes on the expert interview with Mr. Ly Minh Thang of the West Sea Protection Forest Management Board. The interview took place on the 14th April 2023.

Questions for the technical manager of the Forest Protection Department

A) Introduction

1. **Would you like to introduce yourself and the Forest Management Board?**

My name is Ly Minh Thang. I am a Technical Manager of the Forest Protection Department, West Sea Protection Forest Management Board. We have two departments with a total staff number of 56 people including the stations. Our Forest Management Board manages an area of 11,000 hectares.

The Biển Tây (westside of Cà Mau) Forest protection department focuses on Lam Hai (Năm Căn) and Nguyen Viet Khai (Phu Tan). The Biển Tây Forest protection department employs twelve people, including three forest managers and nine field surveyors.

2. **How many shrimp farms are currently monitored by your Forest Management Board?**

There are 3087 production households on the managed forest stand.

3. **What do you consider as main challenges to monitor the mangroves?**

Challenges from climate change and increasing sea level rise, natural erosion, changes in alluvial deposits, agricultural production, aquaculture, financial resources to protect mangroves currently very limited.
We would like to plant more mangroves since now the mangrove cover is just about 40%. But there is no money to invest for planting mangroves.
The budget to protect mangroves is too small. We don't have enough money to support the farmers who protect mangroves.
In recent years, the government invested 30 million Vietnamese Dong to plant 1 ha of mangrove in the protection forest. But just for planting, not for protecting the mangroves later. This is decided every year according to Cà Mau people committee.
Whereas in the production forest the government only funds 8 million Vietnamese Dong per hectare.

4. **What could improve the mangrove monitoring?** (*The number of surveyors, monitoring techniques, skills, or tools?*)

Need to arrange enough human resources about ten people, equipped with knowledge, techniques and tools to carry out the field survey.
Need more people. Improve knowledge (technical & tools) to monitor mangroves.
Software, GIS, MapInfo, mapping techniques.
Don't have enough knowledge about GIS and remote sensing methods at the Forest Management Board.
We have four people who can work with GIS but we need to upgrade them to the next level.

5. **Are there policies and permissions regulating the harvest and planting of mangroves?**

Circular No. 26/TT-BNNPTNT dated December 30, 2022 of the Ministry of Agriculture and Rural Development Regulations on management and traceability of forest products replacing Circular No. 27/2018 of the Ministry of Agriculture.

6. *How are these policies enforced?*

There are forms to follow. Everything is guided in that circular.

B) Monitoring method

7. How do you currently assess the ratio of mangrove cover on shrimp farms?

Actual measurements and satellite images are applied to determine the ratio of mangrove cover on shrimp farms.
We use satellite images of google maps or google earth to manually digitize mangroves on shrimp farms. Then we do a field survey, using handheld GPS devices, to validate the digitized mangrove map.

8. How many working hours or days do you spend on the investigation of the mangrove cover on one shrimp farm?

The GPS field survey takes about two hours per shrimp farm. The field survey investigates the mangrove cover with GPS measurements. A maximum of four shrimp ponds can be surveyed during one day.

9. How do you select the shrimp farms you control?

We have the list, more than 3000 households, we can see where a lack of mangrove is and we go to that location to plant more mangrove. Then we draw or update the base map. Sometimes, we don't have an updated google earth image. So that is why we need to go to the field to update the current status of mangrove cover.
The government will pay for the planting of the mangroves. The farmers do not pay anything for the planted mangroves. The mangrove cover should be 60% in both the protection and production zone.

10. How often do you visit or revisit the shrimp farms?

Visit very often.

11. What exact area do you consider for the mangrove-shrimp farm ratio calculation? Only the pond area or the entire shrimp farm area?

The entire management area.
We don't have mangroves outside of the shrimp ponds because every two years, the shrimp farmers dig out the mud of the pond and put the soil up to the boundaries. Therefore, there is barely plants on the dikes marking the shrimp farm's boundary.
The Forest Management Board only plants mangroves inside the water of the shrimp ponds. Therefore, they do not consider the area outside of the shrimp pond for the mangrove cover.

12. What error range or accuracy of your mangrove to shrimp farm ratio estimations do you consider?

About 10 to 15% error is considered based on the 90 to 85% accuracy stated by the used handheld GPS device.

13. What mangrove cover threshold do you consider to assess if shrimp farms are in compliance? (*Different thresholds for the Production and the Protection Forest?*)

A threshold of 60% mangrove cover on farm is applicable within the forest zones. Since 2010 there is no difference between the threshold for the protection and production forest. Accordingly, the threshold of 60% is set forth for both forest zones.
Before   2010   the   following   regulations   were   active   in   Cà   Mau   province:
For shrimp farms with an area greater than 5 ha: 70% relative mangrove cover for both forest zones
For shrimp farms with an area between 3 to 5 ha: 60% relative mangrove cover for both forest zones
For shrimp farms with an area smaller than 3 ha: 50% relative mangrove cover for both forest zones
Previously there was a regulation of 40% relative mangrove area in the Production zone but it was updated to 60% in 2010.

14. **What is the minimum height a mangrove needs to have to be considered as Mangrove in the assessment?**

A minimum tree height of 5 m is necessary for the mangroves to have a protection function. This height is achieved about 5 years after the planting date and care period. The planted saplings are approximately 30 cm long and have a diameter of 3 cm.
Every year we plant additional trees where dead mangroves are present. After 3 years, we need to have 6,000 trees/ha in the area to be considered as "forest". We use 100 square meters as a representative sampling area to count how many trees are present.

##
#######################

The following Questions are only considered if the restricted time allows.

C) Remote sensing and Geo-information

15. **Do you use satellite remote sensing or unmanned aerial vehicles (UAVs) for mangrove mapping purposes?**

We only use the satellite images available via Google Earth.

16. *(What kind of remote sensing data do you use in terms of Spatial, Temporal, and Spectral resolution?)*

Not used yet

17. *(How do you analyse the imagery?) [Visual analysis, or Classification (manual , pixel-based or object based)?]*

Handmade (manual)

18. *(What potential do you see in remote sensing approaches for the mapping of mangroves on shrimp farms?)*

Teaching institutions need to organize training for technicians on remote sensing, since many units are in need of training and implementation of this method.

19. **What prerequisites must be fulfilled for the application of remote sensing methods**?

The staff only uses basic GIS but has not studied it in depth.

Câu hỏi dành cho người quản lý rừng (Tổng cục Lâm nghiệp Việt Nam (VNFOREST))

A) Giới thiệu

1. Bạn có muốn giới thiệu bản thân và Ban quản lý hoặc Bộ phận của mình không?
2. Có bao nhiêu trang trại nuôi tôm hiện đang được giám sát bởi bộ phận quản lý rừng của bạn?
3. Theo bạn, những thách thức chính đối với việc giám sát rừng ngập mặn là gì?
4. Điều gì có thể cải thiện việc giám sát rừng ngập mặn? (Số lượng người khảo sát, kỹ thuật giám sát, kỹ năng hoặc công cụ?)
5. Có chính sách và giấy phép nào điều chỉnh việc khai thác và trồng rừng ngập mặn không?
6. Các chính sách này được thực thi như thế nào?

B) Phương pháp giám sát

7. Làm thế nào để bạn đánh giá hiện tại tỷ lệ che phủ rừng ngập mặn trên các trang trại nuôi tôm?
8. Bạn dành bao nhiêu giờ hoặc ngày làm việc để điều tra độ che phủ của rừng ngập mặn trên một trang trại nuôi tôm?
9. Làm thế nào để bạn lựa chọn các trang trại nuôi tôm mà bạn kiểm soát?
10. Bạn có thường xuyên đi thăm hoặc thăm lại trang trại nuôi tôm không?
11. Bạn xem xét khu vực chính xác nào để tính tỷ lệ trang trại tôm rừng ngập mặn? Chỉ diện tích ao nuôi hay toàn bộ diện tích đầm nuôi tôm?
12. Phạm vi sai số hoặc độ chính xác của ước tính tỷ lệ rừng ngập mặn trên trang trại nuôi tôm mà bạn xem xét?
13. Bạn xem xét ngưỡng che phủ rừng ngập mặn nào để đánh giá xem các trang trại nuôi tôm có tuân thủ hay không? (Ngưỡng khác nhau đối với rừng sản xuất và rừng phòng hộ?)
14. Chiều cao tối thiểu mà một cây rừng ngập mặn cần có để được xem xét là rừng ngập mặn trong quá trình đánh giá là bao nhiêu?

##

Các câu hỏi sau đây chỉ được xem xét nếu thời gian hạn chế cho phép.

C) Viễn thám và thông tin địa lý

15. Bạn có sử dụng viễn thám vệ tinh hoặc máy bay không người lái (UAV) cho mục đích lập bản đồ rừng ngập mặn không?
16. (Bạn sử dụng loại dữ liệu viễn thám nào về độ phân giải Không gian, Thời gian và Quang phổ?)
17. (Bạn phân tích hình ảnh như thế nào?) [Phân tích hình ảnh hoặc Phân loại (thủ công , dựa trên pixel hoặc dựa trên đối tượng)?]
18. (Bạn thấy tiềm năng gì trong các phương pháp viễn thám để lập bản đồ rừng ngập mặn ở các trang trại nuôi tôm?)
19. Để áp dụng phương pháp viễn thám cần đáp ứng những điều kiện gì?
20. Bạn có bộ phận hoặc chuyên gia về GIS hoặc Geodata không?